DESIGN OF MEDIUM ACCESS CONTROL TECHNIQUES FOR COOPERATIVE WIRELESS NETWORKS

WANG YU

NATIONAL UNIVERSITY OF SINGAPORE

2014

DESIGN OF MEDIUM ACCESS CONTROL TECHNIQUES FOR COOPERATIVE WIRELESS NETWORKS

WANG YU

(*B. Eng., Huazhong University of Science and Technology, China*)

A THESIS SUBMITTED

FOR THE DEGREE OF DOCTOR OF PHILOSOPHY

DEPARTMENT OF ELECTRICAL AND COMPUTER ENGINEERING

NATIONAL UNIVERSITY OF SINGAPORE

2014

Declaration

I hereby declare that the thesis is my original work and it has been written by me in its entirety. I have duly acknowledged all the sources of information which have been used in the thesis.

This thesis has also not been submitted for any degree in any university previously.

Wang Yu

10 July 2014

Wang Yu.

10 - July - 2014

Acknowledgment

First of all, I would like to express my sincere gratitude and appreciation to my advisors Prof. Hari Krishna Garg and Prof. Mehul Motani for their valuable guidance and helpful technical support throughout my Ph.D course. Had it not been for their advices, direction, patience and encouragement, this thesis would certainly not be possible.

I would like to thank Dr. Xin Kang, Dr. Qian Chen and Dr. Tie Luo in Institute for Infocomm Research with whom I have had the good fortune to collaborate.

I would like to thank my colleagues Can Chen, Wen Sun, Shuowen Zhang, Xun Zhou, Yang Hu, Yinghao Guo, Huanhuan Zheng, Xiao Han, Chenglong Jia, Cheng Huang, Gaofeng Wu, Qian Wang, Tianyu Song, Liang Liu, Shixin Luo, Tong Wu, Jie Xu, and Yi Yu in the Communications and Networks Laboratory at the Department of Electrical and Computer Engineering for their friendship and help.

This research was carried out at the NUS-ZJU Sensor-Enhanced Social Media (SeSaMe) Centre. It is supported by the Singapore National Research Foundation under its International Research Centre @ Singapore Funding Initiative and administered by the Interactive Digital Media Programme Office. I would like to thank SeSaMe Centre for the support provided. I would like to thank my colleagues Yan Luo, Yongkang Wong, Tian Gan, Fanxi Chang in SeSaMe Centre for their friendship and help.

Lastly, and most importantly, I would like to thank my parents for their love, support, and encouragement.

Contents

Summary

Cooperation has intrigued many researchers in recent years as an emerging design strategy for both centralized and distributed wireless communication networks. In cooperative networks, terminals may cooperate to achieve common or individual goals by giving, sharing, or allowing something. The main idea behind being cooperative is that each cooperating terminal gains by means of the unified activity. Successful cooperative networks can lead to the development of advanced wireless networks that provide better quality of service in a cost-effective manner. The challenges of designing medium access control techniques for cooperative networks, however, are not well-understood yet. Protocols and algorithms are needed to allocate the networking resources among different terminals and to manage the cooperative actions within networks.

The opportunistic link scheduling algorithm is proposed by Liu et al for infinite backlog traffic demand in [1]. It exploits the variation in channel conditions to improve the throughput of a cellular system. They, however, have not discussed the possibility of using cooperative transmission in helping data transmission in a cellular system. In [2], the authors propose the use of dedicated relays for cooperative transmission in directional wireless networks. Meanwhile, they do not recognize the fact that independent consideration of relay assignment and link scheduling, in general, may not ensure the optimal solution. In [3], cooperation is used to provide the information sharing among neighboring terminals for solving hidden terminal and

deafness problems. They, however, do not consider the possibility that the terminals may use directional transmission instead of omni-directional transmission.

This thesis studies a number of topics in medium access control for cooperative networks. First, we study algorithms for opportunistic scheduling with two-hop cooperative transmission in cellular networks. In this work, we examine the scenario that single user equipment may be served by multiple mobile terminals concurrently in cellular networks. The optimal scheduling algorithm for cooperative cellular networks is obtained under long-term fairness constraints. Second, we extend the idea to multi-hop cooperative transmission in 60 GHz wireless personal area networks. We propose optimal cooperative scheduling algorithms in terms of throughput for various scenarios of traffic demand (bursty or not bursty). The proposed algorithms jointly manage relay assignment and link scheduling for studied networks. The results demonstrate that cooperative algorithms outperform non-cooperative algorithms significantly. Third, we investigate cooperation in designing the medium access control protocol for distributed multi-channel directional ad hoc networks, where terminals contend for channel resources. Different from previous two topics, cooperation is no longer manifested in relaying data frames for other terminals. In this topic, cooperation implies that terminals share local channel usage information with each other. The results illustrate that cooperation effectively solves hidden terminal and deafness problems and improves throughput of studied networks significantly.

In this thesis, we study using cooperation among terminals to improve throughput for both centralized and distributed wireless networks. Theoretical analysis, modeling and simulations are used to guide the design of cooperative algorithms and protocols. Computer simulations demonstrate that cooperation is an effective approach to improve networking performance in terms of quality of service.

List of Figures

List of Tables

List of Notations

a, A	nonbold letters are used to denote scalars
a, **A**	boldface letters are used to denote row vectors
$\mathrm{E}[\cdot]$	the statistical expectation operator
$\lceil\cdot\rceil$	map a real number to the smallest following integer
$\max(x, y)$	the maximum element of x and y
$\min(x, y)$	the minimum element of x and y

List of Abbreviations

ACK	Acknowledgment
ASC	Aggressive strategy with cooperation
ASNC	Aggressive strategy without cooperation
BPSK	Binary phase-shift keying
BTS	Base transmission station
CAMMAC	Cooperative asynchronous multi-channel medium access control
CBP	Cooperation backoff period
CCA	Clear channel assessment
CDMA	Code division multiple access
CDMAC	Coordinated directional medium access control
CFA	Confirm type A
CFB	Confirm type B
CH_NO	Channel number
CLP	Concurrent links pattern
CLS	Cancel signal
CMDMAC	Cooperative multi-channel directional medium access control
CQI	Channel quality indicator
CSC	Conservative strategy with cooperation
CSMA/CA	Carrier sense multiple access /collision avoidance

CSNC	Conservative strategy without cooperation
CTS	Clear to send
dB	Decibel
DBPSK	Differential binary phase-shift keying
DEV	Device
DMAC	Directional medium access control
DNAV	Directional network allocation vector
DoA	Direction of arrival
DTP	Data transmission period
DYSA	Deny signal type A
DYSB	Deny signal type B
FSMC	Finite state markov chain
GMR	Gradient algorithm with minimum/maximum rate constraints
GPS	Global position system
GSM	Groupe spécial mobile
HSDPA	High-speed down-link packet access
IMT	International mobile telecommunications
IoT	Internet of things
ISM	Industrial, scientific and medical
Kbps	Kilobit per second
LOS	Line of sight
LTE	Long-term evolution
LTIME	Left time
MAC	Medium access control
Mbps	Megabit per second
MCS	Modulation and coding schemes

MMAC	Multi-channel medium access control
MT	Mobile terminal
M2M	Machine to machine
NCDMAC	Non-cooperative directional medium access control
NIT	Neighbor information table
NP	Negotiation period
NS2	Network simulator 2
OSI	Open system interconnection
PAC	Practical antenna with cooperation
PANC	Practical antenna without cooperation
PNC	Piconet coordinator
PSSG	Possible spatial sharing gain
QAM	Quadrature amplitude modulation
QoS	Quality of service
QPSK	Quadrature phase-shift keying
RSSI	Received signal strength indication
RS_ADDR	Reason node address
RTS	Request to send
Rx	Receiver
SEC_NO	Sector number
SINR	Signal to interference and noise ratio
SIFS	Short inter-frame space
SMMTSU	Scheduling scheme for multiple mobile terminals serving the same user equipment
SNR	Signal to noise ratio
SSG	Spatial sharing gain

TCOS	Throughput constrained opportunistic scheduling
Tx	Transmitter
UDP	User datagram protocol
UE	User equipment
UMTS	Universal mobile telecommunications system
UP_ADDR	Updated node address
UP_SEC	Updated node sector
WiFi	Wireless fidelity
WLAN	Wireless local area network
WPAN	Wireless personal area network

Chapter 1

Introduction

Wireless communication has experienced rapid development during the last couple of decades. People are nowadays surrounded by different kinds of wireless networks such as cellular networks, wireless local area networks (**WLAN**s), wireless personal area networks (**WPAN**s) and so on. These wireless networks give users the ability to be connected while moving around within a local coverage area. It may also be predicted that the boom of heterogeneous networks, like internet of things (**IoT**) and machine-to-machine (**M2M**) networks, will occur in near future. Witnessing these fast evolutions, people have every reason to expect better and better mobile networking products and services. Since efficient medium access control (**MAC**) techniques are essential for all types of wireless networks, many researchers and engineers are attracted to this field. As wireless networks are formed by multiple terminals, cooperation among them may be introduced to improve the overall networking performance. This thesis focuses on analyzing, studying and proposing efficient MAC techniques for cooperative wireless networks.

King Soloman said "None is so great that he needs no help, and none is so small that he cannot give it". It would be safe to reason that cooperation, widely exploited by nature, has been present from rather early origins of our time. Being understood as a joint action for mutual benefit, it has been the subject of intensive study in the social and biological sciences. From a wireless communication perspective, cooperation may be understood as "taking advantage of the synergetic interaction of multiple terminals to enhance any performance figure" [4]. Typical performance figures include throughput, latency, quality of service (**QoS**), networking coverage and so on. Even though cooperation in wireless networks has not yet reached its full maturity, its realm is already broad. To be focused, we confine our study to cooperation at MAC layer in this thesis. As throughput is typically seen to be the most important and commonly studied indicator of networking performance, this thesis is devoted to enhancing throughput by investigating cooperation in both centralized and distributed wireless networks.

In the remaining parts of this chapter, we briefly introduce the basic background, provide overview on related works and challenges, and present the major contributions and organizations of this thesis.

1.1 Cooperative Medium Access Control

In this section, the background knowledge about MAC is presented. After that, common cooperative techniques in MAC are demonstrated and discussed.

1.1.1 Medium Access Control

MAC techniques are designed to accommodate or schedule data transmission by multiple devices sharing the same wireless medium. In the seven-layer open system interconnection (**OSI**) model of computer networks, media access control is a sublayer of the data link layer as shown in Fig. 1.1. Since medium access control and media access control are often used interchangeably, we use medium access control

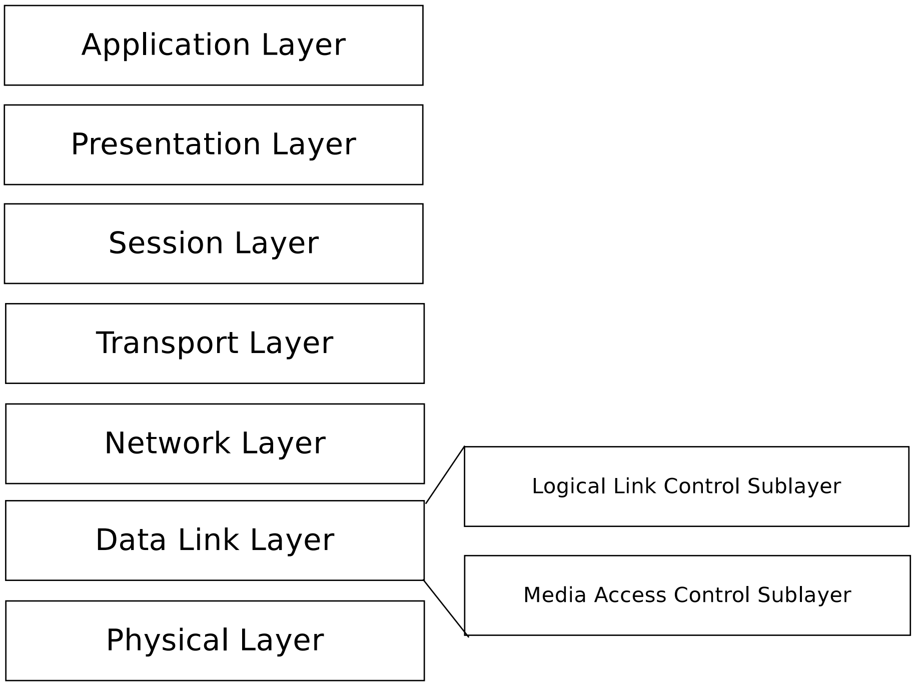

Figure 1.1: Open system interconnection (**OSI**) model of computer networks.

(**MAC**) henceforth. MAC sublayer provides addressing and channel access control techniques that make it possible for several terminals to communicate within a multiple access network that incorporates a shared medium. Generally, there are two kinds of MAC techniques, namely, centralized contention-free link scheduling and distributed contention-based MAC. The details are described below.

1.1.1.1 Contention-Free Link Scheduling for Centralized Networks

If transmission sessions of all devices are arranged by a single scheduler, the network formed by these devices is termed as a centralized network. MAC for a centralized network is termed as link scheduling, and it is usually contention-free. The most common centralized network is a cellular network as shown in Fig. 1.2. The base station is the scheduler responsible for controlling transmission of all mobile devices. That is, the base station manages medium access and allocates medium resource for all mobile devices. Since a centralized scheduler exists, data can be delivered in a

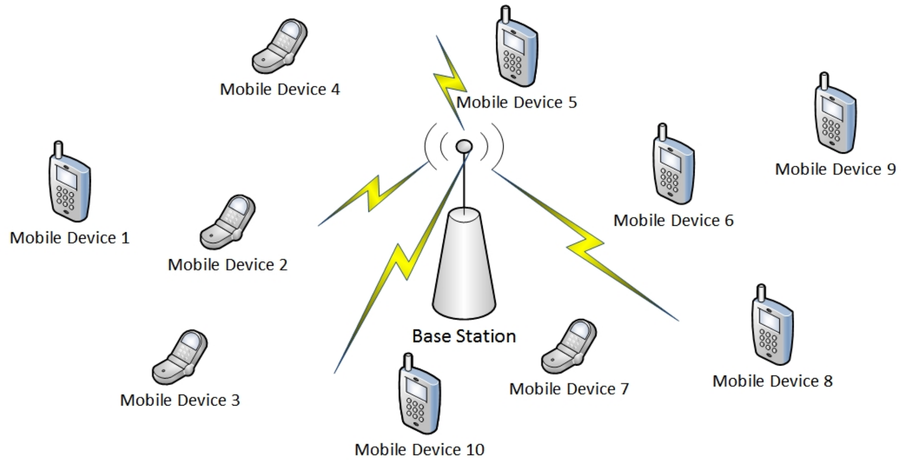

Figure 1.2: System model for centralized networks.

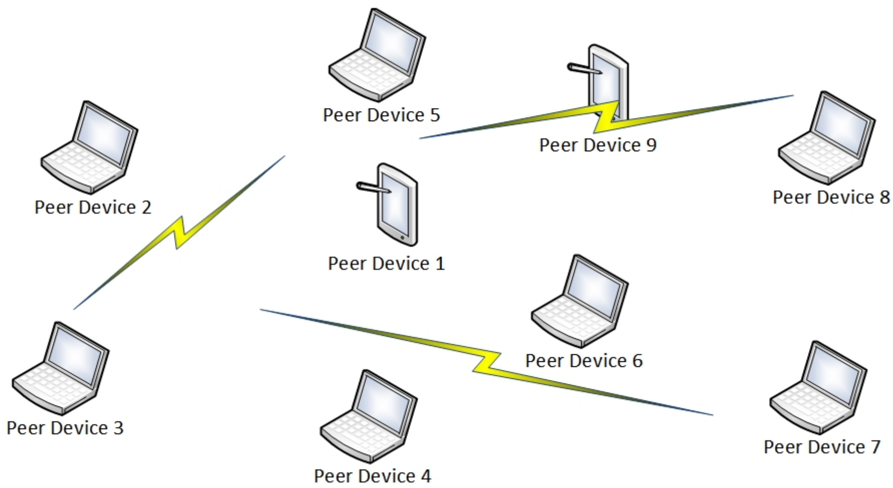

Figure 1.3: System model for distributed networks.

well-organized manner. Meanwhile, the entire centralized network may get corrupted due to failure at the centralized scheduler.

1.1.1.2 Contention-Based MAC for Distributed Networks

If there is no centralized controller, then the network consists of several independent peer devices. Such a network is termed as a distributed network. The most common example of distributed networks is a wireless fidelity (**WiFi**) network based on IEEE 802.11 protocol as shown in Fig. 1.3. Without a scheduler, distributed networks make medium resources available to peer devices in a transparent manner. The regulation, which is followed by peer devices to contend for accessing the medium, is usually termed as MAC protocol. The primary advantage of distributed MAC is that it simplifies establishment procedure of networks and requires no pre-set infrastructure. The disadvantage is that a distributed MAC protocol may not be as efficient as link scheduling in terms of medium resource allocation.

Objective functions are usually formulated when researchers study contention-free link scheduling for centralized networks, since the optimal solution in terms of throughput is expected. In the field of contention-based MAC protocol design, it is not difficult to provide objective function but very difficult to set constraints based on the complicated networking environment. Thus, it is commonly accepted that solving hidden terminal and deafness problems in MAC to reduce packet conflicts and improve throughput is the objective in MAC protocol design. In this thesis, above common rules are accepted and followed. We study optimal solutions for scheduling in cooperative centralized networks and study methods to solve hidden terminal and deafness problems in cooperative distributed networks.

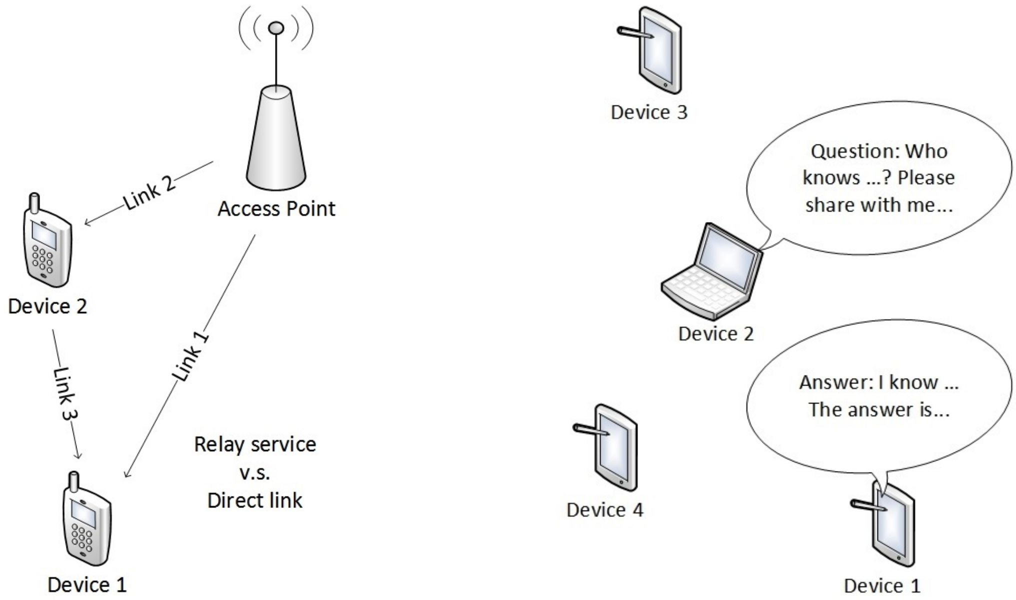

(a) Cooperation by relay service. (b) Cooperation by information sharing.

Figure 1.4: System models for cooperative networks.

1.1.2 Cooperation in Medium Access Control

Cooperation among different devices may reflect in various forms and from different perspectives in MAC sublayer. In this thesis, two types of cooperation based techniques are investigated. First, neighboring devices may provide relay service for each other. For example in Fig. 1.4(a), Device 1 may possess weak signal strength with direct Link 1. Thus, relay service by Link 2 and Link 3 may be a better choice for data delivery from the Access Point to Device 1. Second, neighboring devices may share local information with each other for solving problems in forming or operating networks. For example in Fig. 1.4(b), Device 2 may not have certain information and broadcast its query. If Device 1 happens to know the answer to the query, it may share this local information with Device 2.

1.2 Related Work and Challenges

In this section, an overview is provided on MAC techniques and related cooperative methods in wireless networks. Then, challenges of designing cooperative MAC techniques are discussed briefly.

1.2.1 Link Scheduling in Centralized Wireless Networks

In this section, we review the related literature on link scheduling for omni-directional and directional networks with or without cooperative schemes.

Numerous research works on investigating efficient scheduling algorithms for centralized networks have been reported in the literature [1, 5–22]. Authors in [5–7] are pioneers in studying link scheduling problems and laying foundation for future research, although the networks studied are mainly fixed access ones. Since cellular networks with omni-directional transmission are the most popular and successful centralized wireless networks, early-stage research work on wireless link scheduling is mainly in this area. From groupe spécial mobile (**GSM**) to long-term evolution (**LTE**) networks, the current focus of cellular networks has moved from voice service to data service. Optimal scheduling schemes are investigated for both downlink and uplink transmission of data networks in [18] and [19], respectively. Later researchers have observed that subscribers may have different requirements for their service. In [20], a downlink scheduling algorithm with QoS guarantees to multiple subscribers in a cellular network is proposed. Further, fairness constraint among subscribers is considered in [21]. Observing the time-varying nature of radio environment, the authors in [1] proposed opportunistic scheduling methods to exploit multi-user diversity in cellular systems and presented a framework of opportunistic scheduling in [22]. Several works have followed this framework, applying and extending opportunistic scheduling to many other networking systems [23–28]. While above works discuss link scheduling in omni-directional scenarios, directional networks have also intrigued many researchers due to their higher spatial reuse and throughput performance [2, 29–45]. Recently, directional networks in mmWave band have received attention for their capability to provide multi-gigabit transmission rate. Heuristic and optimal scheduling algorithms are presented in [31] and [46] respectively.

With all these masterworks, it would seem that no further problems exist in the field of link scheduling. Researchers, however, find that it is still not enough to satisfy users sometimes due to poor channel status, limited bandwidth resource and so on. Cooperation has been proposed as a method to improve user experience for customers in [47–58]. Broadly speaking, cooperation in centralized networks implies using relay service among neighboring terminals. Networks become more sophisticated with cooperation, since additional cooperative links are needed to be scheduled along with the original ones. In [47, 48, 51], downlink scheduling is investigated when relay service is enabled in cellular networks. Further, opportunistic scheduling is introduced in cooperative cellular networks to reap benefit from multi-user diversity in [50, 56–58]. Researchers have also considered using cooperative link scheduling for directional networks with relays. In [59], it is shown that the quality and robustness of 60 GHz links can be improved by employing relays in the networks. While dedicated relays are employed for devices in [43, 44, 60], the authors suggested that relays should be selected dynamically based on current channel status for better service in [2, 37, 38]. However, link scheduling and relay assignment are always treated independently in above works, and this may generally not provide the optimal solution.

In summary, link scheduling plays a very important role in centralized wireless networks, and cooperation can potentially help improve networking performance. The main challenge in designing cooperative link scheduling for centralized networks is to jointly consider multiple factors and coordinate a group of links to get the maximal performance under certain system constraints.

1.2.2 Medium Access Control in Distributed Wireless Networks

In this section, related literature on MAC is reviewed for single-channel and multi-channel networks with or without cooperative schemes.

Back in 1970s, ALOHA, possibly one of the most famous MAC algorithms, was presented in [61] to create single-hop networks. Researchers then realized that the performance of ALOHA is not satisfying due to packet conflicts, especially in crowded and heavy-traffic networking environment. Carrier sense multiple access/collision avoidance (**CSMA/CA**) algorithm was first proposed in [62] and later refined in [63]. Then, CSMA/CA was revised and employed in different kinds of networks, and probably has become the most commonly used MAC technique nowadays. In early stages, investigation for MAC began from single-channel scenarios [64–67]. After that, research on multi-channel wireless networks became popular. To operate multi-channel networks properly, efficient MAC protocols are needed to coordinate connection sessions in different channels. In prior literature, one main approach is to use multiple radios and dedicate one radio to monitoring channel usage while others are engaged in data communication [68–70]. This approach may complicate devices' hardware and possibly increase their energy consumption. The other approach is regulating terminal behaviors by common contention window [71–73] or channel hopping sequences [74–76]. This approach faces the difficulty of time synchronization in distributed networks. While above works are examining omni-directional MAC, directional networks have also intrigued researchers for its potential in providing higher spatial reuse ratios and data rates. Recently, MAC for networks formed by terminals using beamforming or directional antennas has become a popular topic as shown in [77–83]. Since these works almost borrowed various ideas from multi-channel MACs, they again complicate networks with either extra hardware or requirement for time synchronization.

Cooperation is employed to solve problems of MAC in distributed wireless networks. Here, cooperation or cooperative MAC usually implies frame relay service among neighboring terminals [84–93]. Since multiple connections including cooperative ones may be established, MAC becomes more complicated for organizing these connections. A thorough survey on omni-directional MAC with cooperative relay service can be found in [94]. Cooperation in MAC, however, may not be limited in the form of relay service. In [3, 95], the authors present that cooperation may also be used for distributed information sharing. By cooperation among idle terminals during link establishment procedures, the hidden terminal problem is eliminated without additional hardware or time synchronization in omni-directional multi-channel ad hoc networks. This cooperation method has been first extended to directional networks with a single data channel in [96], and then extended to multi-channel directional ad hoc networks in [97]. These works demonstrate that cooperation can help reduce packet collision and improve throughput in an effective manner.

In summary, efficient MAC protocols are needed for distributed wireless networks, and cooperation can be employed in MAC from different perspectives. The main challenge in designing cooperative MAC is how to determine the cooperator, the timing and the form of certain cooperation and, at the same time, solve the hidden terminal problem with only local information.

1.3 Theme of the Thesis

The theme of this thesis is using cooperative methods in MAC techniques to improve throughput performance of the wireless network. We are motivated by the fact that there usually exist idle terminals in wireless networks, and we believe that these idle terminals can contribute in neighbors' communication. For example, the idle terminals can relay data frames for their neighbors; or they can share local information and help their neighbors make correct decision in negotiation procedures. The objective of this thesis is to provide novel methods on how we can use cooperation to improve throughput in both centralized and distributed networks.

1.4 Contributions of the Thesis

The motivation comes from the fact that cooperation helps in both social events and engineering design. Theme of the thesis is using cooperation in MAC techniques to improve networking throughput performance. This thesis has investigated the design of efficient MAC techniques to improve throughput performance of cooperative wireless networks. Specifically, the main contributions of this thesis can be categorized into the following three parts:

I. A new opportunistic scheduling algorithm for cooperative cellular networks: An opportunistic downlink scheduling algorithm is presented for the case when there exists user equipment that is served by multiple mobile terminals cooperatively in a time-slotted cellular networks. First, the proposed algorithm is proved to be optimal in terms of overall networking throughput. Then, the algorithm's effect on certain user equipment's throughput is examined. Simulation results demonstrate that the proposed algorithm provides benefit to user equipment with cooperative services and does not harm other users at the same time. This work has been published in [57, 58].

II. A new cooperative scheduling algorithm for 60 GHz WPANs: An optimal cooperative transmission scheme is proposed for 60 GHz WPANs, which considers link scheduling and relay assignment jointly. The throughput maximization issues are studied for scenarios with and without bursty data traffic demand, and formulated as linear programming problems. The optimal solutions based on the column generation method are provided. The results demonstrate that cooperative schemes provide significant throughput improvement as compared to non-cooperative schemes. Moreover, clear throughput gaps are shown between the optimal cooperative solution and an existing benchmark. This work has been presented in [98, 99].

III. A new cooperative MAC protocol for directional ad hoc networks: A cooperative multi-channel directional MAC (**CMDMAC**) protocol incorporating minor-lobe interference is proposed for directional ad hoc networks. While most existing MAC protocols require either additional equipment or clock synchronization to solve deafness and directional hidden terminal problems, CMDMAC needs neither to conquer these problems. Observing that existing directional MAC protocols assume single-data-channel environment in most instances, CMDMAC incorporates directional and multi-channel transmission to provide superior networking performance. Simulation results demonstrate that CMDMAC works efficiently in multi-channel directional ad hoc networks and provides significant throughput improvement. This work has been presented in [96, 97, 100].

1.5 Organization of the Thesis

The reminder of this thesis is organized as follows. Chapter 2 investigates opportunistic scheduling algorithm for cellular networks with user equipment served by multiple mobile terminals. Chapter 3 studies throughput maximization for cooperative 60 GHz WPANs. In Chapter 4, cooperative multi-channel MAC in directional ad hoc networks is examined. Finally, Chapter 5 concludes this thesis and discusses the future work.

Chapter 2

Opportunistic Downlink Scheduling for Cooperative Cellular Networks

In this chapter, an opportunistic downlink scheduling algorithm, which is referred to as scheduling scheme for multiple mobile terminals serving the same user equipment (**SMMTSU**), is presented for the case when there exists user equipment (**UE**) that is served by multiple mobile terminals (**MT**s) in a time-slotted cellular system. We study three scenarios, namely (i) when the MTs are served by the same cellular provider but scheduler has no knowledge of the presence of such UEs; (ii) when the MTs are served by the same cellular provider and the scheduler located in the base station knows the presence of such UEs; and (iii) when such MTs are served by different cellular providers. We establish the optimality and present the main properties of SMMTSU for scenario (ii). In scenario (iii), we show that it is better to use the MTs from one cellular provider using SMMTSU rather than from different cellular providers.

2.1 Introduction

Wireless communication has experienced tremendous growth over the past several decades. Nowadays, we can get different kinds of wireless service from cellular mobile networks to wireless local area networks. As cellular systems have evolved from groupe spécial mobile (**GSM**) to universal mobile telecommunications system (**UMTS**), focus of these systems has shifted from voice to data services. The international mobile telecommunications-2000 (**IMT-2000**) standards for third-generation wireless networks, released in 1999, support high data-rate traffic with 384kbit/s in packet switched mode [101]. After more than ten years of development, wireless networks are a global phenomenon with over 5.3 billion subscribers all around the world. There has been an ever increasing demand for higher-rate-data services with better quality-of-service (**QoS**) support. In order to meet this demand, high-speed down-link packet access (**HSDPA**) scheme has been designed. HSDPA can provide data transfer speeds up to 10.7Mbit/s on the downlink with a time-slotted code division multiple access (**CDMA**) scheme in a cellular system [102]. Most recently, the long term evolution (**LTE**) format was proposed by NTT DoCoMo of Japan and has been adopted as an international standard. We feel that wireless systems will never cease to evolve.

The scheduling policies and resource allocation schemes are very critical in an HSDPA system. For a time-slotted system, a transmission scheduler is needed to decide which user should be scheduled at each timeslot. In wireless networks, the channel conditions of mobile users are time-varying. If round-robin algorithm is used as the scheduling method, a terminal may be scheduled when its signal is relatively poor. It is clear that the throughput of this terminal may be improved if it can be scheduled when it has strong signal. The opportunistic scheduling policy, first proposed by Liu *et al* for infinite backlog traffic demand in [103], exploits the variation of channel conditions to improve the throughput of a cellular system. The scheduler in the base transmission station (**BTS**) assigns resources to users experiencing better channel conditions while simultaneously maintaining fairness among all the users in the cellular system. The work in [103] shows an improvement in the overall throughput of the system. This has drawn much attention and further papers have been published on opportunistic scheduling. The advantage of opportunistic scheduling is providing better throughput performance. The cost is that opportunistic scheduling needs relatively more data thus scheduling system is more complicated. Other information related to problem formulation can be found in [103]. In [104], the maximum constraints on individual users are first introduced into opportunistic scheduling and an algorithm called gradient algorithm with minimum/maximum rate constraints (**GMR**) is proposed. This algorithm seeks to optimize a concave utility function of the users' throughput subject to certain specified lower and upper throughput bounds. Only memoryless channel model is studied in [104]. A related study on opportunistic scheduling with minimum and maximum constraints under finite-state markov chain (**FSMC**) channel model is presented in [105]. An algorithm called throughput constrained opportunistic scheduling (**TCOS**) is proposed to complement the results in [104]. A more complicated case that combines the opportunistic scheduling and modulation/coding selecting scheme is studied in [106] to further improve the throughput of HSDPA systems.

We believe that there is a strong case to be made for a UE that is served by more than one MT that subscribe to one or more cellular operators. The simple use case is the provisioning for differentiated services on a given network. It could also be a way to amortize capacity. Finally, the desirability of this case arises from the fact that it is indeed possible technologically on existing network infrastructures. There are many instances when a UE being served by multiple MTs may prove to be advantageous.

We would like to mention a few such instances here. First, a person with a laptop and two mobiles may wish to download a file from the Internet. She may want to make the MTs work for this download action together to save downloading time. Second, nowadays, mobile modems (also known as dongles) are being integrated into laptops and laptop like devices (iPAD for example) along with wireless fidelity (**WiFi**) functionality. One or more such devices in co-operation with other mobiles within each other's range can form an ad hoc network. When one of the UEs/MTs needs to download a file, other MTs can, if they are available, help in this process. There are many other possibilities for such cases. For instance, this may be a way to improve QoS and provide for relieving some of the congestion that is occurring on cellular systems for data intensive applications such as video downloads without making significant modifications to existing networks. It may be attractive for cellular providers to use their respective infrastructures in a collaborative manner. We have witnessed many instances of such collaboration in the market-place. We believe that though the actual implementation may result in additional complexity, it is beneficial to consider rather unconventional ways and means to exploit existing infrastructure while simultaneously looking to upgrade it for the next generation of services. Moreover, it is observed that we do not require all these devices to belong to the same person.

Three scenarios were compared: (i) when the MTs are served by the same cellular provider but scheduler has no knowledge of the presence of such UEs; and (ii) when the MTs are served by the same cellular provider and the scheduler located in the BTS knows the presence of such UEs; (iii) when the MTs are from different cellular providers.

We denote those UEs that are served by multiple MTs by UE_Bs (B $>$ 1), for example, see UE_1 in Fig. 2.1. The value of B indicates the number of MTs serving such a UE_B. For example, UE_2 means that this is a UE_B served by two MTs. Similarly,

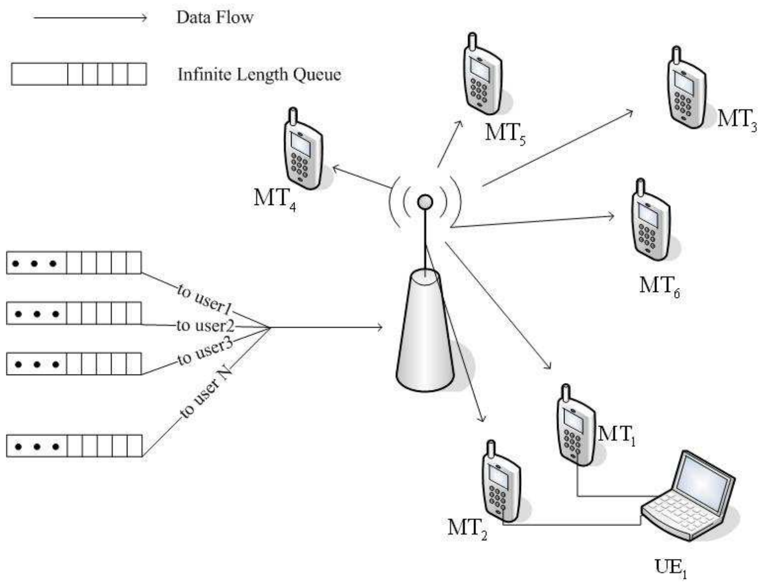

Figure 2.1: System model for downlink cellular network in scenario (i) and (ii).

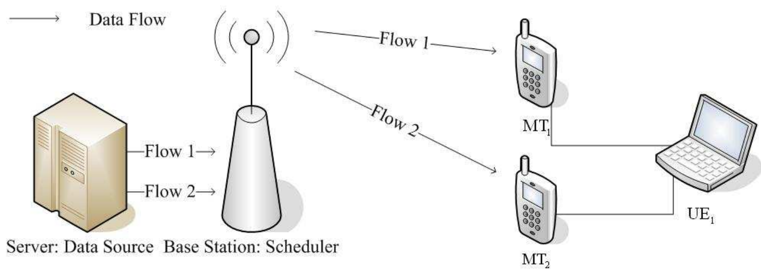

(a) Scenario in which the server divides the data flow.

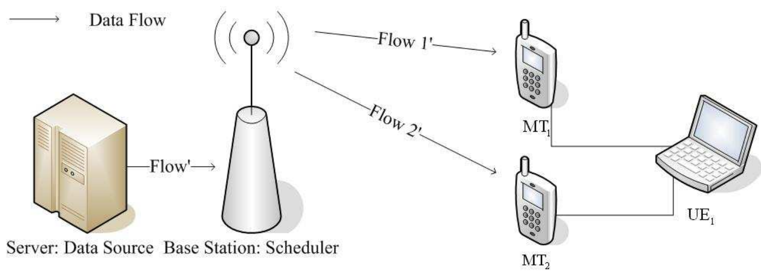

(b) Scenario in which the scheduler divides the data flow.

Figure 2.2: Models for different modes of data flows.

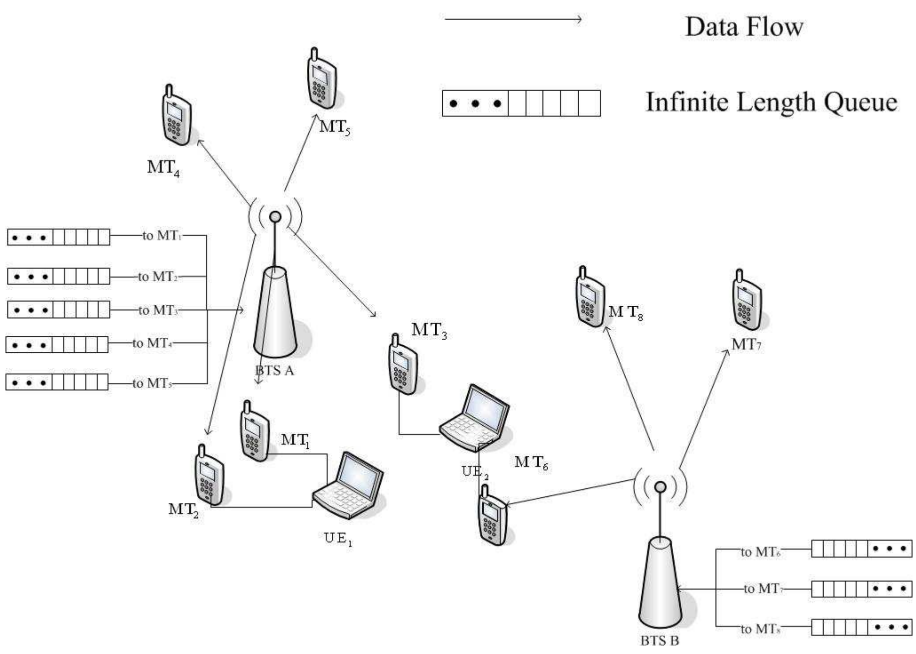

Figure 2.3: System model for downlink cellular network in scenario (iii).

we denote those MTs that serve a UE_B by MT_Bs. For the case B $=$ 1, it is a UE served by a single MT. However, if no additional information about B is given, it is deemed that B $>$ 1. In previous studies on scheduling algorithm, it is always assumed that one UE is only served by one MT. Therefore, even when UE_B (B $>$ 1) exists, the scheduler in the BTS does not use this information. We consider an example to illustrate the differences between the case when the scheduler does not use the information that there are UEs served by multiple MTs and the case when the scheduler uses such information.

In Fig. 2.2(a), the scheduler does not use the information (it may not even have this information) that UE_1 is served simultaneously by MT_1 and MT_2. The server gets data requests from both the MTs. Thus, there are two data flows to the BTS. The scheduler located at the BTS then performs scheduling under certain fairness constraints for MT_1 and MT_2, say assign half the entire time fraction for each of them. This is like an application-layer bandwidth aggregation method as file splitting in Bit Torrent, which does not need any assistance from the BTS. This corresponds to scenario (i).

In Fig. 2.2(b), it is clearly shown that the server sends only one data flow because it gets only one request from UE_1. At the BTS, the scheduler schedules MT_1 or MT_2 for this flow at each timeslot based on their channel conditions. In this case, the fairness constraints are set only for UEs and not for each MT, that is to say the scheduler will assign entire time fractions for UE_1. This may appear to be the same as the first case as both MT_1 and MT_2 are serving UE_1. However, it is quite different because the constraints in the second case are relaxed as compared to the constraints in the first case. An optimal scheduling solution for the overall throughput is presented when there is at least one UE which is served simultaneously by multiple MTs. With the scheduler using more information, SMMTSU provides an improvement in throughput for the UE_Bs (B > 1) and the overall system. This corresponds to scenario (ii).

In Fig. 2.3, A UE_B may be served by multiple MT_Bs from different providers. We assume the probability of a MT being served by certain provider to be 0 (not being served) or 1 (being served). The smart network selection has been extensively studied these years and scheduling algorithms incorporating this promising technique is left for future research. We assume that there is no cooperation between base stations from different cellular service providers. We assume that different schedulers will do scheduling independently. The data flow will be splitting by the scheduler if and only if these MTs are under the service of this scheduler. If the MTs are served by different schedulers, the data flow will be split by data server. The UE_Bs' throughput, when the MT_Bs are served by different cellular providers, is analyzed. We find that it is better to use the service from one cellular provider using SMMTSU rather than to use the services from different cellular providers.

The rest of the chapter is organized as follows. In Section 2.2, our system model is introduced. In Section 2.3, we describe the scheduling problem. In Section 2.4, SMMTSU and its properties are presented. In Section 2.5, we establish numerical results for the system throughput using SMMTSU, opportunistic scheduling algorithm in [103], and round-robin scheme. Conclusions is presented in Section 2.6.

2.2 System Model

In this section, we present the system model. Our work is focused on the downlink scheduling for time-slotted systems and implemented in a single-channel HSDPA system. Consequently, only one MT could be scheduled to transmit at any timeslot for any BTS.

The HSDPA system is a time-slotted system and time is the resource shared among all the users. The time axis in our system is not continuous but divided into equal timeslots. Fast power control is disabled in HSDPA standards [106]. We assume that the transmission power of the BTS is fixed for all timeslots and all the base stations. We do not take the power consumption optimization into consideration in this chapter. An assumption is made that the standards used by all cellular providers are the same. Moreover, different cellular providers should provide services on different bands of frequencies. Therefore, there is no mutual interference between the services of different providers. For any provider, the first ring interference is taken into consideration.

Dynamic modulation and error-correcting codes selecting techniques are used in HSDPA system. The scheduler could select different sets of modulation and error-correcting codes from the set of modulation and coding schemes (**MCS**) based on the channel condition. The MCS is shown in Table 2.1. To simplify the situation and focus on the scheduling issue, we do not consider the error-correcting codes. A periodic channel quality indicator (**CQI**) reporting scheme is included in the specification Release 5 of HSDPA. The definition of the CQI and the CQI reporting

CQI Value	Transport Block Size	Modulation	Data Rate
1	137	QPSK	0.0685
2	173	QPSK	0.0865
3	233	QPSK	0.1165
4	317	QPSK	0.1585
5	377	QPSK	0.1885
6	461	QPSK	0.230
7	650	QPSK	0.325
8	792	QPSK	0.396
9	931	QPSK	0.465
10	1262	QPSK	0.631
11	1483	QPSK	0.7415
12	1742	QPSK	0.871
13	2279	QPSK	0.1140
14	2583	QPSK	1.292
15	3319	QPSK	1.660
16	3565	16-QAM	1.783
17	4189	16-QAM	2.095
18	4664	16-QAM	2.332
19	5287	16-QAM	2.644
20	5887	16-QAM	2.944
21	6554	16-QAM	3.277
22 ~ 30	7168	16-QAM	3.584

Table 2.1: CQI mapping table for UE category 5.

procedures are described in [107]. A UE reports its selected CQI value to BTS periodically. A shorter report cycle results in better throughput though the report overhead and uplink interference are increased [108]. We assume that each UE reports its CQI at the beginning of each timeslot and the overhead of this reporting procedure is ignored. An appropriate SINR-to-CQI mapping is necessary in the HSDPA system. We use the mapping scheme proposed in [109] as follows:

$$\text{CQI} = \begin{cases} 0, & \text{SINR} \leqslant -3.96\ , \\ \lfloor \frac{\text{SINR}}{1.02} + 4.81 \rfloor, & -3.96 < \ \text{SINR} < 26.04\ , \\ 30, & 26.04 \leqslant \text{SINR}\ . \end{cases} \tag{2.1}$$

The unit of signal to interference and noise ratio (**SINR**) is decibel (**dB**). Based on (2.1) we could get the CQI from the SINR. We refer to the CQI mapping table and feasible performance requirement table in [107] and [110] to get the corresponding data rates. We show them together in Table 2.1.

For each of the cellular provider, we assume a single channel case such that only one MT can be scheduled in any timeslot for one BTS. The path-loss variation with distance and slow log-normal shadowing are taken into consideration. Based on the common assumptions for HSDPA in [111], we adopt the following path-loss model:

$$L(x)_{(dB)} = 128.1 + 37.6 log_{10}(x), \tag{2.2}$$

where x is the distance in kilometers between the MT and the BTS. For the shadowing effect, we use the model reported by Gudmundson in [112]. The shadowing term s^k is modeled as a zero-mean stationary Gaussian process given by:

$$E(s^k \cdot s^{k+m}) = \delta^2 \xi_d^{V \cdot m \cdot T_s / d}, \tag{2.3}$$

where ξ_d represents the correlation between two points separated by a distance d, the superscript k indicates the index of a timeslot, T_s is the duration of a timeslot, m is for the time difference represented in the number of timeslots, V is the speed of the MT, and δ is the standard deviation of the Gaussian process.

2.3 Problem Formulation

In this section, we describe the scheduling problem and present our objective function. First, we formulate the problem for single cellular provider scenario. We assume that there are N MTs and M UEs. Our model is described as a time-slotted system and time is the resource shared by all the MTs. Static constant data flows are considered in the formulation. The quantity r_i is used to denote the time fraction assigned to MT_i before the transmission process begins, $\sum_{i=1}^{N} r_i = 1$. k is used to describe the current timeslot and K is the total number of timeslots. We write $\mathrm{MT}_i \in \mathrm{UE}_j$, if MT_i is serving UE_j. $\boldsymbol{D}^k = (D_1^k, ..., D_N^k)$ is defined as the supported rate vector of MTs at timeslot k and the value of each D_i^k must follow the data rates in Table 2.1. $\boldsymbol{R}^k = (R_1^k, ..., R_M^k)$ is the supported rate vector of UEs at timeslot k, which is defined as

$$R_j^k = \max(D_i^k \cdot \mathbf{1}_{\{\mathrm{MT}_i \in \mathrm{UE}_j\}})_{i=1}^{N}. \tag{2.4}$$

$\mathbf{1}_{\{\cdot\}}$ is an indicator function that equals 1 if the condition in the curly brace is true and 0 otherwise. The throughput of MT_i, or γ_i, is defined as

$$\gamma_i = \sum_{k=1}^{K} D_i^k \cdot \mathbf{1}_{\{\mathrm{MT}_i \text{ is scheduled}\}} . \tag{2.5}$$

The throughput of one UE_j, or u_j, is defined as the sum of the throughput of those MTs who are serving this UE and can be expressed as

$$u_j = \sum_{i=1}^{N} \gamma_i \cdot \mathbf{1}_{\{\mathrm{MT}_i \in \mathrm{UE}_j\}} . \tag{2.6}$$

Thus, the UE_Bs' throughput, which is the sum of the throughputs of all the UE_Bs (B $>$ 1), can be represented as $\sum_{j=1}^{M} u_j \cdot \mathbf{1}_{\{\mathrm{UE}_j \text{ is a UE\_B(B>1)}\}}$. The overall system throughput or γ is defined as the sum of the throughputs of all the UEs being served in the system, which is the same as the sum of the throughputs of all the MTs. The fairness constraint is provided by (2.8) and (2.9). In (2.8), it means that the scheduler should serve UE_j at least for duration τ_j. And this should be satisfied for all UEs. In

(2.9), it means we do not consider the fairness constraints separately for MTs serving the same UE. Our objective is to maximize the overall system throughput. The optimization problem P_1 is given by :

$$\gamma^* = \max_Q \sum_{i=1}^{N} \gamma_i = \max_Q \sum_{k=1}^{K} \sum_{j=1}^{M} R_j^k \cdot \mathbf{1}_{\{Q(\boldsymbol{R}^k)=j\}}, \tag{2.7}$$

$$s.t. \quad \frac{\sum_{k=1}^{K} \mathbf{1}_{\{Q(\boldsymbol{R}^k)=j\}}}{\sum_{k=1}^{K} \sum_{j=1}^{M} \mathbf{1}_{\{Q(\boldsymbol{R}^k)=j\}}} \geqslant \tau_j, \ j = 1, 2, \ldots, M, \tag{2.8}$$

where

$$\tau_j = \sum_{i=1}^{N} r_i \cdot \mathbf{1}_{\{\mathrm{MT}_i \in \mathrm{UE}_j\}} \ . \tag{2.9}$$

Q is a policy that determines which UE should be scheduled at a timeslot, and γ is the maximum value of the overall system throughput. If the time is long enough and we pick one timeslot randomly, the left hand side of (2.8) is represented by $P(Q(\boldsymbol{R}) = j)$, which means the probability that this timeslot is occupied by UE_j. For that timeslot, the expectation of the throughput is expressed as $E\left(\sum_{j=1}^{M} R_j \cdot \mathbf{1}_{\{Q(\boldsymbol{R})=j\}}\right)$. The k is dropped because we examine a randomly chosen timeslot. In other words, the analysis is performed on a generic timeslot. The objective function can be simplified as

$$\frac{\gamma^*}{K} = \max_Q E\left(\sum_{j=1}^{M} R_j \cdot \mathbf{1}_{\{Q(\boldsymbol{R})=j\}}\right) . \tag{2.10}$$

$$s.t. \quad P(Q(\boldsymbol{R}) = j) \geqslant \tau_j, \ j = 1, 2, \ldots, M. \tag{2.11}$$

For the multiple cellular providers scenario, each of the providers does this optimization separately because they do not share scheduling information with each other. The performance matrices, overall system throughput, and UE_B (B $>$ 1) throughput, are the same as those in single provider scenario.

2.4 Proposed Solution

In this section, we present an algorithm to solve the problem P_1 in Section 2.3 and then describe some properties of this algorithm.

2.4.1 Scheduling Policy

The following policy Q is optimal for problem P_1 in Section 2.3:

$$Q(R_j^k, v_j^k) = \arg\max_j (R_j^k + v_j^k) \ , \tag{2.12}$$

where the v_j^ks are real parameters used to reach the fairness constraints of the UEs in the system. Here, $\boldsymbol{v}^k$ is defined as $\boldsymbol{v}^k = (v_1^k, ..., v_M^k)$. These parameters could be found using the technique of stochastic approximation in [1]. The fairness constraints and the method to update the v_j^ks are given by:

1. $\min(v_j^k) = 0, \quad j = 1, 2, \ldots, M;$
2. if $P(Q(\boldsymbol{R}) = j) \geqslant \tau_j$, where $\tau_j = \sum_{i=1}^{N} r_i \cdot \mathbf{1}_{\{\mathrm{MT}_i \in \mathrm{UE}_j\}}$, then $v_j^k = 0$, $j = 1, 2, \ldots, M$;
3. $v_j^{k+1} = v_j^k - s \cdot (\mathbf{1}_{\{Q(\boldsymbol{R})=j\}} - \tau_j), \quad j = 1, 2, \ldots, M.$

Here, s is a small constant that indicates a step to track system variations. The scheduler uses the policy Q to determine which UE to schedule. Then, it uses Q^* to schedule the best performing MT serving that scheduled UE. SMMTSU is the combination of Q and Q^*. For processing SMMTSU, the following steps are taken:

1. Use Q to determine which UE should be scheduled based on $\boldsymbol{R}^k$ and $\boldsymbol{v}^k$;
2. Use Q^* to determine which MT should be scheduled based on Step 1 and $\boldsymbol{D}^k$.

Since no fairness requirement exist among MTs serving the same UE, the constraint is loosed as compared to the case when fairness is considered for MTs serving the same UE. Intuitively, the performance must be better or at least the same.

2.4.2 Policy Properties

Proposition 2.1: For any cellular provider, the policy defined in Subsection 2.4.1 is the optimal solution to the problem P_1. It maximizes the overall system throughput and satisfies the long-term minimum throughput constraints for each UE.

It is easy to prove based on the work of [1]. If we change the subject investigated and constraints from mobile to user equipment, this problem can be re-written in a form similar to that in [1]. Generally, it provides a better overall throughput for relaxing the constraints of the optimization problem in [1]. For the proof, please refer to Appendix A.1.

Proposition 2.2: For any cellular provider, the throughput of the UE_B (B $>$ 1) is improved under SMMTSU as compared to the [1] and the Round Robin scheme.

Here, the throughput of the UE_B (B $>$ 1) is defined in Section 2.3 as the sum of the throughput of those MTs who are serving this UE_B. We establish the correctness of the proposition as follows. Recall that Q and Q^* represent the SMMTSU scheduling policies in UE and MT level, respectively. Moreover, $Q^{'}$ and $Q^{\sharp}$ are used to represent other scheduling policies in UE and MT level. The benefit of using SMMTSU as compared to other scheduling policies is that the UE_B can harvest the data rate differences between the serving MTs. A 2-MT case, which means there are only 2 MTs in the system, is used to illustrate the correctness of this proposition. We assume that MT_1 and MT_2 are serving the same UE_1. We define

$$C_j^k = \sum_{i=1}^{N} D_i^k \cdot \mathbf{1}_{\{\text{MT}_i \in \text{UE}_j\}} \tag{2.13}$$

as the performance ability of UE_j. Combining with $\mathbf{1}_{\{Q^*=i\}} + \mathbf{1}_{\{Q^* \neq i\}} = 1$, we have

$$E\left[C_1\right] = E\left[\sum_{i=1}^{2} D_i \cdot \left(\mathbf{1}_{\{Q^*=i\}} + \mathbf{1}_{\{Q^* \neq i\}}\right)\right]. \tag{2.14}$$

Rewrite this equation,

$$E\left[\sum_{i=1}^{2} D_i \cdot \mathbf{1}_{\{Q^*=i\}}\right] = E\left[C_1 - \sum_{i=1}^{2} D_i \cdot \mathbf{1}_{\{Q^*\neq i\}}\right] . \tag{2.15}$$

For $Q^{'}$ and $Q^{\sharp}$, a similar result can be gained as

$$E\left[\sum_{i=1}^{2} D_i \cdot \mathbf{1}_{\{Q^{\sharp}=i\}}\right] = E\left[C_1 - \sum_{i=1}^{2} D_i \cdot \mathbf{1}_{\{Q^{\sharp}\neq i\}}\right] . \tag{2.16}$$

We notice that

$$E\left[D_i \cdot \mathbf{1}_{\{Q^*\neq i\}}\right] \leq E\left[D_i \cdot \mathbf{1}_{\{Q^{\sharp}\neq i\}}\right] , \tag{2.17}$$

as the scheduling policy $Q^{'}$ and $Q^{\sharp}$ do not use the information of the existence of UE_B. Thus the scheduler still keeps fairness between the MTs. It means $Q^{\sharp} \neq i$ does not guarantee that MT$_i$ is the worst performing MT in this 2-MT example. However, with SMMTSU, the scheduler is only limited to the fairness constraints in the UE level, which means no constraint for individual MTs in this 1-UE scenario. From (2.15), (2.16) and (2.17), we get

$$E\left[D_i \cdot \mathbf{1}_{\{Q^*=i\}}\right] \geq E\left[D_i \cdot \mathbf{1}_{\{Q^{\sharp}=i\}}\right] . \tag{2.18}$$

For the reason that $Q^{'}$ and $Q^{\sharp}$ are not specified, the result that Q and Q^* outperform $Q^{'}$ and $Q^{\sharp}$ in terms of the UE_Bs' throughput supports this proposition.

Proposition 2.3: For any cellular provider, when all MT_Bs (B $>$ 1) simultaneously serving certain UE_B have the same data rate and this situation occurs for all UE_Bs, the overall system throughput reaches its minimum value.

When data rates of the MT_Bs serving the same UE_B are in the same value, the scheduler cannot gain benefit from using the best performing MT for the system. For the proof, please refer to Appendix A.2.

Proposition 2.4: For any cellular provider, for the case when the value of B for all UE_Bs (B $>$ 1) are the same, the overall system throughput is improved as the number of UE_Bs is increased.

The proof can be described in following way. We define

$$\overline{\boldsymbol{R}}_j^k = \{D_i^k \cdot \mathbf{1}_{\{\mathrm{MT}_i \in \mathrm{UE}_j\}}\}_{i=1}^N - \{R_j^k\} \tag{2.19}$$

as a vector consisting of the data rates of those MTs serving the UE_j excluding the one which is scheduled at timeslot k. Based on the proof in Appendix A.2, we know that the source of throughput improvement of SMMTSU as compared to the scheduling scheme in [1] is

$$E\left[(m_j - 1) \cdot R_j \cdot \mathbf{1}_{\{Q=j\}} - \mathrm{sum}(\overline{\boldsymbol{R}}_j \cdot \mathbf{1}_{\{Q=j\}})\right], \tag{2.20}$$

which is non-negative. Here, we define $\mathrm{sum}(\cdot)$ as a function which gets the summation of all the items of a set. Increasing the number of UE_Bs creates more such terms which directly leads to an improvement in the throughput.

Proposition 2.5: For the multiple cellular providers scenario, the UE_Bs' throughput when the MT_Bs are from the same cellular provider using SMMTSU is better than the throughput when the MT_Bs are from different cellular providers.

This scenario is shown in Fig. 2.3 and the overlaid networks are shown in Fig. 2.4. The cells are ideal hexagons. Two cellular providers, A and B, are assumed in the system. A and B own their independent downlink channels. The relative locations or distances between BTS_A and BTS_B are unknown (but distances between BTS_As are the same). Another assumption is the different cellular providers are under the same load. Moreover, the expectation of a MT's supported data rate at certain timeslot depends on its location and the channel variation. The main difference of having multiple providers as compared to single provider is that different providers do not cooperate in the scheduling process and cannot benefit from the information of the existence of UE_B. A 3-MT case is taken as example to illustrate this difference. It is assumed that MT_1, MT_2 and MT_3 are serving UE_1. If all three MTs are served by A, when one of them is scheduled it must be the best performing MT at that very

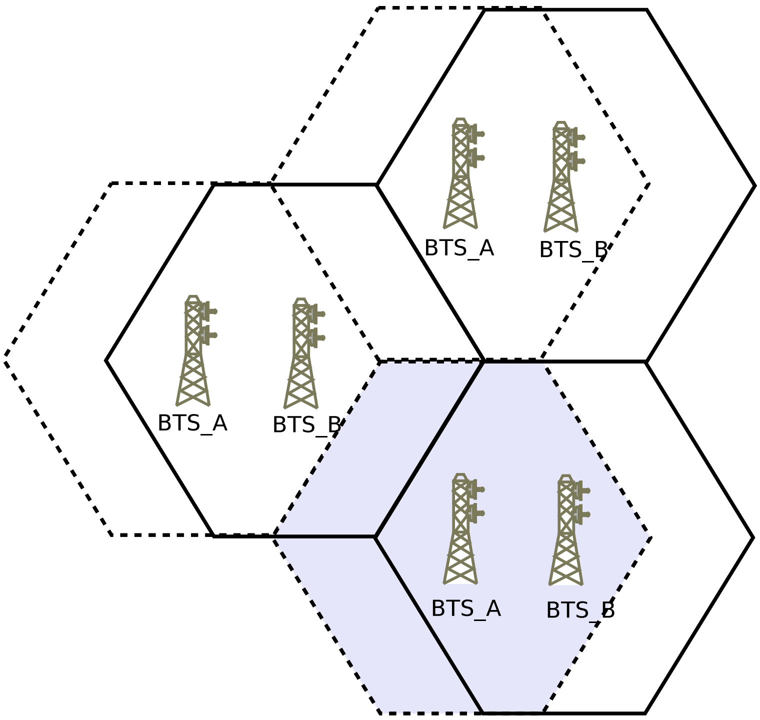

Figure 2.4: Cellular networking model with multiple service providers.

moment. This is the advantage of SMMTSU. However, if MT_1 and MT_2 are served by A and MT_3 is served by B, A and B will do the scheduling independently. Thus, UE_1 can only benefit from the data rate gap between MT_1 and MT_2.

We would like to emphasize the meaning of this proposition. It means that the throughput of a UE_B is expected to be larger when it chooses its MT_Bs from the same cellular provider, no matter how the two cellular networks are overlaid. For the proof, please refer to Appendix A.3.

2.5 Numerical Results

In this section, we first study the case of throughput with one cellular provider. We present simulation results for both the overall and UE_Bs' throughput improvement achieved by SMMTSU as compared to the scheduling algorithm in [1] and the Round

Cell Radius	1500 m
Reuse Factor	3
MT Number	100
Transmission Power	40 dBm
Propagation	$128.1 + 37.6log_{10}(d)$
Scheduling Slot Duration	2 ms
MT Speed	3.6 km/h and 90 km/h
MT Channel Estimation	Perfect
MT Thermal Noise	-174 dBm/Hz
MT Simulation Duration	200 s

Table 2.2: Simulation parameters for SMMTSU.

Robin scheduling scheme. The difference between above three algorithms is shown in Fig. 2.5. Then, we show the throughput results under the worst case with SMMTSU. All the r_is are set to be $\frac{1}{N}$ where N is the number of the MTs to do the comparison between SMMTSU and the Round Robin scheme. An assumption is made that the MTs serving a certain UE are not changed for the duration and the list of UEs served by MTs is updated at the beginning of the simulation. We further study the scenario when the MTs serving the same UE come from different cellular providers. With different providers having no information that the UEs are served by multiple MTs, the servers takes the responsibility to divide the data flows. Comparisons are done between SMMTSU and the scheme in [1]. The simulation parameters are summarized in Table 2.2. All UEs take random walk movement model. For all the data flows, the flow rates are fixed in the simulation.

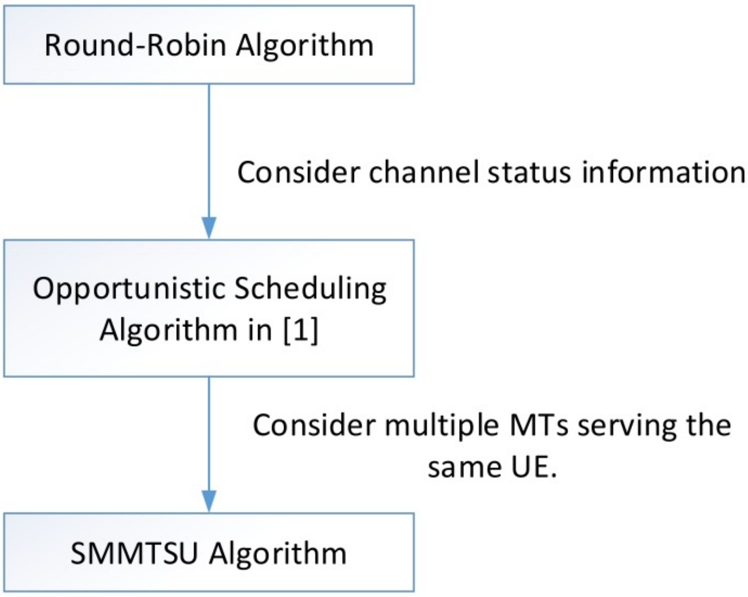

Figure 2.5: Difference between scheduling algorithms.

2.5.1 Overall System Throughput Improvement

For this subsection, we study the scenarios (i) and (ii), which means that all the MTs are from the same cellular provider.

In Fig. 2.6(a), we present the overall throughput improvement with different numbers of UE_2s. It shows that the overall throughput improvement under SMMTSU is generally 20% over the Round Robin scheme. And there is a clear trend of overall throughput improvement with more UE_Bs, which is consistent with *Proposition 2.4*. It is also shown that in the worst case the overall throughput under SMMTSU is approximately the same as the scheduling scheme in [1]. The reasons are explained in *Proposition 2.3*. In Fig. 2.6(b), when the numbers of MT_Bs are same, fewer UE_Bs bring more throughput improvement. We can take the case with 12 MT_Bs as an example. It is seen that the overall throughput improvement ratio for the case when there are 3 UE_Bs is about 7%, but the improvement ratio for the case when there are 6 UE_Bs is only 4%. This situation is the same for all the simulation

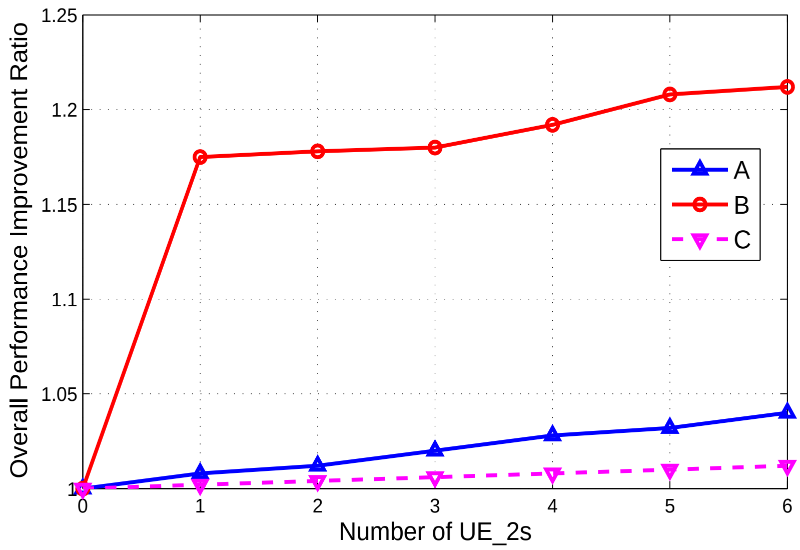

(a) Overall system throughput improvement ratio with different numbers of UE_2s. A: overall throughput improvement ratio as compared to the scheduling scheme in [1]. B: overall throughput improvement ratio as compared to Round Robin scheme. C: overall throughput improvement ratio as compared to the scheduling scheme in [1] in the worst case.

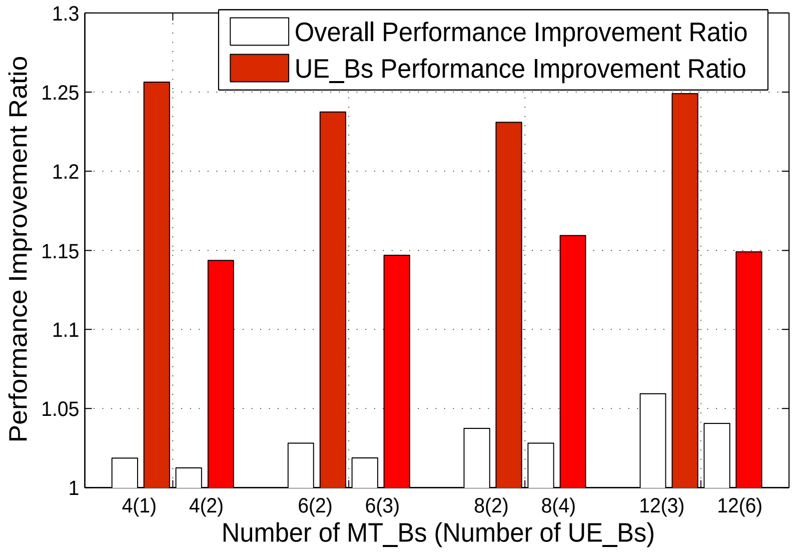

(b) Throughput improvement ratio of SMMTSU as compared to the scheduling scheme in [1] with the same number of MT_Bs and different numbers of UE_Bs.

Figure 2.6: Improvement of throughput performance without mixed UE_Bs.

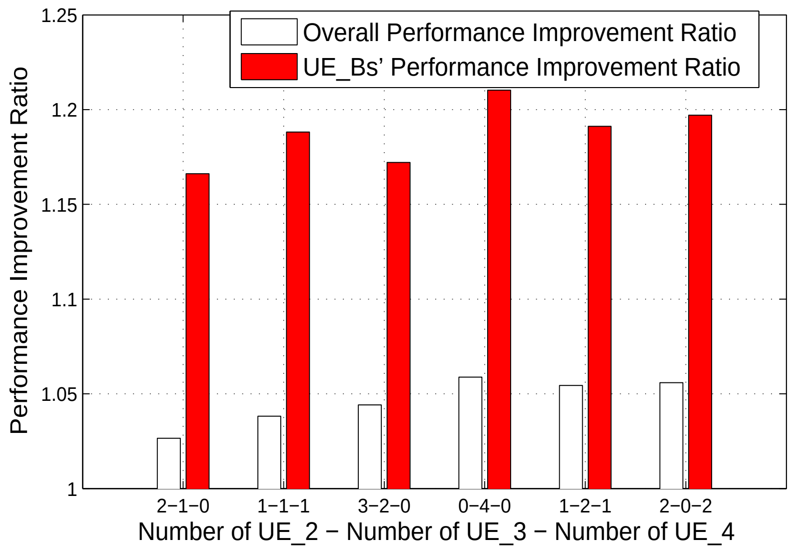

Figure 2.7: Improvement of throughput performance with UE_2, UE_3 and UE_4 coexisting.

results. It is because with one UE_B being served by more MTs, the difference of data rates among all MT_Bs may be larger. Therefore, there may be additional benefits that the scheduler could gain from these gaps.

In Fig. 2.7, the cases where UE_2, UE_3 and UE_4 co-exist are studied. In the real world, UE_2s, UE_3s and UE_4s may coexist. The simulation is also done for this case and the results are shown here. Generally, there is a 4% throughput improvement. For the case 2-1-0, we know that the number of UE_Bs and MT_Bs are 3 and 7, respectively. Both the number of MT_B and UE_B are the smallest among all the cases, which leads to the smallest throughput improvement ratio. The result can be understood for there are the fewest users benefiting from SMMTSU. For the cases 1-1-1 and 3-2-0, there are 9 MT_Bs in both. With fewer UE_Bs, the throughput improvement ratio becomes larger. Moreover, for the last three cases in Fig. 2.7, both the number of UE_Bs and MT_Bs are the same. There is no easy way to judge which combination of MT_Bs may provide larger throughput improvement ratio, but

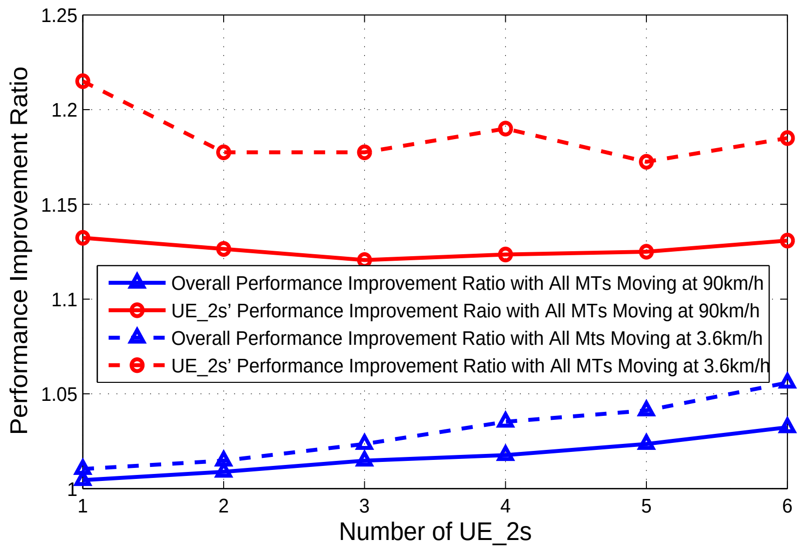

Figure 2.8: Improvement of throughput performance in mobile scenarios.

generally speaking, if the number of MT_Bs is kept unchanged, then more UE_Bs leads to worse improvement ratio; if the number of UE_Bs keeps unchanged, then more MT_Bs leads to more improvement ratio. In our simulation, the throughput improvement ratios are very similar for the last three cases, however, we argue that the same numbers of UE_Bs and MT_Bs do not always lead to this kind of result. From this figure, we could know that our scheduling policy can improve the overall throughput for the case where different kinds of UE_Bs coexist.

In Fig. 2.8, we study the effect of different speeds on SMMTSU. We can see that SMMTSU works better with all MTs moving at lower speed. It is already well explained that SMMTSU mainly benefits from the different data rates among the MT_Bs serving the same UE_B by opportunistically scheduling the MT_B with best propagation state. In Section 2.2, the propagation and channel model are shown and $s(0)$ is generated by the random function based on $s(k) \sim N(0, 4.3)$ in our simulation. A stationary Gaussian process is determined by its expectation $E\{s(k)\}$ and autocorrelation $R\{s(k)\}$. We could represent the conditional expectation of $s(k)$

as:

$$\begin{cases} E\{s(k+m)|s(k)\} = \frac{R(m)}{R(0)} \cdot s(k) , \\ R(m) = \delta^2 \cdot \xi_d^{m \cdot T_s \cdot V/d} . \end{cases} \tag{2.21}$$

V is the speed of the MT, and T_s is the duration of a timeslot. We could know from (2.21) that the shadowing effect will be larger as the speed of the MTs increases. As the shadowing factor gets larger, the channel gets worse thereby leading to smaller CQI values. Based on [107] and [110], the data rates of the MTs are much smaller with lower CQI values. With all the MTs working in lower data rates, it is obvious that the data rate differences among the MT_Bs serving the same UE_B will be smaller. In this case, the possibility of SMMTSU to provide any benefit from the differences is smaller. In Fig. 2.8, it is shown that SMMTSU improves the throughput of both kinds of UE_Bs, however, SMMTSU works better with the UE_Bs moving at smaller speed.

We conclude that, SMMTSU can improve the overall throughput of the cellular system under different speeds and different kinds of UE_Bs.

2.5.2 UE_Bs' Throughput Improvement

In our scheduling scheme, we provide the scheduler with the knowledge that there are UEs served by multiple MTs and study how much throughput improvement the UEs may gain from such knowledge. Based on our analysis and the simulation, the key advantage of SMMTSU is that it improves the UE_Bs' throughput as compared to [1].

We first study the scenarios with only one cellular provider. In Fig. 2.6(b), we see from the grey bars that if the number of MT_Bs is constant, more UE_Bs leads to smaller throughput improvement. This is because with the UE_Bs served by more MTs, the variance of the MT_Bs' data rates may become larger. Therefore, the system has more opportunities to benefit from this difference. In Fig. 2.7, the case when UE_2, UE_3 and UE_4 coexist is studied. It is shown that the throughput improvement ratios

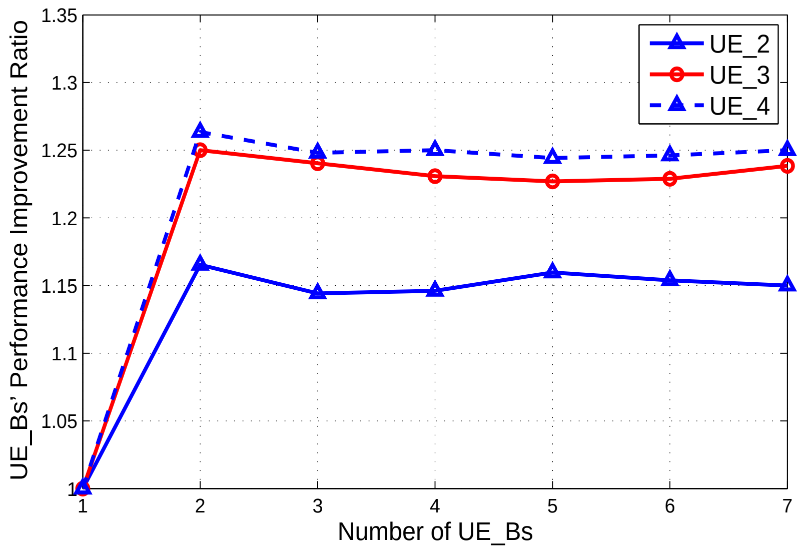

Figure 2.9: Comparison of UE_Bs' throughput performance between SMMTSU and the scheme in [1].

are generally from 15% to 20%. Again, like what we analyze in last subsection, we cannot easily tell which combinations of MT_Bs provide better throughput just based on the numbers of UE_Bs and MT_Bs. However, we still can know from this figure that SMMTSU can improve the UE_Bs' throughput for the case when the different types of UE_Bs coexist.

In Fig. 2.8, the throughput improvements of UE_Bs at different speeds are studied. In this case, all the MTs are moving at the same speed, i.e. 3.6 km/h or 90 km/h. It is clear that both kinds of UE_Bs benefit from SMMTSU. To further analyze the simulation result, we see that SMMTSU works better when all the MTs are moving at 3.6 km/h. The reasons are the same as explained for the overall system throughput in last subsection. In Fig. 2.9, throughput improvement of SMMTSU over the policy in [1] is studied under different numbers of UE_Bs. It is seen that the throughput improvement ratio of UE_3 and UE_4 is around 25%. We also find that the improvement ratio is steady for each line after the first UE_Bs' appearance, which means each UE_B gains similar throughput improvement.

In Fig. 2.10(a), the UE_Bs' throughput for the case when the MTs may be served by different cellular providers is compared to that when the MTs are served by the same cellular provider. We assume that SMMTSU is used within the same cellular provider. It is also assumed that the communication load and signal quality are the same for both of the cellular providers. Case 1(1) and 2(1) are taken as examples. We can see that there is about 8% throughput improvement benefit for both cases if MT_Bs are served by the same cellular provider. We conclude that having all the MT_Bs under services of the same cellular provider is the best strategy. We also examine how the speeds affect the UE_B throughput when MTs are served by different cellular providers in Fig. 2.10(b). The results are similar to the case when MTs are from the same provider. Our results suggest the cellular providers may use SMMTSU as their scheduling policy which may help to attract more users.

In Fig. 2.11, the UE_Bs' (B $>$ 1) throughput is compared to the UE_1 in different cases. With SMMTSU, the base station can opportunistically schedule the best performing MT_B which is serving the UE_B (B $>$ 1). Thus, UE_B (B $>$ 1) is expected to get a throughput larger than the sum of the throughputs of those MT_Bs working individually. This is what we have explained in *Proposition 2.2*. If we use U_{avg} to denote the average throughput of UE_1, the average throughput of UE_2 is expected to be larger than $2 \cdot U_{avg}$ and that of UE_3 is expected to be larger than $3 \cdot U_{avg}$. Similar results are expected for UE_Bs with other values of B. In Fig. 2.11, we show the simulation results that match with our analytical results. We see that the throughput of UE_2 is around 2.2 times that of UE_1. For UE_3 and UE_4, even greater benefit is gained from SMMTSU. Thus, there is motivation for people to use UE_B (B $>$ 1) than UE_1 to get better service with larger average throughput for their UEs.

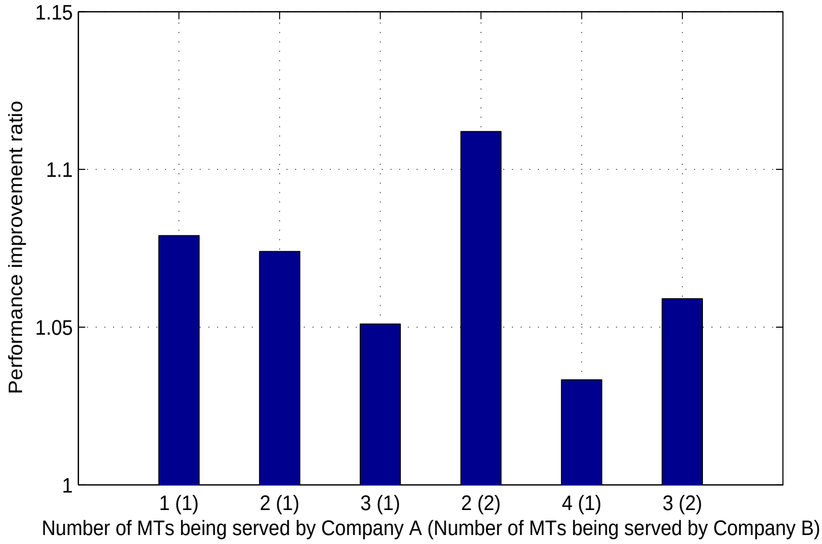

(a) UE_Bs' throughput improvement ratio between MTs are from different cellular providers and the same cellular provider.

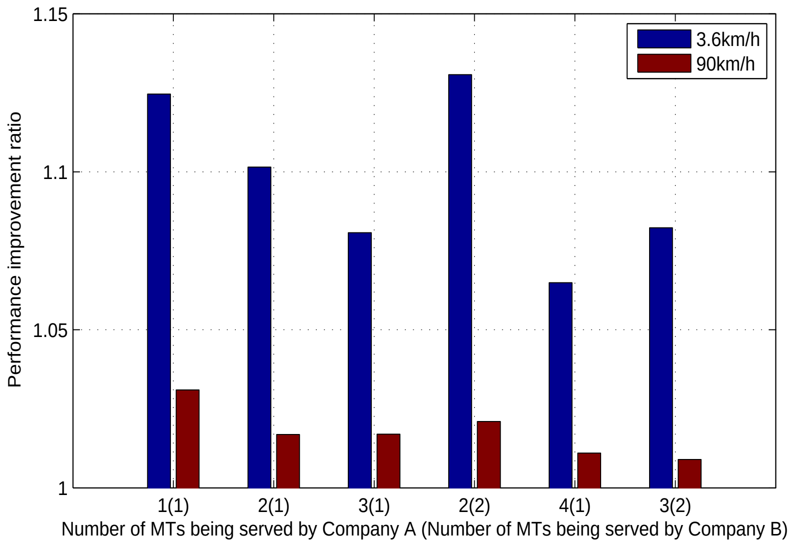

(b) UE_Bs' throughput improvement ratio between MTs are from different cellular providers and the same cellular provider under different speeds.

Figure 2.10: UE_Bs' improvement of throughput performance with multiple service providers.

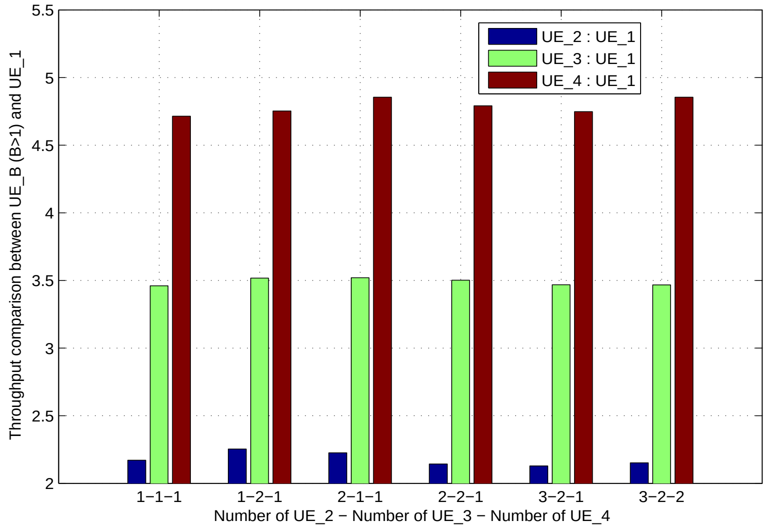

Figure 2.11: Comparison of throughput performance between UE_B (B $>$ 1) and UE_1.

2.6 Chapter Summary

In this chapter, we have presented a new downlink opportunistic scheduling algorithm named SMMTSU for the case when a cellular system consists of UEs served by multiple MTs with the objective of improving the overall system throughput. We first study the single channel case with all the MTs being served by the same cellular provider. We simulated SMMTSU for the HSDPA system model and showed that the algorithm proposed here results in an improvement in the overall system throughput along with positive effect on the throughput of UEs served by multiple MTs. We notice that usually there are more than one cellular provider providing the cellular communication services and study the scenario when the MTs serving the same UE may be served by different cellular providers. We prove that it is better to use the service from one cellular provider under SMMTSU rather than using the service from different cellular providers. We conclude that SMMTSU is an efficient policy for downlink scheduling. It is duly noted that we don't take packet-level delay into consideration. Hence, this algorithm may be better suited for the case of best effort downloading or file transferring. However, with the increased data rate, the downloading delay for the entire file is also expected to be reduced.

Chapter 3

Link Scheduling for 60 GHz WPANs with Cooperative Transmission

In this chapter, the topic of cooperative link scheduling for 60 GHz wireless personal area networks (**WPANs**) is investigated. With using beamforming antennas, 60 GHz WPANs are able to provide larger spatial reuse as compared to omni-directional networks. To further explore the high spatial reuse property, we propose a node cooperation scheme to improve throughput of 60 GHz WPANs. Two scenarios are studied based on the demand for data communication. The first scenario is that all devices' transmission demands can be met in the current frame. The second scenario is that some devices' transmission demands may not be met in the current frame due to time limit. The throughput maximization problems of these scenarios are formulated as linear programming problems. Optimal solutions are provided based on the column generation method. Simulations are performed for scenarios with devices using either realistic or ideal antenna models. The results demonstrate that cooperative transmission scheme can significantly improve throughput performance as compared to its non-cooperative counterparts.

3.1 Introduction

60 GHz directional communication technology offers various advantages over the conventional omni-directional communication systems, such as higher spatial reuse and large unlicensed bandwidth. It is believed to be one of the most promising technologies to provide gigabit wireless indoor communication. Currently, the most popular usage of 60 GHz technology is to build WPANs, which are small networks for wireless indoor services. These small networks provide wireless indoor services, such as wireless display, distribution of HDTV and rapid upload/download [113]. Before reaping benefits from 60 GHz transmission, the following issues have to be handled. First, 60 GHz band suffers from significant free space propagation loss, generally 20 dB more than that in 5 GHz band [114]. Second, the strongest component of 60 GHz transmission tends to be line-of-sight (**LOS**). Thus, 60 GHz transmission is vulnerable to long distance and obstacles between transceivers. The intuitive motivation is to use multiple links with faster rate to replace a single direct link with lower rate.

Fig. 3.1 illustrates the aforementioned issues. In Fig. 3.1(a), there are 11 devices (**DEV**s) in the WPANs. One DEV is selected as the piconet coordinator (**PNC**) and performs link scheduling for each WPAN. Wireless links are represented by arrows with index on them. $Flow_{(i,j)}$ is an end-to-end data flow with the source destination pair DEV_i-DEV_j. $L_{(1,5)}$ is a feasible direct route for $flow_{(1,5)}$, but $L_{(1,5)}$ may not be the best choice for $flow_{(1,5)}$ due to the long distance between DEV_1 and DEV_5. In Fig. 3.1(b), $L_{(9,11)}$ is a feasible direct route for $flow_{(9,11)}$, but a crowd of people standing between the transceivers block the LOS direction of $L_{(9,11)}$. Cooperative transmission means DEVs may relay data frames for neighbors, which is a promising approach to tackle the aforementioned problems. In the first example, if $flow_{(1,5)}$ goes through the multi-hop route $L_{(1,2)}/L_{(2,4)}/L_{(4,5)}$, higher throughput may be achieved with shorter distance

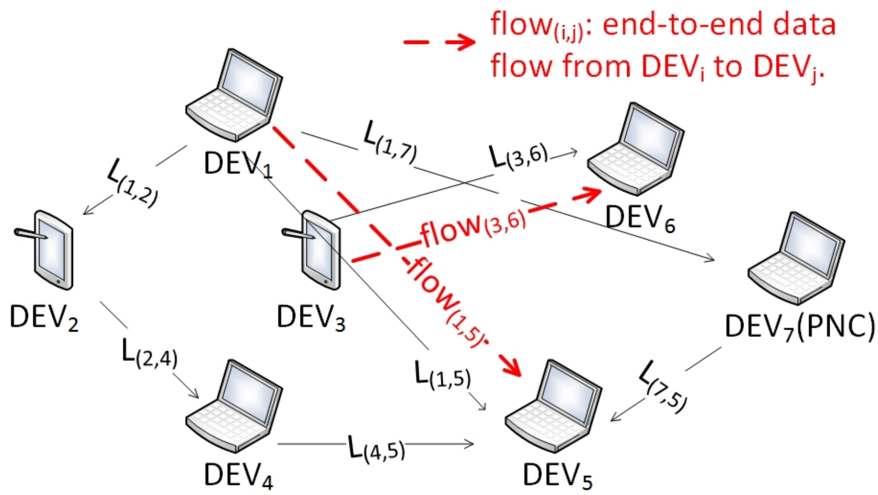

(a) A WPAN with long direct links.

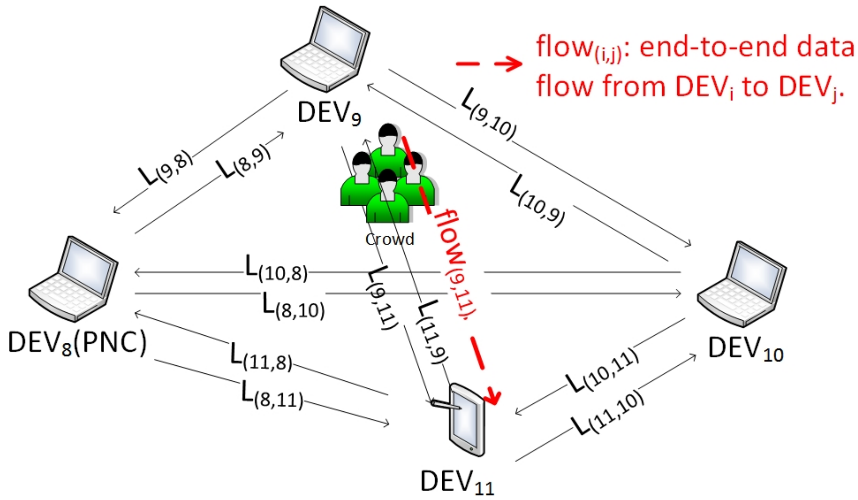

(b) A WPAN with direct links being blocked.

Figure 3.1: WPAN models. (Piconet coordinator (**PNC**) is the scheduler. Devices (**DEV**s) are denoted by DEV_1 to DEV_{11}. $\mathrm{L}_{(i,j)}$ is a wireless link from DEV_i to DEV_j.)

of each hop. In the second case, if $flow_{(9,11)}$ uses route $L_{(9,8)}/L_{(8,11)}$, it may avoid being blocked and have a higher throughput.

In this work, a cooperative transmission scheme is proposed for 60 GHz WPANs. Cooperation strategy is defined as the scheme to arrange relays and schedule transmission for WPANs. We study two scenarios: i) achievable data demand; and ii) bursty data demand. Given that each frame has a maximum length, achievable data demand means that all demand for data communication can be completed within the current frame, while bursty demand means that some devices' demand may not be met in the current frame. Both scenarios may be observed in real applications. For instance, demand is achievable when people watch some real time online video, since data is generated sequentially; demand may be bursty, when people do some best-effort downloading task, since data is already there.

Numerous simulations are performed to provide guideline for real protocol design. Effect of beam-widths, flow rates and other factors are examined under both ideal and practical antenna models. Comprehensive performance analysis is provided for different spatial reuse strategies. The minor-lobe effect of practical antenna model is incorporated and the proposed optimal solutions are compared with existing benchmarks. The cooperative approach proposed in this work can also be extended to other kinds of networks using directional antenna.

The chapter is organized as follows. In Section 3.2, the related works are reviewed. In Section 3.3, the system model is provided. In Section 3.4, the problem formulation is presented. In Section 3.5, the solutions of the problems are described. In Section 3.6, the numerical results are given. The last section concludes this chapter.

3.2 Related Work

A brief literature review on cooperative link scheduling in 60 GHz networks is provided in this section.

The research on link scheduling in 60 GHz networks starts with no cooperation or relay service being considered. The optimal scheduling problem under fairness constraints in 60 GHz network is solved in [46]. Then, a few heuristic sub-optimal scheduling algorithms are provided. In [40], an exclusive region based scheduling algorithm is proposed based on perfect channel information. In [33], the authors propose a spatial reuse strategy which can schedule multiple transmissions appropriately based on beamforming information. In [31], a graph coloring-based heuristic scheduling algorithm is proposed to reduce overall transmission time. Besides aforementioned algorithms, a protocol is designed for 802.15.3c based WPANs to exploit spatial reuse in [29].

However, researchers recognize that direct links may not possess strong signal quality in 60 GHz networks due to the large path loss and possible blockages [34]. Cooperative transmission is proposed to solve this problem, which means the neighboring devices may relay data frame for each other. The idea of using relays is not new in the field of omni-directional networks. In [54, 115–118], different cooperative transmission schemes are proposed for the omni-directional cooperative ad hoc, cellular and mesh networks. The framework of using column generation in capacity maximization is described for omni-directional networks in [119].

Then, study on cooperative transmission is extended to directional networks, but data frames are assumed to be relayed for at most one time. This means no multihop (more than two hop) transmission is allowed. Cooperative transmission with dedicated relays for each source device is studied in [43, 44, 59, 60], and demonstrates better throughput performance than non-cooperative transmission. Moreover, a cooperative medium access control protocol is proposed for 60 GHz WPAN based on optimal beamforming information in [120]. However, we know that one-hop relay generally may not provide best relay service.

Therefore, cooperative transmission with multihop relay service is studied. In [42], joint routing and scheduling problem is investigated in multi-hop directional wireless mesh networks, but relay is only used if the destination cannot be reached by direct links. Since WPANs are small networks, devices can reach each other while some long-distance links possess poor rates. If the method in [42] is used, no cooperative transmission will appear in WPANs. However, the overall throughput may be poor, if the low-rate links are scheduled. In [45], the authors examine joint link scheduling and routing for 60 GHz wireless mesh networks. They propose heuristic algorithms for this problem and perform extensive simulations. Again, direct links are used by default as long as they exist.

Observing above issues, the researchers raise that PNC should decide whether to use cooperative or direct transmission based on current channel status in 60 GHz WPANs. In [2, 37, 38], heuristic algorithms are proposed for scheduling cooperative transmission in 60 GHz WPANs. However, link scheduling is performed only after relay assignment being done ahead. It is known that separate consideration of relay assignment and link scheduling may not provide the optimal end-to-end solution. In our previous work [98], we consider the multi-hop relay assignment and link scheduling problem jointly in 60 GHz WPANs. The throughput maximization problem is formulated as linear programming problems and the optimal solution is provided. In [98], we assume that the demand of data from all sources can be transmitted within current frame. Observing that the demand may not be completed in current frame due to network capacity, throughput maximization problem with bursty demand is studied in this work. Link scheduling and relay assignment are jointly considered for 60 GHz WPANs. And multihop relay service is provided for links which possess weak signal strength. Besides, more comprehensive performance analysis are provided to verify the proposed cooperative transmission scheme.

3.3 System Model

In this section, information about system model, antenna model and channel model is provided.

3.3.1 Network Model

A centralized 60 GHz WPAN consisting of a PNC and multiple peer DEVs is considered as illustrated in Fig. 3.1(a). Each DEV is assumed to be equipped with one single electronically steerable directional antenna, i.e., the antenna that is able to direct its beam towards other DEVs for transmission or reception. As WPAN is a small network, all DEVs are assumed to be within other DEVs' transmission range. In addition, we assume slotted transmission, i.e., one slot for one frame. Since we focus on scheduling algorithms, a general frame structure as [31] is used as shown in Fig. 3.2. One device is selected as the PNC. The PNC polls transmission requests and pushes the schedules to the DEVs during the control period. It then performs scheduling for the conflict-free data transmission during data transmission period (**DTP**). The length of DTP is assumed to be adaptive with a maximum value T. Next frame may start right after the current one ends.

Based on traffic demands, we examine two scenarios. First, if all DEVs' data traffic demand can be finished in the current frame, we say that it is achievable data demand. In this case, PNC tries to minimize the transmission time. An instance of such a scenario occurs when DEVs are using online video streaming service and communication with achievable data rates appears in WPANs. Second, if some

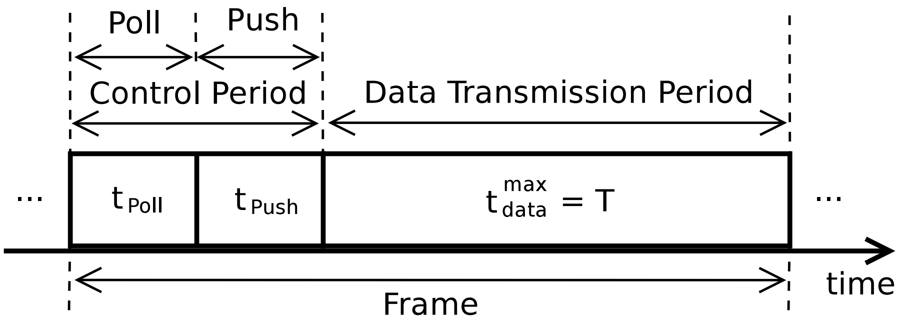

Figure 3.2: Frame structure.

DEVs' data traffic demand may not be fulfilled within current frame, we say that there is bursty data demand. In this case, PNC tries to maximize amount of received data within current frame. An instance of such a scenario occurs when DEVs in WPANs conduct best effort downloading service and a bunch of data is to be delivered from server side. Adaptive rates are used for the data transmissions in the 802.11ad 60 GHz WPAN standard [121]. Channel status of links are assumed to be the same during one frame and PNC can obtain this information as assumed in [2, 116, 117].

3.3.2 Antenna and Channel Model

To be consistent with the most popular standard in 60 GHz WPAN and make it easier for other researchers to compare, the antenna model in [121] is adopted to approximate a practical antenna, which is

$$\begin{cases} \text{main-lobe gain: } G_m = 10log_{10}(\frac{1.6162}{sin(\alpha/2)})^2; \\ \text{side-lobe gain: } G_s = -0.4111 \cdot ln(\alpha) - 10.579, \end{cases} \tag{3.1}$$

where α is beamwidth. G_s is set to zero for ideal antenna model. The Friis equation (in dB) as in [121] is used as propagation model and power is in the log sense:

$$P_R(\alpha, f, d, \sigma) = P_T + G_T(\alpha) + G_R(\alpha) - L(f, d, \sigma), \tag{3.2}$$

where f is frequency and d is distance. P_T and P_R denote the transmission and reception power, respectively. G_T and G_R denote the transmitter's and receiver's antenna gains, respectively. $L(f, d, \sigma)$ represents pathloss. σ is shadow fading factor normally distributed with standard deviation 1.5 dB.

$$L(f, d, \sigma) = 32.5 + 20lg(f) + 20lg(d) + \sigma. \tag{3.3}$$

3.3.3 Spatial Reuse Strategy

Three spatial reuse strategies are i) conservative strategy for ideal antenna model: two links can coexist when devices from one link are not in the main-lobe sectors of the devices from the other link; ii) aggressive strategy for ideal antenna model: two links can coexist when devices from different links do not direct their main-lobe sectors towards each other at the same time; and iii) impartial strategy for practical antenna model: whether two links may coexist or not is determined by capture effect based on signal-to-noise ratios (**SNR**) under physical interference model.

The reason we study these strategies is as follows. First, perfect SNR information is difficult to collect in real environment so spatial reuse strategy is usually based on relative location information. Performance gap between i) and iii) is largely due to imperfect information. Second, minor-lobe is ignored in ideal antenna model. Thus, the performance gap between ii) and iii) shows the minor-lobe effect.

3.4 Problem Formulation

In this section, the problem formulation is presented. The variables are described in Table 3.1, and detailed information are described below.

In this section, the problem formulation is presented. The variables are described in Table 3.1. We assume that there are K nodes in the network, and the entire set of

Variable	Description
K	Number of devices in the studied WPAN
ψ_i	Concurrent links pattern (**CLP**) with index of i
Ψ	Set of all feasible CLPs
i, j, u, w	Indexes of DEVs
(i, j)	Link from DEV$_i$ to DEV$_j$
$v_{i,j}^m$	Status of (i, j) in ψ_m
$r_{i,j}$	Transmission rate of (i, j)
$r_{i,j}^m$	Transmission rate of (i, j) in ψ_m
d_n	data demand of flow n
$x_{i,j}^n$	Amount of data of flow n through (i, j)
τ_m	Active time for ψ_m
f_n	Amount of data received for flow n

Table 3.1: Defined and used variables

links is L. To focus on the scheduling part, we do not consider the handshakes in any specific protocols. For convenience, we define a term referred to as concurrent links pattern (**CLP**), and represent the i_{th} CLP by ψ_i. A CLP is used to show a group of links which can be activated simultaneously, and can be mathematically expressed as a binary vector where each item corresponds to the working state (active/idle) of a link. For example in Fig. 3.1(b), $L_{(8,9)}$ and $L_{(11,10)}$ form a CLP ψ_g. If we denote the link sequence in the CLP as {$L_{(9,8)}$, $L_{(8,9)}$, $L_{(11,8)}$, $L_{(8,11)}$, $L_{(10,11)}$, $L_{(11,10)}$, $L_{(10,9)}$, $L_{(9,10)}$, $L_{(9,11)}$, $L_{(11,9)}$, $L_{(10,8)}$, $L_{(8,10)}$}, ψ_g equals {0, 1, 0, 0, 0, 1, 0, 0, 0, 0, 0, 0}. Denote Ψ as the set of all feasible CLPs with cardinality $M = |\Psi|$. (i, j) represents a link from DEV$_i$ to DEV$_j$. Link (i, i) does not exist, thus it is not considered in $\forall(i, j) \in L$. Let

$C[(i,j),(u,w)]$ be an indicator function that represents whether two links (i,j) and (u,w) can coexist, and this information is assumed to be available based on either conservative or aggressive spatial reuse strategy during the beamforming process. Thus:

$$C[(i,j),(u,w)] = \begin{cases} 1, & (i,j) \text{ and } (u,w) \text{ can coexist;} \\ 0, & \text{they cannot coexist.} \end{cases} \tag{3.4}$$

Let m be an index of a generic CLP ψ_m. Binary $v_{i,j}^m$ represents whether (i,j) is active (1) or idle (0) in ψ_m. Thus, ψ_m is a vector combined by $v_{i,j}^m$ for all (i,j), $\psi_m = \{v_{i,j}^m,\ \forall(i,j)\}$. Since each device is equipped with a single half-duplex radio, it should not be scheduled more than once in ψ_m. Due to the half-duplex requirement of single-radio DEV$_i$, we have:

$$\sum_{j=1\&j\neq i}^{K} v_{i,j}^m + \sum_{j=1\&j\neq i}^{K} v_{j,i}^m \leq 1,\ \forall i,\ \forall m. \tag{3.5}$$

The links' coexistence constraints in ψ_m are given as in (3.6), which are determined by $C[(i,j),(u,w)]$ as follows:

$$v_{i,j}^m + v_{u,w}^m \leq 1 + C[(i,j),(u,w)]\ ,\forall(i,j),\ \forall(u,w). \tag{3.6}$$

$r_{i,j}$ is used to represent the current transmission rate of (i,j). The rate of (i,j) in ψ_m can be calculated as:

$$r_{i,j}^m = v_{i,j}^m \cdot r_{i,j}\ . \tag{3.7}$$

We assume that there are N flows, and a flow n is characterized by source device, destination device, and data demand, or $(S(n), D(n), d_n)$.

Our objective is to maximize the throughput of this WPAN. Throughput equals the sum of received data divided by overall transmission time. That is:

$$\text{Throughput} = \frac{\text{Received Data}}{\text{Transmission Time}}. \tag{3.8}$$

Here, transmission time measures the duration since the start of data transmission till the end of data transmission.

3.4.1 Scenario I: Achievable Data Demand

There are N flows in the studied WPAN. n is the index for a flow and $n \in \{1, 2, \cdots, N\}$. In the Scenario I, all data demands can be fulfilled within the current frame. Since all data are successfully delivered, the numerator in (3.8) is determined by source devices' demands and fixed. Therefore, maximizing the throughput is equivalent to minimizing the transmission time. At any moment of the transmission period, there is a group of active links, or in other words, a CLP working for the data transmission. Therefore, minimizing the overall transmission time is equivalent to minimizing the sum of the scheduled periods of all the CLPs as shown in (3.9). τ_m is the active time for CLP $\boldsymbol{\psi}_m$, and the **objective** of minimizing the transmission time can be represented as $\min_{\tau_1,\tau_2,\cdots,\tau_M} \sum_{m=1}^{M} \tau_m$.

Cooperative transmission: The problem of time minimization with cooperative transmission is formulated as

$$\text{Problem } P_{1,M}: \min_{\tau_1,\tau_2,\cdots,\tau_M} \sum_{m=1}^{M} \tau_m \ , \tag{3.9}$$

subject to

$$\sum_{j=1\&j\neq i}^{K} (x_{i,j}^n - x_{j,i}^n) = \begin{cases} d_n, & i = S(n),\ \forall n; \\ -d_n, & i = D(n),\ \forall n; \\ 0, & i \neq S(n) \text{ or } D(n),\ \forall n; \end{cases} \tag{3.10}$$

$$\sum_{m=1}^{M} \tau_m \cdot r_{i,j}^m \geq \sum_{n=1}^{N} x_{i,j}^n,\ \forall (i,j); \tag{3.11}$$

$$\sum_{j=1\&j\neq i}^{K} v_{i,j}^m + \sum_{j=1\&j\neq i}^{K} v_{j,i}^m \leq 1,\ \forall i,\ \forall m; \tag{3.12}$$

$$\tau_m \geq 0, \quad m = 1, 2, \cdots, M; \tag{3.13}$$

$$v_{i,j}^m + v_{u,w}^m \le 1 + C[(i,j),(u,w)]\ ,\forall (i,j),\ \forall (u,w). \tag{3.14}$$

(3.10) provides the flow conservation constraint. For source, destination and relay devices, differences between amounts of the outgoing and incoming data are d_n, $-d_n$ and 0, respectively. $x_{i,j}^n$ denotes the amount of data of flow n through (i,j). (3.11) provides the link capacity constraints, which means that the link capacity should be larger than the sum of amounts of data through this link. (3.12) and (3.14) are explained in (3.5) and (3.6) respectively. (3.13) means τ_m should be non-negative value, since it represents active transmission time.

Non-cooperative transmission: The problem of time minimization without cooperative transmission is formulated as

$$\text{Problem } P_{2,M}: \min_{\tau_1,\tau_2,\cdots,\tau_M} \sum_{m=1}^{M} \tau_m\ , \tag{3.15}$$

subject to

$$\sum_{m=1}^{M} \tau_m \cdot r_{i,j}^m \ge \begin{cases} d_n, & i = S(n)\ \&\ j = D(n); \\ 0, & \text{any other } (i,j); \end{cases} \tag{3.16}$$

$$\sum_{j=1\&j\neq i}^{K} v_{i,j}^m + \sum_{j=1\&j\neq i}^{K} v_{j,i}^m \le 1,\ \forall i,\ \forall m; \tag{3.17}$$

$$\tau_m \ge 0, \quad m = 1,2,\cdots,M; \tag{3.18}$$

$$v_{i,j}^m + v_{u,w}^m \le 1 + C[(i,j),(u,w)]\ ,\forall (i,j),\ \forall (u,w). \tag{3.19}$$

Since only the source and destination DEVs are engaged in the non-cooperative scenario, the flow conservation and link capacity constraint can be merged into (3.16).

3.4.2 Scenario II: Bursty Data Demand

In this scenario, there are bursty data demands and not all data demands can be fulfilled in the current frame. The objective is to maximize the throughput of studied WPAN.

When there are bursty data demands, the WPAN may not be capable to transmit them completely within the current frame. Since the maximum duration of DTP is fixed and the throughput equals the amount of data received divided by DTP, the objective of maximizing throughput is equivalent to maximizing the amount of data received as shown in (3.20). We use f_n to represent amount of data received for flow n, thus $f_n \geq 0$. The objective of maximizing amount of data received can be represented as $\max_{f_1, f_2, \cdots, f_N} \sum_{n=1}^{N} f_n$.

Cooperative Transmission: Maximization of amount of data received with cooperative transmission can be formulated as

$$\text{Problem } P_{3,M}: \max_{f_1, f_2, \cdots, f_N} \sum_{n=1}^{N} f_n = -\min_{f_1, f_2, \cdots, f_N} \sum_{n=1}^{N} -f_n \ , \tag{3.20}$$

subject to

$$f_n \leq d_n, \forall n; \tag{3.21}$$

$$\sum_{j=1 \& j \neq i}^{K} (x_{i,j}^n - x_{j,i}^n) = \begin{cases} f_n, & i = S(n),\ \forall n; \\ -f_n, & i = D(n),\ \forall n; \\ 0, & i \neq S(n) \text{ or } D(n),\ \forall n; \end{cases} \tag{3.22}$$

$$\sum_{m=1}^{M} \tau_m \cdot r_{i,j}^m \geq \sum_{n=1}^{N} x_{i,j}^n,\ \forall (i,j); \tag{3.23}$$

$$\sum_{j=1 \& j \neq i}^{K} v_{i,j}^m + \sum_{j=1 \& j \neq i}^{K} v_{j,i}^m \leq 1,\ \forall i,\ \forall m; \tag{3.24}$$

$$\sum_{m=1}^{M} \tau_m \leq T; \tag{3.25}$$

$$\tau_m \geq 0, \quad m = 1, 2, \cdots, M; \tag{3.26}$$

$$v_{i,j}^m + v_{u,w}^m \leq 1 + C[(i,j), (u,w)] \ ,\ \forall (i,j),\ \forall (u,w). \tag{3.27}$$

The constraint (3.21) ensures that the amount of data received does not exceed the demand for data. The flow conservation constraints are shown in (3.22). For source, destination and relay DEVs, differences between the amounts of outgoing and incoming data are f_n, $-f_n$ and 0, respectively. $x^n_{i,j}$ is defined as the amount of data of flow n through link (i,j). The link capacity constraints are shown in (3.23). The constraint (3.25) guarantees that the transmission time will not exceed the DTP.

Non-Cooperative Transmission: Maximization of amount of data received without cooperative transmission can be formulated as

$$\text{Problem } P_{4,M}: \; -\min_{f_1,f_2,\cdots,f_N} \sum_{n=1}^{N} -f_n \,, \tag{3.28}$$

subject to

$$f_n \leq d_n, \forall n; \tag{3.29}$$

$$\sum_{m=1}^{M} \tau_m \cdot r^m_{i,j} \geq \begin{cases} f_n, & \text{if } i = S(n) \;\&\; j = D(n); \\ 0, & \text{any other } (i,j); \end{cases} \tag{3.30}$$

$$\sum_{m=1}^{M} \tau_m \leq T; \tag{3.31}$$

$$\tau_m \geq 0, \quad m = 1, 2, \cdots, M; \tag{3.32}$$

$$\sum_{j=1\&j\neq i}^{K} v^m_{i,j} + \sum_{j=1\&j\neq i}^{K} v^m_{j,i} \leq 1, \; \forall i, \; \forall m; \tag{3.33}$$

$$v^m_{i,j} + v^m_{u,w} \leq 1 + C[(i,j),(u,w)] \,, \forall (i,j), \; \forall (u,w). \tag{3.34}$$

Since only the source and destination DEVs are engaged in the non-cooperative scenario, the flow conservation and link capacity constraint can be merged into (3.30).

3.5 Solution via Column Generation

In this section, we first provide a brief introduction to column generation method, then show the solution for the problems.

To solve the problems formulated in the previous section directly, we have to enumerate all the CLPs. However, the number of the entire set of CLPs for a network with N nodes is $M = \sum_{i=1}^{N(N-1)} C_{N(N-1)}^{i}$, which is an extremely large number even for a moderate N. Common desktop computers may run out of memory with using this method, while only a small number of the CLPs will be scheduled in the final result. Therefore, we use the column generation method [122] to decompose the original problem into a master problem and a pricing problem. With column generation method, we do not need to consider all CLPs at the same time but only check potential ones sequentially. Thus, it saves memory and computation time.

3.5.1 Introduction of the Column Generation

Column generation is an efficient algorithm for solving larger linear programs, which can be deemed as an extension to Simplex method [122]. The key idea is that many linear programs are too large to consider all the variables explicitly. Since most of the variables will be non-basic in the optimal solution, only a subset of variables need to be considered. Column generation uses this idea to generate only the variables which have the potential to improve the objective function. Original optimization problem is decomposed into two problems: master problem and pricing problem. The master problem is the original problem with only a subset of variables. The pricing problem is a new problem created to identify a new variable. The objective function of the pricing problem is the reduced cost of the new variable with respect to the current dual variables, and the constraints require that the variable obey the naturally occurring constraints.

The master problem is solved first with a subset of variables, dual price can be obtained for each constraint. This information is utilized in the objective function of the pricing problem. Then, the pricing problem is solved. If the objective value of the pricing problem is negative, a variable with negative reduced cost can be identified. This variable is then added to the master problem, and the master problem is re-solved.

Re-solving the master problem will generate a new set of dual values, and the process is repeated until no negative reduced cost variable is identified. That is, the master problem reaches the optimal solution.

3.5.2 Solution for Scenario I

We use the column generation method to solve our problems. The **master problem** of $P_{1,M}$ is formulated as:

$$\text{Problem } P_{1,M'}: \min_{\tau_1,\tau_2,\cdots,\tau_{M'}} \sum_{m=1}^{M'} \tau_m\ , \tag{3.35}$$

subject to:

$$\sum_{j=1\&j\neq i}^{K} (x_{i,j}^n - x_{j,i}^n) = \begin{cases} d_n, & i = S(n),\ \forall n; \\ -d_n, & i = D(n),\ \forall n; \\ 0, & i \neq S(n) \text{ or } D(n),\ \forall n; \end{cases} \tag{3.36}$$

$$\tau_m \geq 0, \quad m = 1, 2, \cdots, M'; \tag{3.37}$$

$$\sum_{m=1}^{M'} \tau_m \cdot r_{i,j}^m \geq \sum_{n=1}^{N} x_{i,j}^n,\ \forall (i,j). \tag{3.38}$$

It is noticed that M in the original problem (3.9) becomes M' in the master problem (3.35). There is $M' \leq M$, which means the master problem only depends on part of the CLPs. To solve the master problem, a group of feasible CLPs should be given. For the problem considered in this work, the initial CLPs contain only the direct links corresponding to source-destination pairs of the flows. After solving the master problem, the optimal values of dual variables are obtained for the link demand constraints in (3.38) as $\overline{\pi}_{i,j}$. Therefore, the reduced cost for a new column (CLP) with the specific index m' is:

$$\overline{\xi}_{m'} = 1 - \sum_{(i,j)\in \boldsymbol{L}} \overline{\pi}_{i,j} \cdot r_{i,j}^{m'}\ . \tag{3.39}$$

The reduced cost in the linear optimization program indicates how much the objective function value can be reduced with the new basis. Here, the value of the objective function $P_{1,(M'+1)}$ of the new master problem including CLP m' is equal to:

$$P_{1,(M'+1)} = P_{1,M'} + \overline{\xi}_{m'}. \tag{3.40}$$

If the reduced cost $\overline{\xi}_{m'}$ is negative, it means the new CLP m' can reduce the current objective function value $P_{1,M'}$. To minimize $P_{1,(M'+1)}$, the minimum $\overline{\xi}_{m'}$ is needed. That is, the maximum $\sum_{(i,j)\in\boldsymbol{L}} \overline{\pi}_{i,j} \cdot r^{m'}_{i,j}$ is needed in (3.39). With (3.7), minimizing (3.39) can be re-formulated as the **pricing problem**:

$$\max_{v^{m'}_{i,j}, \forall (i,j)} \sum_{(i,j)\in\boldsymbol{L}} \overline{\pi}_{i,j} \cdot r_{i,j} \cdot v^{m'}_{i,j} \ , \tag{3.41}$$

subject to:

$$\sum_{j=1\&j\neq i}^{K} v^{m'}_{i,j} + \sum_{j=1\&j\neq i}^{K} v^{m'}_{j,i} \leq 1, \ \forall i; \tag{3.42}$$

$$v^{m'}_{i,j} + v^{m'}_{u,w} \leq 1 + C[(i,j),(u,w)], \ \forall (i,j), \ \forall (u,w). \tag{3.43}$$

The solution of the pricing problem is a new CLP $\boldsymbol{\psi}_{m'}$. If the reduced cost $\overline{\xi}_{m'}$ for $\boldsymbol{\psi}_{m'}$ is negative, the new $\boldsymbol{\psi}_{m'}$ is added to the bases of the previous master problem and re-solve it. After several iterations, the reduced cost becomes positive, which means no CLP can reduce the objective function value of the current master problem. Then, the objective function value of master problem in current iteration is optimal for the original $P_{1,M}$. $P_{2,M}$ can also be solved by a similar method.

3.5.3 Solution for Scenario II

The solution for $P_{3,M}$ comes as follows. The master problem is formulated as

$$\text{Problem } P_{3,M''}: \min_{f_1,f_2,\cdots,f_N} \sum_{n=1}^{N} -f_n \ , \tag{3.44}$$

subject to

$$f_n \leq d_n, \forall n; \tag{3.45}$$

$$\sum_{j=1\&j\neq i}^{K} (x_{i,j}^n - x_{j,i}^n) = \begin{cases} f_n, & i = S(n),\ \forall n; \\ -f_n, & i = D(n),\ \forall n; \\ 0, & i \neq S(n) \text{ or } D(n),\ \forall n; \end{cases} \tag{3.46}$$

$$\sum_{m=1}^{M''} \tau_m \cdot r_{i,j}^m \geq \sum_{n=1}^{N} x_{i,j}^n,\ \forall (i,j); \tag{3.47}$$

$$\tau_m \geq 0, \quad m = 1, 2, \cdots, M''; \tag{3.48}$$

$$\sum_{m=1}^{M'} \tau_m \leq T. \tag{3.49}$$

Again, M in the original problem (3.20) becomes M'' in the master problem (3.44), $M'' \leq M$. This means the master problem only depends on part of the CLPs. After solving the master problem, we can get the optimal dual variables for (3.47) and (3.49) as $\overline{\alpha}_{i,j}$ and $\overline{\beta}$, respectively. Therefore, we can write the reduced cost for a new column (CLP) with the specific index m'' as

$$\overline{\xi}_{m''} = 0 - \sum_{(i,j)\in \boldsymbol{L}} \overline{\alpha}_{i,j} \cdot r_{i,j}^{m''} - \overline{\beta}\ . \tag{3.50}$$

The reduced cost in the linear optimization program indicates the amount of objective function value which can be reduced with the new basis. Here, the objective function value $P_{3,(M''+1)}$ of the new master problem including CLP m'' can be expressed as

$$P_{3,(M''+1)} = P_{3,M''} + \overline{\xi}_{m''}. \tag{3.51}$$

If the reduced cost is negative, the new CLP m'' can reduce the current objective value $P_{3,M''}$. To minimize $P_{3,(M''+1)}$ in (3.51), minimum $\overline{\xi}_{m''}$ is needed. That is, the maximum $\sum_{(i,j)\in \boldsymbol{L}} \overline{\alpha}_{i,j} \cdot r_{i,j} \cdot v_{i,j}^{m''} + \overline{\beta}$ is needed. With (3.7), minimizing the reduced cost can be re-formulated as the **pricing problem**

$$\max_{v_{i,j}^{m''}, \forall (i,j)} \sum_{(i,j)\in \boldsymbol{L}} \overline{\alpha}_{i,j} \cdot r_{i,j} \cdot v_{i,j}^{m''} + \overline{\beta}\ , \tag{3.52}$$

subject to

$$\sum_{j=1\&j\neq i}^{K} v_{i,j}^{m''} + \sum_{j=1\&j\neq i}^{K} v_{j,i}^{m''} \leq 1, \ \forall i. \tag{3.53}$$

$$v_{i,j}^{m''} + v_{u,w}^{m''} \leq 1 + C[(i,j),(u,w)], \ \forall(i,j), \ \forall(u,w). \tag{3.54}$$

The solution of the pricing problem is a new CLP $\psi_{m''}$. If the reduced cost for $\psi_{m''}$ is negative, we add the new $\psi_{m''}$ to the bases of the previous master problem and then re-solve it. After several iterations, the master problem may reach the optimal solution, which is also optimal for the original problem $P_{3,M}$. We can solve $P_{4,M}$ by a similar approach.

3.6 Performance Evaluation

n this section, we first describe simulation setup and simulation parameters. After that, the numerical results for both scenarios I and II are shown and investigated. Following acronyms are used in the figures: impartial strategy for practical antenna model with cooperation (**PAC**), impartial strategy for practical antenna model without cooperation (**PANC**), conservative strategy for ideal antenna model with cooperation (**CSC**), conservative strategy for ideal antenna model without cooperation (**CSNC**), and aggressive strategy for ideal antenna model with cooperation (**ASC**), aggressive strategy for ideal antenna model without cooperation (**ASNC**).

First, the effect of cooperation is shown by comparing cooperative and non-cooperative cases. Second, the effect of minor-lobe is shown by comparing PAC and ASC. Third, the effect of perfect information is shown by comparing PAC and CSC. Fourth, the proposed cooperative scheme is compared to its counterpart in [2]. The cooperative scheme in [2] is designed for 60 GHz WPAN and considers multi-hop relay service. This is the reason that the scheme in [2] is chosen as benchmark. The difference between scheduling strategies is shown in Fig. 3.3.

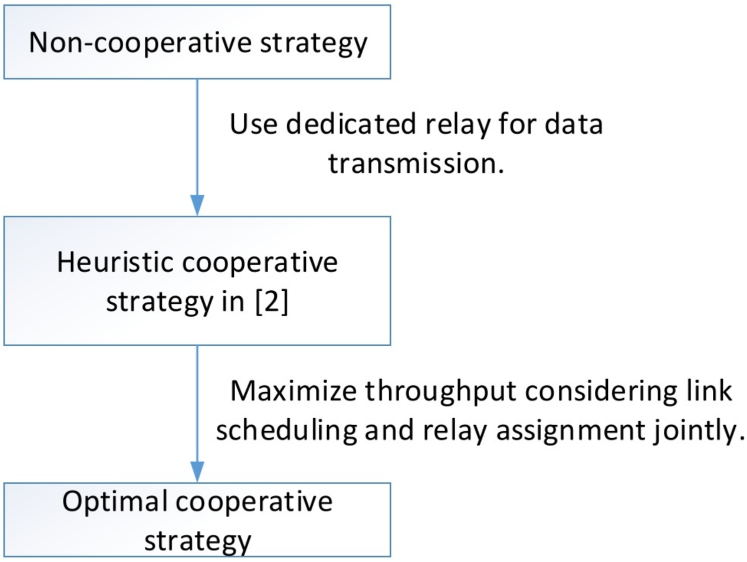

Figure 3.3: Difference between scheduling strategies.

3.6.1 Simulation Parameter

C++ and CPLEX [123] are used for simulations. Network topologies are generated using C++. Then, the constraints of linear programming problem is generated according to the studied topology. After that, CPLEX is used solve the linear programming problem. Throughput gain is defined as the ratio between throughput under different schemes or antenna models. The simulation configuration is as follows. The DEVs are randomly deployed in a square area of side 15 meters. As shown in Table 3.2, we use the modulation and coding schemes (**MCS**) in [121]. Transmission power is fixed at 10 dBm. Noise factor and implementation loss are set as 10 and 5 dB, respectively. 50 networking topologies are randomly generated. The simulation results are then averaged and shown.

MCS	Modulation	Code Rate	Data Rate (Mbps)
0	DBPSK	1/2	27.5
1	π/2-BPSK	1/2	385
2	π/2-BPSK	1/2	770
3	π/2-BPSK	5/8	962.5
4	π/2-BPSK	3/4	1155
5	π/2-BPSK	13/16	1251.25
6	π/2-QPSK	1/2	1540
7	π/2-QPSK	5/8	1925
8	π/2-QPSK	3/4	2310
9	π/2-QPSK	13/16	2502.5
10	π/2-16QAM	1/2	3080
11	π/2-16QAM	5/8	3850
12	π/2-16QAM	3/4	4620

Table 3.2: Modulation and coding scheme for single carrier

3.6.2 Simulation Analysis of Scenario I

In Scenario I, we assume that transmission time does not reach the maximum DTP length in Fig. 3.2. Thus, we maximize the throughput of WPANs via minimizing transmission time. Four aspects are discussed, namely, antenna beamwidth, number of DEVs, number of flows and data demand per flow. The proposed scheduling scheme is also compared to that used in [2].

In Fig. 3.4, the effect of antenna beamwidth on transmission time is shown. 20 DEVs are randomly deployed. 4 flows are initialized and amount of data per flow is set as 0.5 Mbits. Since all flows are end-to-end data flows, which can lead to flows in different links. The number 4 is chosen, since there are only 20 DEVs in this WPAN. If a large number is used, the simulation becomes very time-consuming. Transmission time increases with wider beamwidth for all cases. For CSC, the throughput gain between using 15° and 90° antenna is about 100 times. This is due to the fact that wider beamwidths provide smaller spatial reuse ratios, and the consequential fewer concurrent links lead to smaller capability for data transmission. The need for cooperative transmission is low with 15° antenna, since the direct links possess good qualities. Cooperative transmission also does not help much with 90° antenna, because the cooperative scheme needs more concurrent active links. Larger throughput gains between cooperative and non-cooperative transmission schemes are attained at moderate beamwidths. For example, cooperative transmission scheme is 10 times better with 45° beam as compared to non-cooperative scheme.

In Fig. 3.5, the effect of different numbers of DEVs on transmission time is shown. The antenna beamwidth is set as 30°. 4 flows are initialized and amount of data per flow is set as 0.5 Mbits. Generally, cooperative schemes provide shorter transmission time as compared to the corresponding non-cooperative schemes. For CSC, ASC and PAC, the transmission time decreases with number of DEVs. This result is as expected because WPANs have better cooperation choices with more relay DEVs. Moreover, we observe that the transmission time fluctuates for the non-cooperative schemes. This demonstrates that number of DEVs does not have an obvious effect on throughput for non-cooperative transmission. The reason is that additional idle DEVs do not bring benefit to the direct transmissions.

In Fig. 3.6, the effect of different numbers of flows on transmission time is shown. 20 DEVs are randomly deployed. The antenna beamwidth is set as 30° and amount of data per flow is set as 0.5 Mbits. Our first observation is that transmission time increases for larger number of flows for all cases. Then, we see that cooperative transmission schemes provides shorter transmission time as compared to their counterparts. The figure also shows that the difference of transmission time between cooperative and non-cooperative schemes becomes larger as the number of flows increases. That indicates that the network capacity is improved by using cooperative transmission schemes.

In Fig. 3.7, the effect of different amounts of data per flow is shown. 20 DEVs are randomly deployed. The antenna beamwidth is set as 30°. 4 flows are initialized in the studied WPAN. It is observed that the transmission time for each line increases almost linearly with amount of data per flow. Since the best routes for given flows are fixed in the corresponding WPAN, the end-to-end data rates for these flows are also fixed. Thus, transmission time increases linearly with amount of data per flow. For transmitting the same amount of data, ASC needs the shortest time. PAC can achieve almost the same performance as ASC, which means minor-lobe of the used antenna model is not strong.

In Fig. 3.8, we compare different cooperative schemes with different antenna models. 20 DEVs are randomly deployed and antenna beamwidth is set as 30°. 4 flows are initialized and amount of data per flow is set as 0.5 Mbits. The throughput under the practical antenna model is close to the throughput under the ideal antenna

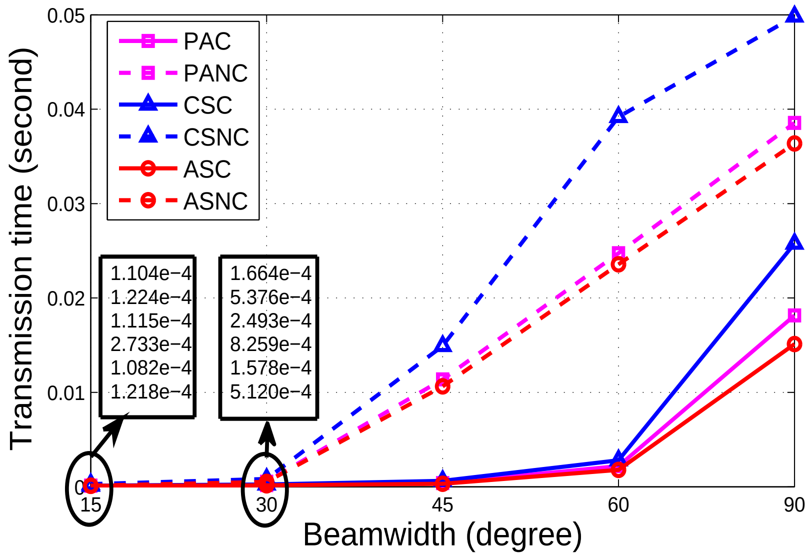

Figure 3.4: Transmission time with different antenna beamwidths in Scenario I. (The sequence of the numbers in the text boxes is consistent with that in the legend.)

model with aggressive strategy. The reason is that the side-lobe gain of the realistic antenna model used in this work is low as shown in (3.1). If an antenna with larger side-lobe gain is used, throughput will be closer to that using conservative strategy with ideal antenna. Moreover, the cooperative strategy in [2] requires more time to transmit the same amount of data as compared to the method described in this work. This is due to the reason that the scheme used in [2] is limited to two-hop device cooperation, and furthermore, the link scheduling and relay assignment are treated as independent problems.

3.6.3 Simulation Analysis of Scenario II

In Scenario II, the length of DTP is fixed at 1 micro-second in the simulations. We maximize the throughput of WPAN via maximizing the received amount of data for given demands. Effects from four aspects are discussed, namely, antenna beamwidth,

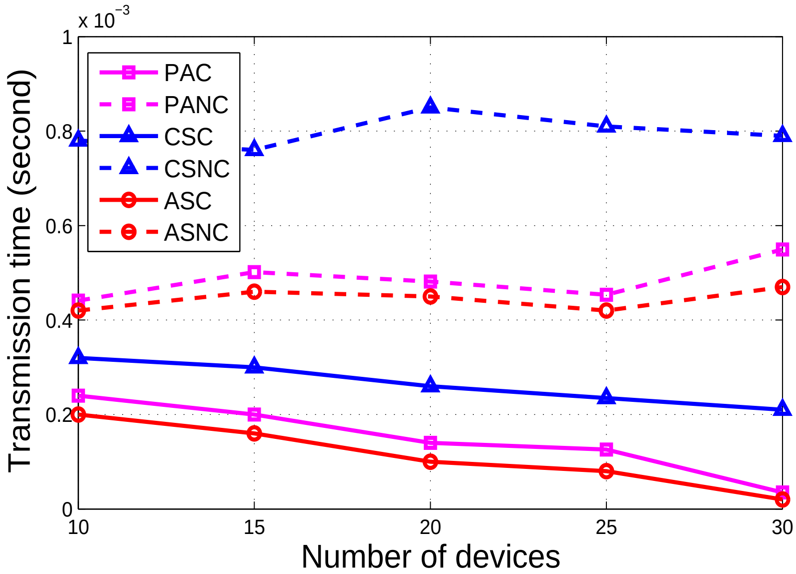

Figure 3.5: Transmission time with different numbers of DEVs in Scenario I.

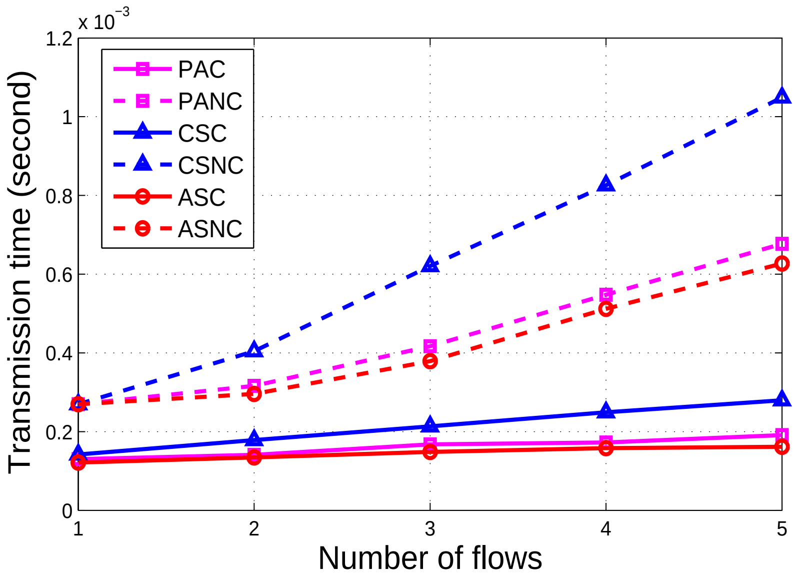

Figure 3.6: Transmission time with different numbers of flows in Scenario I.

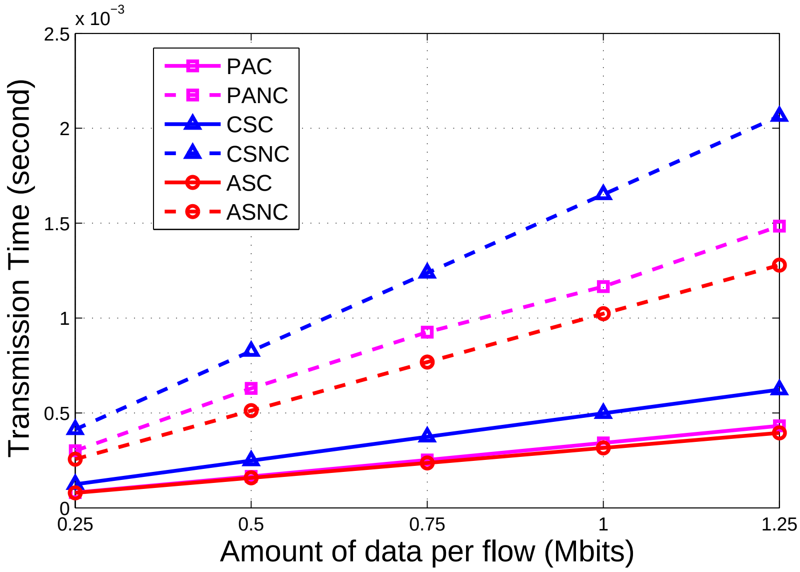

Figure 3.7: Transmission time with different amounts of data per flow in Scenario I.

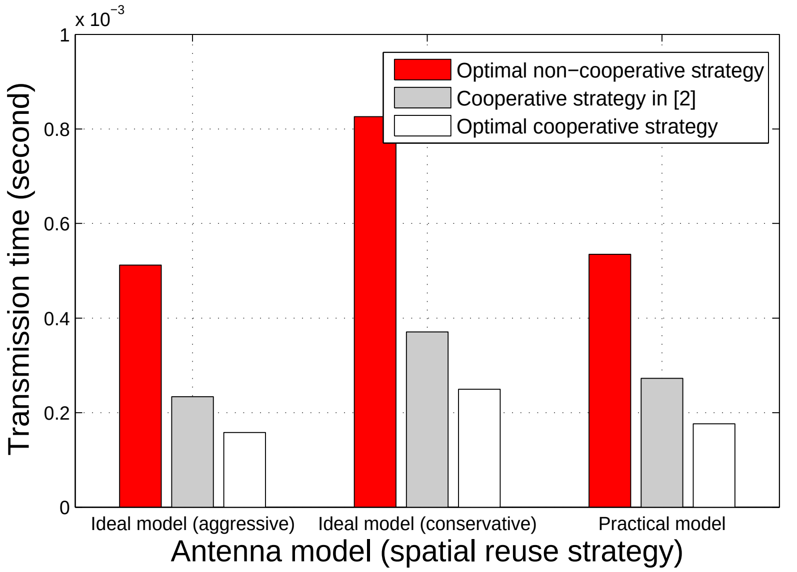

Figure 3.8: Comparison among non-cooperative algorithm, cooperative algorithm in [2], and optimal cooperative algorithm in Scenario I.

number of DEVs, number of flows and data demand per flow. Again, the scheduling schemes in this work are compared with [2].

In Fig. 3.9, the effect of different beamwidths is shown. 20 DEVs are randomly deployed. 4 flows are transmitted and amount of data per flow is set as 4 Mbits. It is observed that the amount of data received is larger when cooperative transmission is used as compared to the case when non-cooperative transmission is used. The throughput gain between the cooperative and non-cooperative scheme is in the range 1.5 to 3. The largest gain is attained when the antenna beamwidth is 45°. For narrow beams, the need for node cooperation is low due to the good quality of direct links. For wide beams, cooperative transmission is less effective due to low spatial reuse ability.

In Fig. 3.10, the effect of different number of DEVs is shown. The antenna beamwidth is set as 30°. 4 flows are initialized and amount of data per flow is set as 4 Mbits. For cooperative scheme, the amount of data received increases with the number of DEVs. The throughput gain between 30 and 10 DEVs is about 1.2 in CSC. Moreover, we observe that number of DEVs has a limited effect on the amount of data received in WPAN with non-cooperative transmission.

In Fig. 3.11, the effect of different numbers of flows is shown. 20 DEVs are randomly deployed. The antenna beamwidth is set as 30°. Amount of data per flow is set as 4 Mbits. It is clear that the amount of received data increases with number of flows. It is also observed that the gradients for all the lines decrease with number of flows. This is because that the WPAN is saturate. Moreover, it is observed that the cooperative transmission generally provides 50% larger throughput than the non-cooperative transmission.

In Fig. 3.12, the effect of different amounts of data per flow is shown. 20 DEVs are randomly deployed and the antenna beamwidth is set as 30°. 4 flows are initialized. The overall amount of received data increase with demand, and the gradients of the lines decrease during this process. For all cases, the throughput gain is around 1.5 or 2 times between cooperative and non-cooperative schemes. When the amount of data per flow equals 4 Mbits, PAC, CSC and ASC received about 40% to 80% more data as compared to the non-cooperative schemes.

In Fig. 3.13, we compare various cooperative schemes with different antenna models. 20 DEVs are randomly deployed and the antenna beamwidth is set as 30°. 4 flows are initialized and amount of data per flow is set as 4 Mbits. Since there is no other work discussing bursty data demand, the scheme in [2] is simply extended to comprise bursty demand and used as a benchmark. As in [2], a relay is selected within feasible region for a direct link, when LOS path is blocked. The throughput of the benchmark is in the middle of the throughput with non-cooperative and cooperative schemes proposed in this work. For the three spatial reuse strategies in the figure, the cooperative scheme in this work transmits 21%, 34% and 27% more data than the benchmark. This shows that the scheme proposed in this work provides better cooperative service.

3.6.4 Discussion

First, cooperative schemes generally outperform the non-cooperative ones. We observe that the throughput gain between the cooperative scheme and the non-cooperative scheme in Scenario I is larger than that in Scenario II. The reason is as follows. In Scenario I, all data has to be received, thus the transmission time is mainly determined by the worst flow. It is clear that cooperative transmission may be more helpful for the worst flow. In Scenario II, not all data needs to be received. To maximize the amount of received data, both cooperative and non-cooperative schemes schedule the best flow first. For the flows with best throughput, the difference in end-to-end data rates between cooperative and non-cooperative schemes may not be

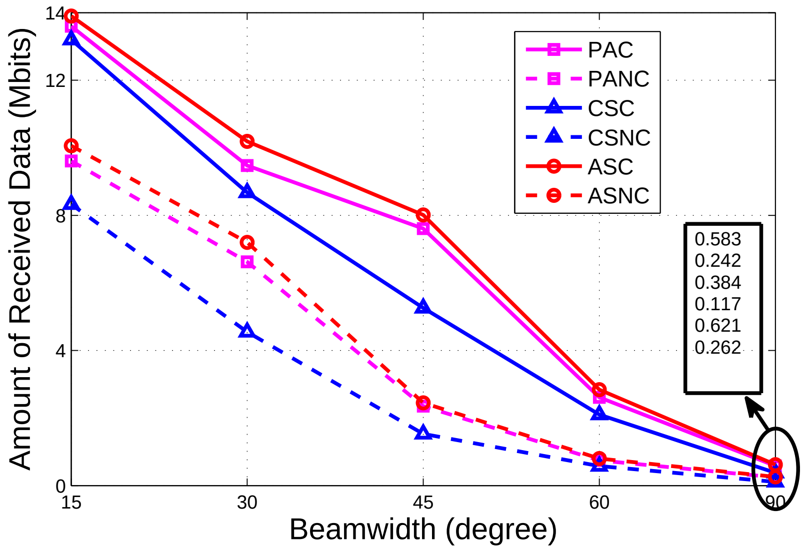

Figure 3.9: Amount of received data with different antenna beamwidths in Scenario II. (The sequence of the numbers in the text boxes is consistent with that in the legend.)

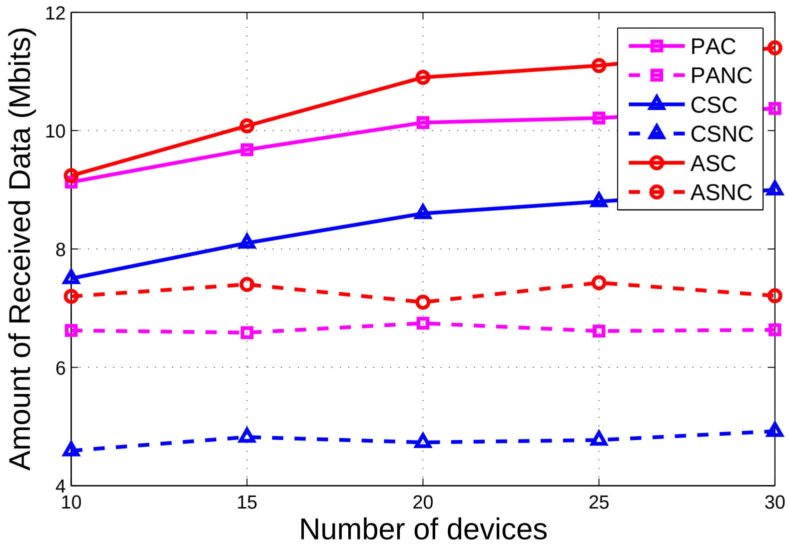

Figure 3.10: Amount of received data with different numbers of DEVs in Scenario II.

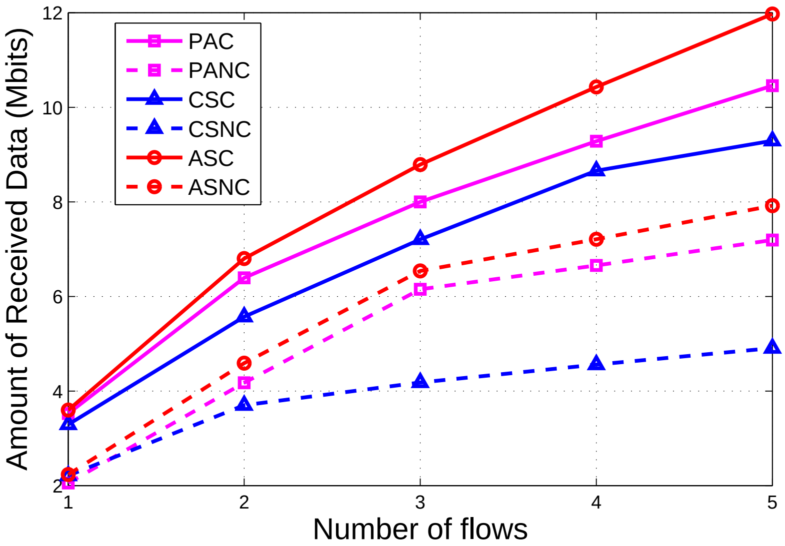

Figure 3.11: Amount of received data with different numbers of flows in Scenario II.

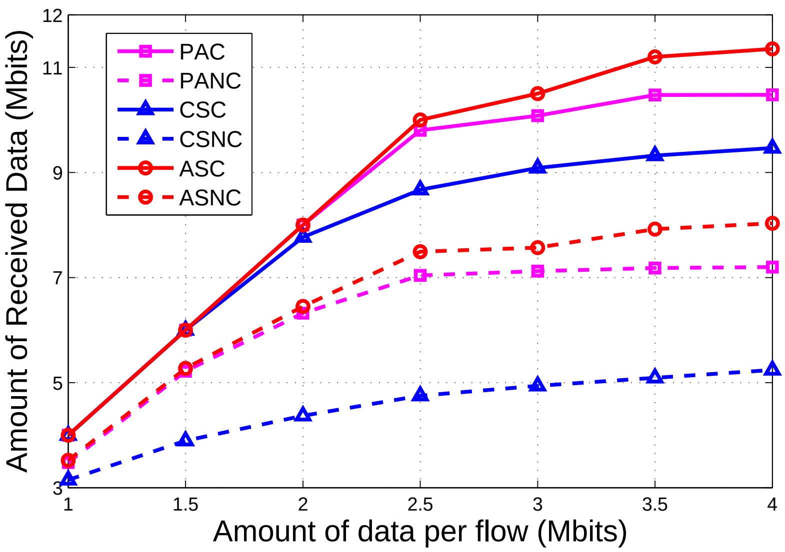

Figure 3.12: Amount of received data with different data demand per flow in Scenario II.

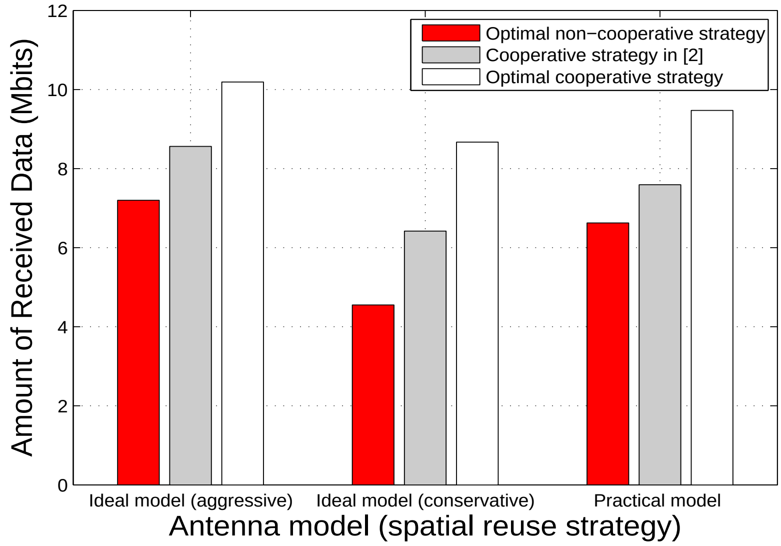

Figure 3.13: Comparison among non-cooperative algorithm, cooperative algorithm in [2], and optimal cooperative algorithm in Scenario II.

that large. This is the reason why the throughput gain is around 10 in Scenario I, while it is usually less than 2 in Scenario II. Second, we observe that the performance of PAC is within 10% lower than ASC, which means that the minor-lobe effect is not very strong. Third, we observe that the performance of PAC can be 20% better than that of CSC, which shows the tradeoff between perfect and imperfect information. Fourth, column generation method can reduce computation time from hour to minute level, but it is still too long to implement in real system. Therefore, heuristic algorithms with cooperation which can provide real-time scheduling are needed, and the optimal methods proposed here can provide the guideline to the design of heuristic algorithms.

3.7 Chapter Summary

In this chapter, we propose the use of cooperative transmission to improve the throughput of directional 60 GHz WPANs. Both achievable and bursty data demand scenarios are studied. The throughput maximization objectives are formulated as linear programming problems and solved by the column generation method. We have the following observations. First, throughput increases with larger number of DEVs, larger data amount per flow, larger number of flows or smaller antenna beamwidths in the studied cooperative WPANs. Second, the throughput ratio of PAC to ASC is usually around 95%, this indicates that the side-lobe of the realistic antenna model used in this work does not have strong effect in throughput. Third, the proposed cooperative transmission scheme may provide around 20% to 45% higher throughput than the protocol used in [2] in the studied scenarios. In summary, the proposed cooperative transmission scheme can significantly improve the throughput of 60 GHz WPANs.

Chapter 4

Cooperative Multi-Channel Directional Medium Access Control for Ad Hoc Networks

In this chapter, we propose a cooperative multi-channel directional medium access control (**CMDMAC**) protocol incorporating minor-lobe interference for directional ad hoc networks. While most existing MAC protocols require either extra equipment or clock synchronization to solve deafness and directional hidden terminal problems, CMDMAC needs neither to conquer these problems. Observing that directional transmission assumes single-data-channel in most instance, CMDMAC incorporates directional and multi-channel transmission to provide superior networking performance. Theoretical analysis for CMDMAC is provided and its performance is validated via NS2 simulation.

4.1 Introduction

Since directional transmission can provide higher data rates, omni-directional networks are falling into disfavor especially in new networking applications, such as high definition video streaming. Moreover, due to high spatial reuse ratio, directional networks offer advantage in dense environments, such as Internet-of-Things (**IoT**) and Machine-to-Machine (**M2M**) networks. To reap the benefits of directional transmission, efficient directional Medium Access Control (**MAC**) protocols are needed. New standards like 802.11ad and 802.15.3c have been proposed, but both work in a centralized manner.

In this chapter, we work on directional MAC protocols for ad hoc networks. Two key challenges in designing directional MAC protocols for ad hoc networks are the hidden terminal and deafness problems. Existing solutions are generally based on one of two approaches, namely i) network-wide synchronization and ii) multiple radios with one radio dedicated for control messages. However, synchronization is difficult to achieve in ad hoc networks. Besides, we can not expect all terminals to be equipped with two or more radios in the emerging IoT, M2M or other heterogeneous networks, as smart phones with multiple Wireless Fidelity (**WiFi**) radios are seldom seen in the market. Another scenario where multiple radios may not be available for each terminal is sensor network, since there will be strict concern about hardware size and power consumption.

The main focus of this chapter is on designing a directional MAC that can solve hidden terminal and deafness problems without network-wide synchronization and multiple radios for directional ad hoc networks. With the objective of improving aggregate throughput for directional ad hoc networks, we propose a Cooperative Multi-channel Directional Medium Access Control protocol (**CMDMAC**). Multi-channel and directional transmission are two known multiplexing techniques that can be used to improve networking performance. However, they are studied separately in most literature on MAC protocols due to complexity considerations. CMDMAC incorporates multi-data-channel transmission to further improve networking performance. Each terminal is assumed to be equipped with a single half-duplex radio, which may be tuned to different channels. To solve hidden terminal and deafness problems under a multi-channel directional environment, CMDMAC operates with one control channel and multiple data channels and uses cooperation among neighbors. All control messages are exchanged omni-directionally in control channel while data packets are transmitted directionally in data channels. Moreover, a single radio is not a necessary condition for CMDMAC. Terminals equipped with multiple radios may also perform CMDMAC.

The rest of this chapter is organized as follows. In Section 4.2, related work is reviewed. In Section 4.3, the system model is introduced. In Section 4.4, we discuss the problems and challenges in directional and multi-channel MAC design. In Section 4.5, we present the details of the proposed CMDMAC protocol. In Section 4.6, we present a theoretical analysis for CMDMAC. In Section 4.7, we evaluate the performance of CMDMAC and compare to other MAC protocols via simulations. Conclusions are drawn in Section 4.8.

4.2 Related Works

In the area of directional MAC protocols, Takai et al. have done pioneering work [124], in which they first proposed methods like directional virtual carrier sensing. In [125], the authors summarized the key design problems in directional MAC but not all issues were solved satisfactorily. In [126], it was argued that directional MAC with practical antenna models needed more attention, but global position system (**GPS**) sensors were needed to provide accurate location information for each terminal. In

[127], it was found that existing solutions rarely deal with the impact of minor lobes and they proposed a MAC protocol for multi-hop networks based on network-wide synchronization. In [128], a radio dedicated for control messages was used to solve the hidden terminal problem. In [129], the authors proposed a protocol using sector sweep to overcome the hidden terminal problem and proposed a method to collect neighbor information for directional networks. In [130], double radios were used to identify deaf terminals. In [131], data frames were fragmented to reduce packet collisions but only hidden terminals in the main sectors of the communicating pairs were eliminated. In [132], a protocol was proposed where an additional busy tone equipment was needed for each terminal. In [133], a contention window is used for terminals to negotiate and solve the hidden terminal problem. There also exist research papers on providing efficient directional MACs for 60 GHz personal networks [31, 37, 44].

In existing multi-channel MAC works, there are two main approaches to solve hidden terminal and deafness problems. The first one is using multiple radios and dedicating one of them for control channel messages [69, 70, 134]. It is clear that the hardware complexity is increased for this approach and hence cost and energy consumption. We also cannot expect that all terminals will be equipped with multiple radios in a heterogeneous network. In fact, we seldom find a smart phone with two WiFi devices. The other approach is regulating the irregular nodes' behavior by using well-known approaches based on contention time slots [71–73], or channel hopping sequences [135]. However, this approach requires network-wide synchronization which is a difficult task for multi-hop ad hoc networks [136]. In [3], CAMMAC was proposed and cooperation was used to solve the multi-channel collision problem in omni-directional networks. In CAMMAC, nodes use two-hop topology information to tell whether two omni-directional links can co-exist in certain channel. Since directional transmission is taken into consideration in CMDMAC, the condition for two links to co-exist becomes different. The contribution of CMDMAC is to extend

CAMMAC to solve hidden terminal problem in directional networks. Nodes with CMDMAC have to jointly consider channel usage information, direction information, and topology information to decide whether a new link under negotiation procedure can be established or not. There are also some approaches trying to provide efficient multi-channel MACs for cognitive ratio networks [137–140].

Based on the literature review, we observe the following. Regardless of whether it is for directional or multi-channel MACs, most researchers depend on either additional hardware or network synchronization to solve the associated problems. Moreover, while incorporating multi-channel and directional transmission may improve networking performance, there are few works that have studied these two aspects together. In this chapter, we propose CMDMAC combines directional and multi-channel transmission. It does not need any extra hardware for control message exchange and may work asynchronously.

4.3 System Model

In this section, we introduce the network and antenna models employed in this chapter.

4.3.1 Network Model

An asynchronous ad hoc network which works in the unlicensed band, for example Industrial, Scientific and Medical (**ISM**) band, is considered. Terminals are randomly located and each of them is equipped with a single half-duplex transceiver. Terminals and nodes are used interchangeably henceforth. As shown in Fig. 4.1, multiple independent channels are available: one is dedicated for the exchange of omni-directional control messages; others are used for the transmission of directional data packets. We further assume that radios can work in both omni-directional and

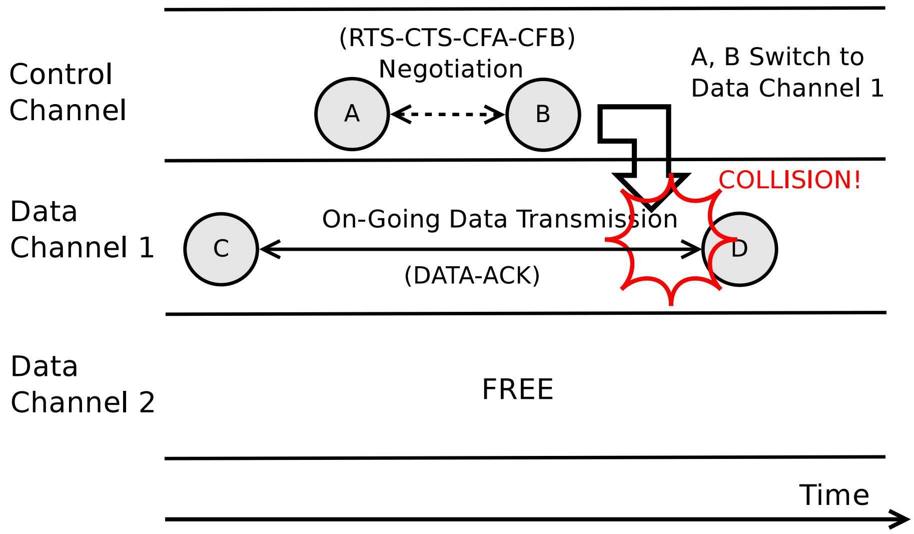

Figure 4.1: System model and the multi-channel hidden terminal problem.

directional modes [126, 127] and that radios can be tuned among different channels [137, 138].

A two-ray propagation model is used. The reception power P_R is given by

$$P_R = \frac{P_T \cdot G_T \cdot G_R \cdot H_T^2 \cdot H_R^2}{D^4}, \tag{4.1}$$

where P_T is transmission power; G_T is the antenna gain of transmitter (**Tx**); G_R is the antenna gain of receiver (**Rx**); H_T is the height of Tx's antenna; H_R is the height of Rx's antenna; and D is the distance between the Tx and Rx.

4.3.2 Antenna Model

We employ the most widely used directional antenna model [141] as shown in Fig. 4.2(a). The antenna gain for minor-lobe is a non-zero value 0.4 in this example, while the antenna gain for main-lobe is much larger than 1. Both minor- and main-lobes have uniform antenna gains. The antenna consists of M non-overlapping sectors. For example, M is equal to 6 in Fig. 4.2(b). Moreover, the antenna is capable of switching among different sectors without any switching delay [129, 133]. Direction of Arrival

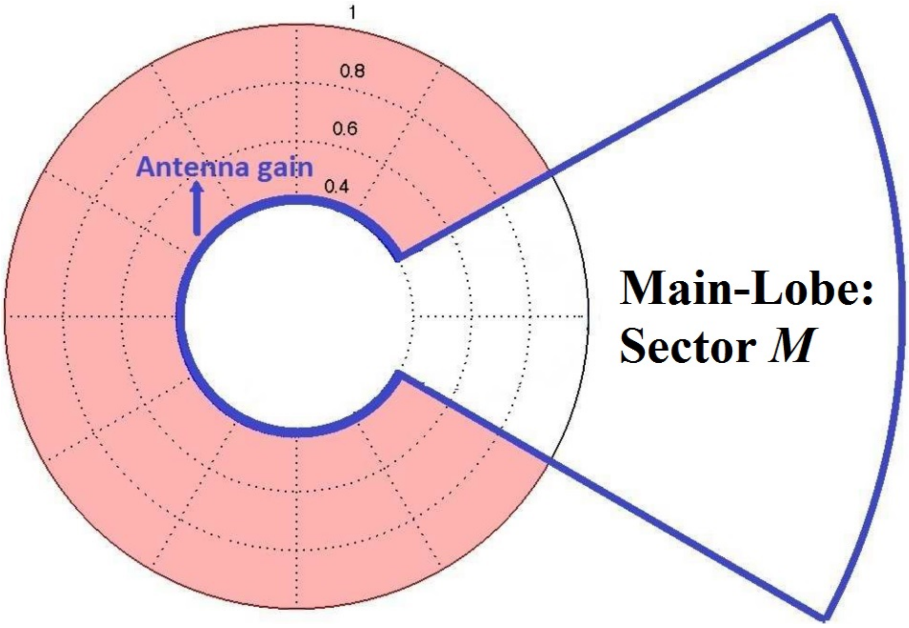

(a) Antenna gains model.

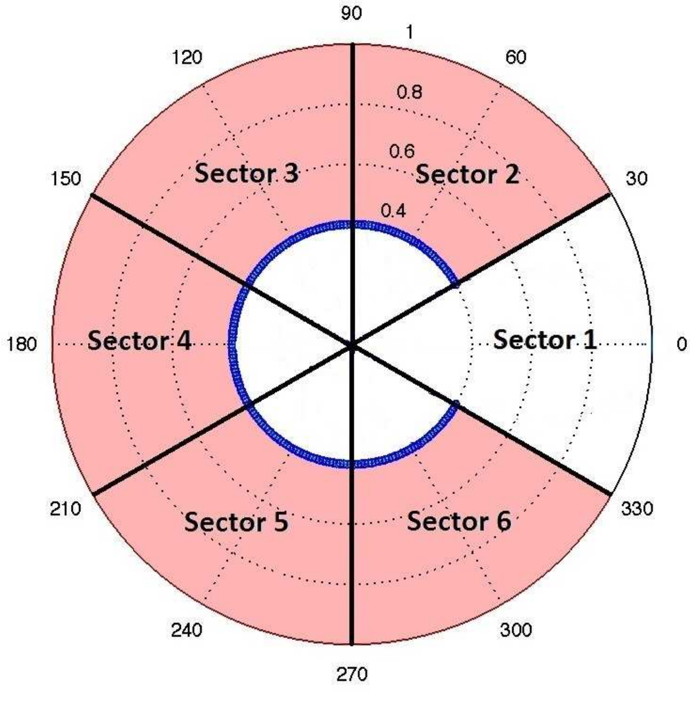

(b) Antenna sector model.

Figure 4.2: Antenna model.

(**DoA**) technique is assumed to be used and terminals can estimate the direction of the received signal [127].

4.4 Problems in Multi-Channel Directional MAC

In this section, we introduce the challenges in multi-channel directional MAC design, taking minor-lobe interference effects into consideration.

4.4.1 Vulnerability of Receivers

Vulnerability of receivers means interference from all directions can interrupt the ongoing data reception. The case using ideal antenna model is shown in Fig. 4.3(a). B is receiving from A. As C is in Rx B's minor-lobe Sector 2 and the antenna gain for Sector 2 is 0, there will be no interference from C to B, thus no packet collision taking place. The case considering minor-lobe effect is shown in Fig. 4.3(b). B is receiving from A. The interference from C to B is non-zero, which potentially results in packet collision.

4.4.2 Multi-Channel Directional Hidden Terminal Problem

The directional hidden terminal problem with a single data channel is illustrated as follows. In Fig. 4.4(a), nodes A, B, C and D are engaged in data transmission while nodes E and F establish their link. After transmissions in links 1 and 2, B wants to transmit to C. Without knowing the existence of link 3, the new directional link may cause collision to E. This kind of problem is defined as directional hidden terminal problem. The multi-channel hidden terminal problem with omni-directional transmission is discussed as follows. In Fig. 4.1, nodes A and B are carrying out the negotiation in the control channel without knowing that C and D are communicating

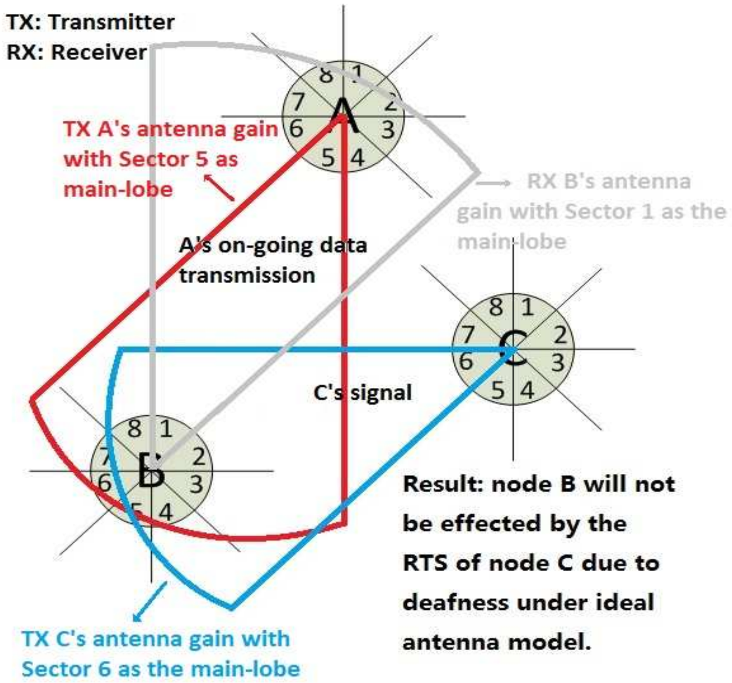

(a) Interference-free receiver with ideal antenna model.

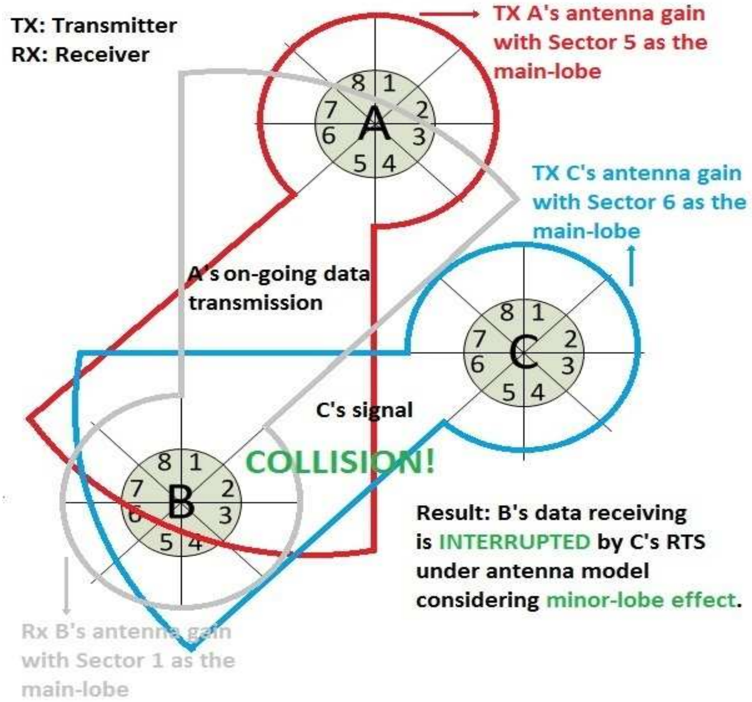

(b) Vulnerability of receiver with considering minor-lobes.

Figure 4.3: Minor-lobe interference to receivers.

in data channel 1. Meanwhile, data channel 2 is free. If A and B switch to data channel 1 for data transmission, it is obvious that they may bring collision to the current link of C and D. Therefore, it is important to coordinate different terminals in the network. This kind of hidden terminal problem is defined as multi-channel hidden terminal problem.

The situation studied in this chapter is a combination of above two cases. We term it ”multi-channel directional hidden terminal problem”. Direction and channel together determine whether a node may become hidden terminal towards another terminal. For the case shown in Fig. 4.4(b), let’s assume there are two data channels. The grey curve indicates the transmission range of node B. If the new link 4 is in data channel 2 while link 3 is in data channel 1, there will be no collision. For the case in Fig. 4.1, let’s assume A, B, C and D are located as two parallel link, like links 4 and 5 in Fig. 4.4(a). Even if the link of C and D is in data channel 1, there will be no collision since A and B are not in the interference range of C and D hence the two links can co-exist.

4.4.3 Deafness Problem

In the multi-channel directional networking environment, deafness is caused when the negotiation information of the intended Rx is missed. The Tx may keep sending requests. This wastes control channel resources and reduces system performance.

4.4.4 Collision Due to Different Gains

For the reason that transmission and interference ranges in directional and omni-directional mode are different, a node may interfere with another node much farther than its omni-directional transmission range. This is due to the coexistence of omni-directional and directional modes [129]. The transmission power adaption may also lead to a more efficient power usage.

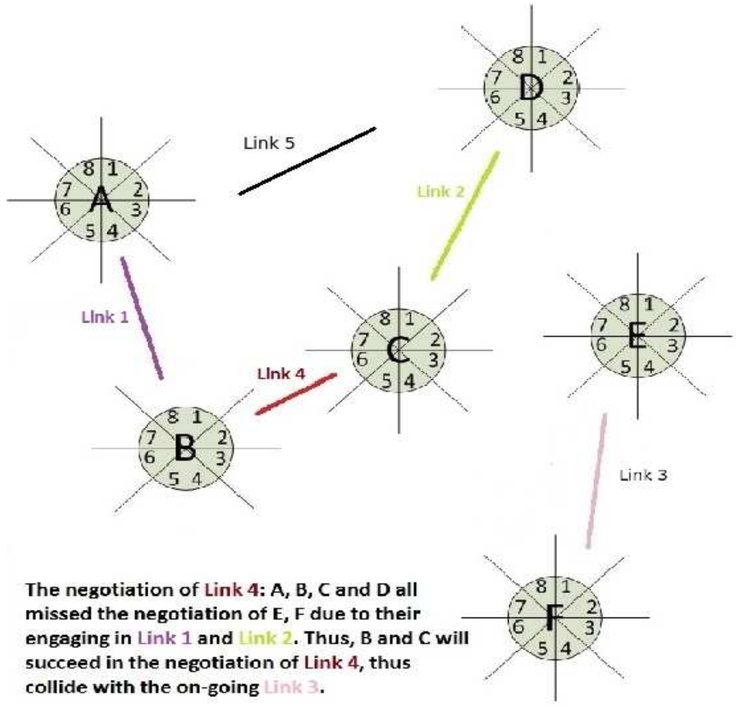

(a) The directional hidden terminal problem.

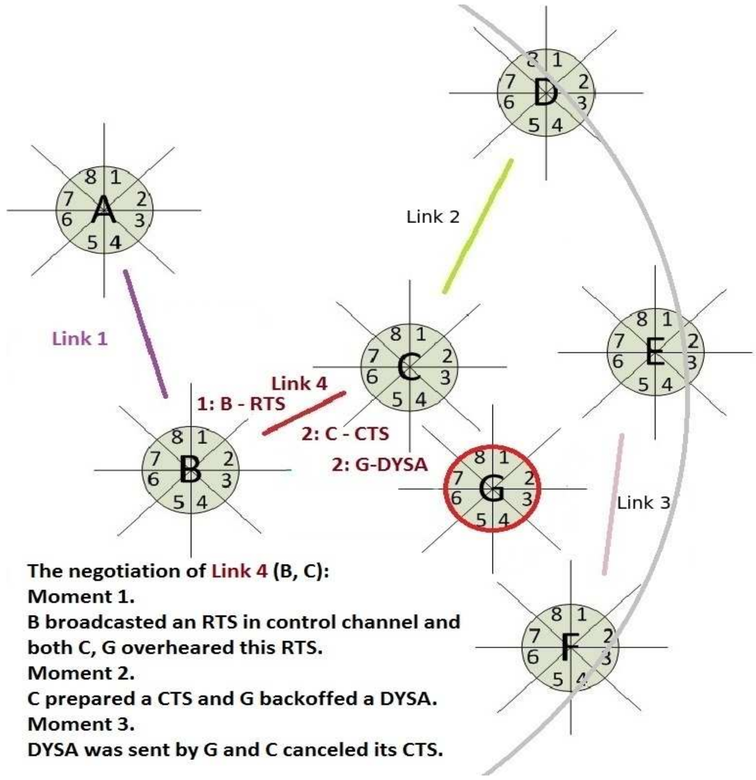

(b) An example to further illustrate the feature of cooperation.

Figure 4.4: Illustration of terminals' cooperation.

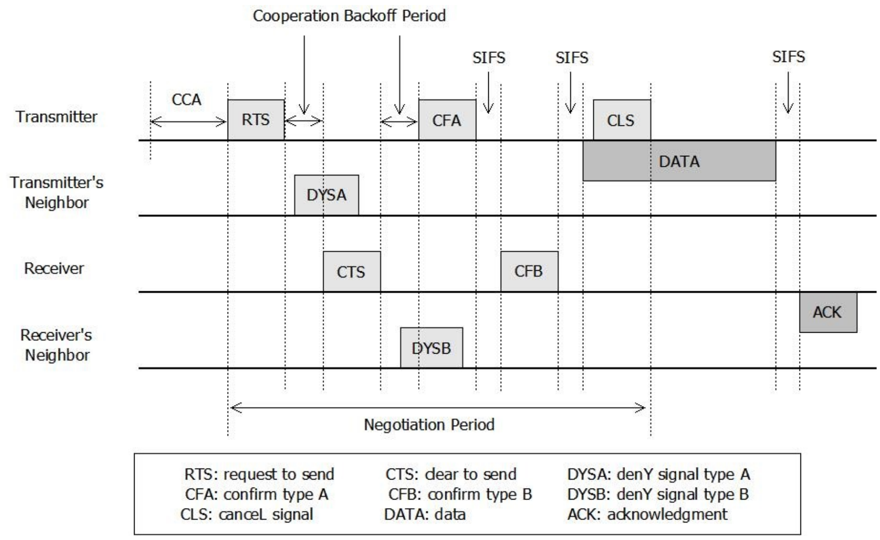

Figure 4.5: Negotiation procedures and data channel handshake of CMDMAC.

4.5 CMDMAC Protocol Design

In this section, CMDMAC will be presented in detail. The basic idea of CMDMAC is information sharing. A dedicated control channel is used while multiple data channels may exist. A four-step negotiation procedure is designed to work on the control channel as shown in Fig. 4.5. With successful negotiation, terminals switch to the selected data channel for data transmission. The terminals will switch back to control channel after the data transmission is completed. The unique feature of CMDMAC is that terminals use their local channel usage records to help Txs and Rxs make decisions and prevent packet conflicts. Moreover, power adaption is used to ensure the transmission ranges in control and data channels to be the same to reduce the collision due to different gains.

In remaining part of this section, related designs for CMDMAC are described along with detailed negotiation procedure and algorithms.

4.5.1 Neighbor Information Table

A Neighbor Information Table (**NIT**) which contains two-hop neighbors' relative location information is maintained by each terminal. An example is shown in Fig. 4.1 according to node G in Fig. 4.4(b). A to G are all wireless nodes. Take C(8, 1) in Node Index G's row as an instance: 8 means that C is in G's Sector 8, and 1 means C is G's up-close neighbor. We say that two neighboring nodes are up-close if they can interfere with each other through their minor-lobes (and set up-close = 1). Now, let's assume C is transmitting in the data channel with sector 6 and G is receiving in the data channel with sector 4 in Fig. 4.4(b). That is, they do not use their main-lobes to point towards each other. As they are up-close nodes, the minor-lobe of C can still interfere with G's current reception. A node can build its one-hop NIT by receiving frames from neighboring nodes with DoA, and broadcast this information within the management frames. Thus, all the nodes can build the two-hop NIT.

For the static topology in this work, we assume that two-hop neighbor information is provided by the management frames of an upper layer protocol. For the mobile topology, we assume that initial two-hop neighbor information is only provided once by the management frames at the beginning of network establishment. After the initial set-up, nodes update the sector information for their neighbors using control frames. In RTS/CTS, transmitter TX_ADDR indicates the relative direction SEC_NO for neighbor RX_ADDR. Thus, terminals that receive RTS/CTS can update the corresponding neighbor information for this transmitter TX_ADDR. Similarly, if DYSA/DYSB is received, neighbor information for TX_ADDR can be updated based on UP_ADDR and UP_SEC. That is, terminal UP_ADDR is in sector UP_SEC of transmitter TX_ADDR. Same information update procedure is also implemented in CFA/CFB. Each node keeps a local table to record non-updated duration for all its neighbors. We use two factors to decide which neighbor to be updated in the current

Node Index	1-Hop Information: Neighbor Index (Sector, Up-Close)
G	E(2, 0), F(4, 0), B(7, 0), C(8, 1)
E	F(5, 0), G(6, 0), C(6, 0), D(8, 0)
F	E(1, 0), G(8, 0), C(8, 0)
B	C(2, 0), E(2, 0), G(3, 0), A(8, 0)
C	D(1, 0), E(2, 0), G(4, 1), F(4, 0), B(6, 0), A(7, 0)

Table 4.1: Neighbor information table.

frame: 1) whether the neighbor's direction information changed recently; 2) time that has lapsed since last update. If there is no neighbor that satisfies factor 1), then 2) can finalize the decision. If there is one neighbor that satisfies factor 1), then this neighbor is updated. If there are multiple neighbors that satisfy factor 1), the one that has waited for the longest time is updated.

4.5.2 Frame Structure

The formats of all frames are shown in Fig. 4.6. Request to send (**RTS**) and clear to send (**CTS**) frames are used to initialize negotiation. In RTS/CTS, the expected data channel and sector are included in channel number (**CH_NO**) and sector number (**SEC_NO**), respectively. The neighbors who hear the RTS/CTS may know which data channel and sector the negotiating pairs expect to use. Moreover, they also update NITs based on the received information. Confirm type A (**CFA**) and confirm type B (**CFB**) are used to confirm reception of CTS and CFA. In CFA/CFB, the duration of link is included in **TIME**. The neighbors who hear these frames can update their DNAV according to their local clocks. Further, updated node address (**UP_ADDR**) and updated node sector (**UP_SEC**) are used to update the NITs. Deny signal type

RTS/CTS

FC (2 bytes)	TX_ADDR (6 bytes)	RX_ADDR (6 bytes)	CH_NO (1 bytes)	SEC_NO (1 bytes)	SEQ_NO (1 bytes)	FCS (2 bytes)

DYSA/DYSB

FC (2 bytes)	TX_ADDR (6 bytes)	RS_ADDR (6 bytes)	RS_CHSEC (2 bytes)	LTIME (2 bytes)	UP_ADDR (6 bytes)	UP_SEC (1 bytes)	FCS (2 bytes)

CFA/CFB

FC (2 bytes)	UP_ADDR (6 bytes)	UP_SEC (1 bytes)	TIME (2 bytes)	SEQ_NO (1 bytes)	FCS (2 bytes)

ACK/CLS

FC (2 bytes)	SEQ_NO (1 bytes)	FCS (2 bytes)

Abbreviation List:

FC: frame control	TX_ADDR: transmitter address	RX_ADDR: receiver address
CH_NO: channel number	SEC_NO: sector number	SEQ_NO: sequence number
FCS: frame check sequence	RS_ADDR: reason node address	RS_CHSEC: active sector and channel
LTIME: left time	UP_ADDR: updated node address	UP_SEC: updated node sector

Figure 4.6: Frame structures of CMDMAC.

A (**DYSA**) and deny signal type B (**DYSB**) are used by cooperators to stop current negotiation. In DYSA/DYSB, reason node address (**RS_ADDR**) identifies the active node who leads to this "veto" frame and left time (**LTIME**) shows the remaining active time of the corresponding link. Acknowledgment (**ACK**) is the same as in IEEE 802.11 protocol. In some special cases, Tx sends CFA but receives no CFB, which means this is an unsuccessful negotiation. Then, cancel signal (**CLS**) is sent by Tx to announce the cancellation of confirmation, e.g. CFA, to Tx's neighbors. CLS has the same structure as ACK.

4.5.3 Negotiation Procedure for Link Establishment

Cooperation is used in CMDMAC to solve the directional multi-channel hidden terminal problem. The basic idea of cooperation is information sharing among Tx, Rx and cooperators. If a cooperator knows that Tx or Rx is negotiating for an occupied channel resource, it may deny this negotiation and provide suggestion on channel selection.

A four-way handshake procedure is performed in the control channel as shown in Fig. 4.5. A Tx with CMDMAC verifies the absence of other traffic before transmitting based on Carrier Sense Multiple Access (**CSMA**). A Tx then initializes a negotiation by sending an RTS. Upon receiving the RTS, the Rx checks its Directional Network Allocation Vector (**DNAV**) [124] to see whether this RTS should be accepted. If the Rx identifies that there are active nodes in the expected sector, it prepares a DYSA; otherwise, it prepares a CTS. At the same time, the Tx's other neighbors, who hear the RTS, also check their DNAVs and the NIT. If a neighbor recognizes that the current negotiation will build a link which may collide with certain on-going data transmission, it prepares a DYSA; otherwise, it keep silent. Then, the Tx's cooperators with DYSAs enter the Cooperation Backoff Period (**CBP**) and execute a CSMA-based mechanism. They randomly back off and the earliest one sends out its "veto" frame. If the medium is busy after the CBP, the Rx cancels its CTS.

If Tx does not receive CTS, the negotiation ends; otherwise, the Tx prepares the CFA to announce the establishment of a new link. Meanwhile, the Rx's neighbors who hear the CTS also check their DNAVs to see whether they should veto to block the expected link. If a neighbor identifies that this expected link may collide with an on-going data transmission, it prepares a DYSB. After the CTS, the Rx's cooperators with DYSBs enter the second CBP. If there is no DYSB and CFA is correctly received by the Rx, the Rx sends CFB to confirm link establishment. In a few cases that Tx sends the CFA but receives no CFB, it needs to send CLS to invalidate previous CFA. Reception of both RTS and CFA (or both CTS and CFB) with no CLS implies successful link establishment. The nodes, which hear the new link establishment, update their DNAVs. With successful negotiation, certain pairs of nodes switch to the data channel and start to transmit after a Short Inter-Frame Space (**SIFS**). As in the original 802.11, if a data packet is received, the Rx replies with an ACK.

A negotiation which consists of potential hidden terminals is stopped by DYSA or DYSB. This solves the multi-channel directional hidden terminal problem. Moreover, with reception of DYSA or DYSB, the Tx knows the reason why it cannot start this link and can take further decisions. This solves the deafness problem.

4.5.4 Algorithm Details

The pseudo codes for Tx, Rx and cooperators are shown in Algorithms 1, 2 and 3, respectively. A terminal is defined to be engaged in a negotiation period (**NP**), when it is cooperating or negotiating as shown in Fig. 4.5. Any attempt to enter multiple NPs is forbidden to protect the on-going negotiations, regardless of whether it is a Tx, Rx or cooperator. There are two ways to exit the current NP: i) wait for it to end; ii) receive or send a DYSA/DYSB.

Algorithm 1 Pseudo code for Tx operation

```
if (Medium is free) then
    Send RTS and enter negotiation period;
    if (Receive CTS after CBP) then
        Defer for CBP;
        if (Medium is free) then
            Send CFA;
            if (Receive CFB after SIFS) then
                Switch to expected sector in the proposed data channel;
                Defer for SIFS and send DATA;
            else
                Backoff and send CLS;
            end if
        else
            Cancel CFA;
        end if
    end if
end if
Exit current negotiation period and start RTS retransmission backoff.
```

Algorithm 2 Pseudo code for Rx operation

```
Receive RTS;
if (Rx is not cooperating or negotiating) then
    Enter negotiation period;
    if (The expected sector in the data channel proposed by RTS is not available)
    then
        Defer for a random period within CBP;
        if (Medium is free) then
            Send DYSA;
        else
            Cancel DYSA;
        end if
    else
        Defer for CBP;
        if (Medium is free) then
            Send CTS;
            if (Receive CFA after CBP) then
                Defer for SIFS and send CFB;
                Switch to expected sector of the data channel proposed by RTS;
            end if
        else
            Cancel CTS;
        end if
    end if
end if
Exit current negotiation period and start RTS transmission backoff.
```

4.5.5 Node Cooperation

An example is shown to illustrate how CMDMAC works in Fig. 4.4(b). Link 3 was established in data channel 1 during the transmissions of links 1 and 2. After the transmissions of links 1 and 2, B wants to initialize a new transmission to C. Thus, B broadcasts an RTS in the control channel and expects to start the transmission in data channel 2. Upon hearing this RTS, C checks its DNAV and accepts this request with preparing a CTS. At the same time, neighbor G checks its DNAV and NIT, and finds that E is active in B's expected sector of the expected data channel. Thus, G backs off and replies a DYSA. Upon receiving the DYSA, B and C know that E is working and may still work for LTIME. Then, B can make its further decision based on the current channel usage situation. As illustrated in this example, neighboring nodes actively cooperate in the process of negotiation to identify the potential hidden terminals and

Algorithm 3 Pseudo code for Cooperator operation

```
Receive packet P;
if ( P == RTS && cooperator is not cooperating in another incomplete negotiation) then
    Enter the cooperation period for this negotiation;
    if (The expected transmission of RTS may lead to channel conflicts) then
        Defer for a random time within CBP;
        if (Medium is free) then
            Send DYSA;
        else
            Cancel DYSA;
        end if
    else
        Defer for 2*(CBP+SIFS)+TimeLength(CTS+CFA
        +CFB);
    end if
else if ( P == CTS && cooperator is not cooperating in another incomplete negotiation) then
    Enter the cooperation period for this negotiation;
    if (The expected transmission of CTS may lead to channel conflicts) then
        Defer a random time within CBP;
        if (Medium is free) then
            Send DYSB;
        else
            Cancel DYSB;
        end if
    else
        Defer for 2*SIFS+TimeLength(CFA+CFB)+CBP;
    end if
end if
if (P == RTS/CTS/DYSA/DYSB) then
    if (Cooperator is in negotiation period) then
        Exit current negotiation period;
    end if
    Start RTS transmission backoff;
end if
```

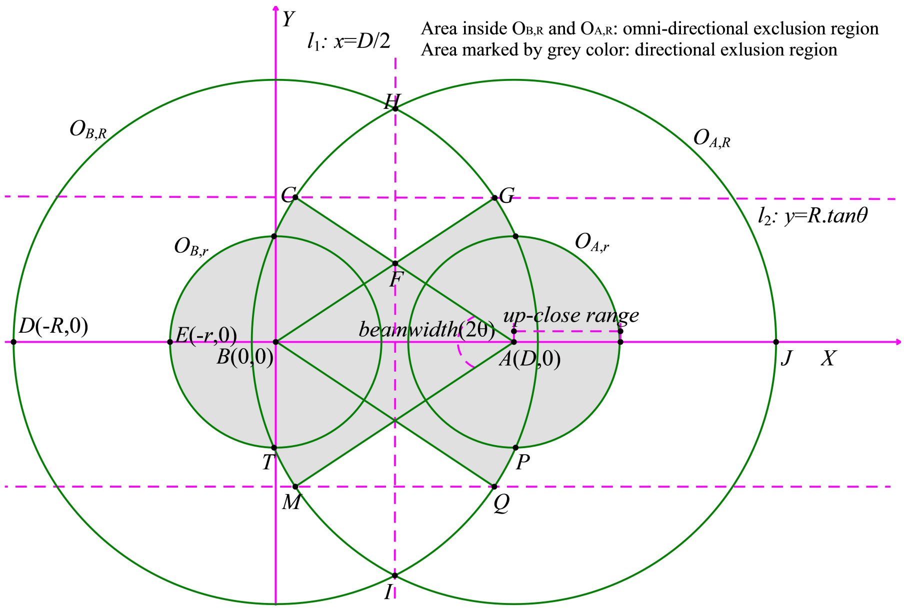

Figure 4.7: Exclusion region of omni-directional and directional transmission.

deaf nodes. This helps to solve the hidden terminal and deafness problems asynchronously without additional devices.

4.6 Protocol Analysis

In this section, we present a theoretical analysis for CMDMAC via three propositions. First, we discuss how minor-lobe interference affects the co-existence condition for directional links. Second, we demonstrate how different antenna beamwidths affect potential spatial sharing gain. Third, we demonstrate that a single dedicated control channel can support multi-channel directional transmissions.

Proposition 4.1: Minor-lobe effects of directional antennas change the co-existence condition for directional links.

Proof: Co-existence means that two links can be active simultaneously in the same location. We define exclusion region as a spatial region in a certain channel where no other active terminals exist except the current active pair of transceivers.

The co-existence condition for different links is that they do not lie in other links' exclusion regions. A general case of exclusion region of a link is shown in Fig. 4.7, where two terminals are located at A and B. The exclusion region of this link in omni-directional mode is covered by $O_{A,R}$ and $O_{B,R}$. The exclusion region in directional mode is covered by the grey area, which is determined by beamwidth and up-close range. P_t is omni-directional transmission power. G_m and G_s are the main- and minor-lobe gains of directional antenna, respectively. h is the height of antenna. *IF_THRESH* is the power threshold of interference range. The up-close range r of antenna with minor-lobe can be obtained by

$$r = \sqrt[4]{\frac{\frac{P_t}{{G_m}^2} \cdot {G_s}^2 \cdot h^4}{\mathit{IF\_THRESH}}}\ , \tag{4.2}$$

given the conditions that $P_R = \mathit{IF\_THRESH}$, $G_T = G_R = G_s$, $H_T = H_R = h$, $P_T = \frac{P_t}{{G_m}^2}$ in (4.1). For any two terminals from different active links in the same channel, if they are in a distance less than or equal to r, they may interfere with each other resulting in packet conflict. Using ideal antennas with G_s being 0, r is 0 and this terminal's exclusion region is fan-shaped. Using non-ideal antennas with G_s being non-zero, r is non-zero and this link's exclusion region is the grey area in Fig. 4.7.

Proposition 4.2: Larger beamwidths provide smaller possibility of spatial sharing for directional ad hoc networks.

Proof: This proposition illustrates the benefit of using directional transmission. A main feature of directional transmission is its higher spatial sharing gain (**SSG**) as compared to omni-directional transmission. We define a metric called possible spatial sharing gain (**PSSG**), which reflects the possible SSG that directional transmission can provide as compared to omni-directional mode. We use the exclusion region ratio between omni-directional and directional transmission to estimate PSSG. As expected, we find that larger beamwidths lead to smaller PSSGs, as shown in Appendix B.1. With the parameters in our simulation, the PSSG with 30° beamwidth is 2.57 as shown in

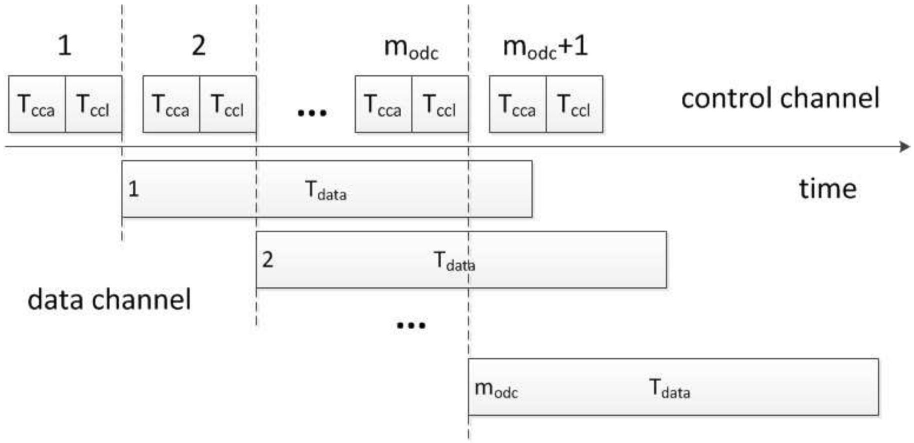

Figure 4.8: Illustration of control channel analysis.

Appendix B.2. In the simulations, we find that the SSG is about 1.4 in saturation, which is smaller than PSSG. This is because that PSSG only estimates the possible gain. Real SSG is a case-by-case index and can be affected by many factors, such as network topology and traffic flow.

Proposition 4.3: One dedicated control channel can be used to coordinate multiple concurrent directional links in a multi-data-channel scenario.

Proof: This proposition illustrates the capability of using directional and multi-channel transmission altogether. Using a dedicated channel facilitates terminals to exchange control messages. However, the drawback is that a single control channel may face congestion and become performance bottleneck when there are many terminals in the network. Without losing generality, we suppose a complete communication process comprises of clear channel assessment (**CCA**), control channel link-establishment handshake, and data channel handshake as shown in Fig. 4.8.

1. T_{cca}: duration of a CCA period.

2. T_{ccl}: duration of a successful control channel link-establishment handshake.

3. T_{data}: duration of a successful data channel handshake.

T_{cca} and T_{ccl} are overhead due to the use of CMDMAC. Assume there are N data channels, the use of control channel leads to bandwidth loss by $\frac{1}{N+1}$. The bottleneck problem of control channel is analyzed as follows. We assume that there are a large enough number of data channels in this area. We also assume that there are a large number of terminals which are trying to establish links in this area. We define a metric m_{odc} (m_{ddc}) to be the maximum number of omni-directional (directional) data channels that can be simultaneously used for a given protocol. For m_{odc}, we assume that data transmission is done in omni-directional mode. Based on Fig. 4.8, we have

$$m_{odc} = \left\lceil \frac{T_{data}}{T_{cca} + T_{ccl}} \right\rceil . \tag{4.3}$$

As there are a large enough number of data channels, thus $T_{cca} = T_{cca}^{min}$. As T_{cca}^{min} and T_{ccl} are fixed for CMDMAC, m_{odc} is mainly determined by T_{data}, which is dominated by the data payload size. For the directional case, we assume that there are SSG concurrent links in one data channel in the given area. We can estimate m_{ddc} as

$$m_{ddc} = \frac{m_{odc}}{\text{SSG}} . \tag{4.4}$$

According to the PHY parameters in our simulation [142], we have $T_{ccl} = 138.5$ bytes, $T_{cca} = 37.5$ bytes, $T_{data} = 1573.5$ bytes. Thus, we get $m_{odc} = 8.94$. If we take SSG $=$ PSSG, then m_{ddc} is 3.47. However, we find that the SSG is around 1.40 and the corresponding m_{ddc} is 6.38 in the simulations. Moreover, if we increase the value of data payload length or use shorter PLCP preamble and headers, CMDMAC can support larger number of data channels. Since both 3.47 and 6.38 are larger than 1, this result demonstrates that one control channel is capable of coordinating multiple directional links in a multiple data channel network as described in *Proposition 4.3*.

Simulator	NS2
Tx power (CC/DC)	24.5 dBm/ 4.5 dBm
Rx threshold	-64.375 dBm
Capture threshold	10 dB
Transmission rate	1 Mbps
Cooperation backoff period	40 μs
G_m/G_s	10 dB
Propagation model	two-ray model
Topology dimensions	500 m * 500 m
Simulation time	120 s

Table 4.2: Simulation parameters for CMDMAC.

4.7 Performance Evaluation

In this section, we evaluate the performance of CMDMAC using NS-2. For comparison, we define a non-cooperative version of CMDMAC called Non-Cooperation Directional MAC (**NCDMAC**). The only difference between CMDMAC and NCDMAC is whether or not the neighboring nodes cooperate in solving the hidden terminal and deafness problems. Specifically in NCDMAC, the neighboring nodes do not send DYSA/DYSB to cooperate. We also compare against with omni-directional 802.11 protocol provided by NS-2.

4.7.1 Simulation Configuration

The simulation parameters are shown in Table 4.2. The transmission and interference range are determined by the value of $\frac{G_m}{G_s}$ for the two-ray propagation model. By adapting Tx powers for control and data channel, the transmission ranges in both control and data channel are made 250m. K nodes are randomly located and K non-disjoint User Datagram Protocol (**UDP**) flows with constant rate are generated as data sources, where each node is the source and destination of one flow. UDP flows mean that the protocol used in transport layer is UDP. Non-disjoint means that nodes cannot participate as both sources and sinks in the network. The capture effect is implemented based on the comparison of reception power in NS-2. Other parameters not mentioned are set as default values in NS-2.

In the field of MAC protocol design, simulations are usually used to support the argument and proposed protocols. First, results of simulations are usually used to compare and study the benefits of the new protocol. Second, the overall performance of network can be affected by a lot of factors, especially the topologies. However, no one can simulate all the topology settings. Thus, researchers usually generate random topologies. It is commonly accepted to average results on 10 to 20 simulations and set simulation duration to be around 100 seconds, such as in the popular benchmarks [3, 125, 129] in the field of MAC protocol design. The duration is set as 200 seconds, because 200 seconds are enough for network initialization and entering into data transmission period. Since the network initialization is quick in NS2 simulations, 200 seconds are long enough for testing the accurate throughput with constant flow rates for a topology. This setting is also consistent with [3, 125, 129] which are popular benchmarks in the field of MAC protocol design.

Two performance metrics are examined to compare CMDMAC and NCDMAC: i) end-to-end (aggregate) throughput, defined as the total data delivered from source to destination divided by the simulation duration; ii) packet error rate (PER), defined as the ratio of number of packets not correctly received to number of packets sent in MAC layer. We use average aggregate throughput as it is a popular metric. It also reflects the average end-to-end delay for the unsaturated networking cases. We use PER, as it

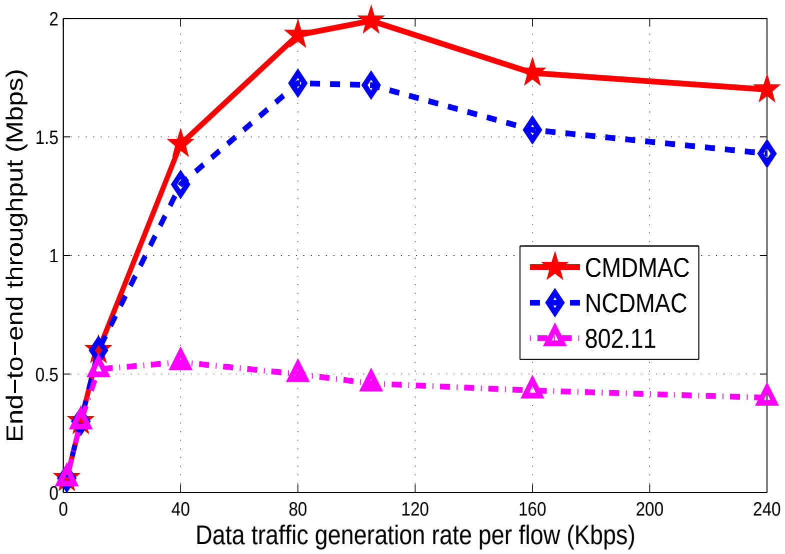

Figure 4.9: Impact of traffic load in single-data-channel scenarios.

is a one-hop metric and can reflect how much our cooperation reduces the data packet collisions. We also talk about saturation break point, as the point before which all the data demands can be satisfied. Packets may accumulate and queue occupancy may grow at some nodes after this point.

4.7.2 Single Data Channel Scenario

In this subsection, we show the simulation results of scenarios with single data channel. Impact of traffic load, packet sizes and beamwidths are examined.

In Fig. 4.9, we show the impact of different traffic loads. We randomly deploy 50 nodes and vary the traffic load of each flow from 1.2 Kbps to 240 Kbps. Beamwidth is set as 30° and data payload size is 1500 bytes. When traffic load is light, throughput is nearly the same for CMDMAC and NCDMAC. Then, we see that 802.11 quickly saturates at around 0.5 Mbps while CMDMAC and NCDMAC keeps going up. As traffic load increases, the throughput difference between CMDMAC and NCDMAC becomes larger. CMDMAC reaches saturation with heavier traffic load

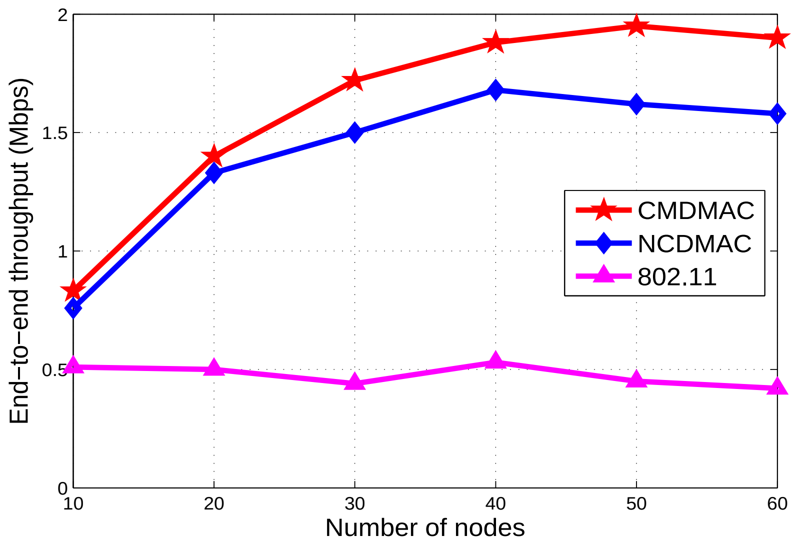

Figure 4.10: Impact of node density.

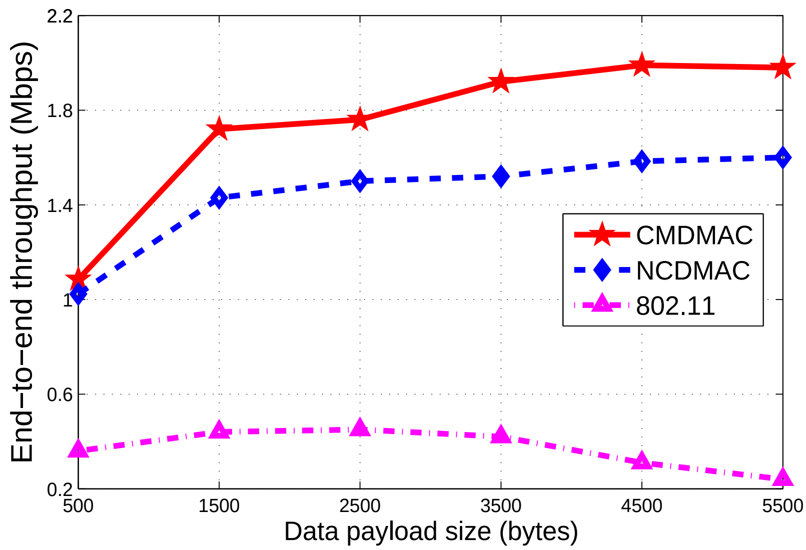

Figure 4.11: Impact of packet size in single-data-channel scenarios.

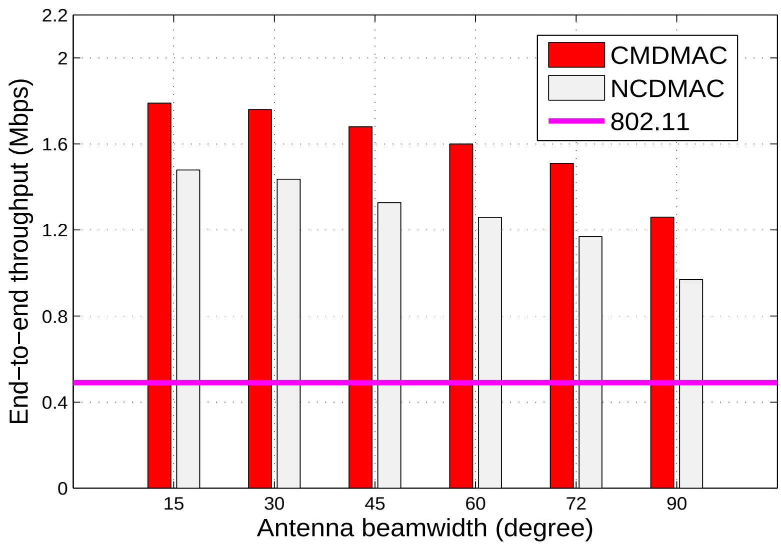

Figure 4.12: Impact of beamwidth in single-data-channel scenarios.

and gets 15% larger throughput as compared to NCDMAC. We observe that the maximum throughput is about 2 Mbps which is smaller than 5 Mbps. This is because the network is saturate around 100 Kbps.

In Fig. 4.10, we show the impact of different node densities. We randomly deploy 10 to 60 nodes and set the traffic load of each flow to be 100 Kbps. Beamwidth of antenna is set to be 30° and data payload size is 1500 bytes. It is clearly seen that CMDMAC outperforms NCDMAC. We see that difference between CMDMAC and NCDMAC is smaller when node density is low as compared to that when node density is high. It is expected that there will be fewer packet conflicts when node density is low, thus CMDMAC may not bring much benefit. A simple scenario is that there is no conflict if there is only a pair of nodes. There is no need for cooperator in that case. If there is no cooperator, CMDMAC is the same as NCDMAC. However, we may expect cooperators to exist and help eliminate packet conflicts, if density is high.

In Fig. 4.11, we show the impact of different data packet sizes. We randomly deploy 50 nodes and vary the data payload size from 500 to 5500 bytes. Beamwidth is set as 30° and traffic load is 240 Kbps. First, the end-to-end throughput keeps increasing with using larger packet sizes. Both CMDMAC and NCDMAC benefit from larger data packet sizes because the larger packet size offsets handshake overheads more effectively. Second, we notice that the throughput difference between CMDMAC and NCDMAC becomes larger as packet size grows. With larger size packets, the number of packets reduces. Meanwhile, the collision of one packet becomes more harmful to throughput. The throughput reduction of 802.11 is due to similar reason. For the case of packet size equals to 5500 bytes, CMDMAC outperforms NCDMAC by 20%.

In Fig. 4.12, we show the impact of different beamwidths. We randomly deploy 50 nodes, set the data rate of each flow at 240 Kbps (50 flows) and vary the beamwidths from 15° to 90°. We notice that CMDMAC always outperforms NCDMAC. Moreover, we see that the throughput with wider beamwidths are smaller than that with narrower beamwidths. This is because that narrower beamwidths provide larger link co-existence possibilities as explained in *Proposition 2*, and more co-existence links support larger throughput. Further, we find that the largest spatial sharing gain for CMDMAC with 15° sector to omni-directional 802.11 is about 350%.

4.7.3 Multiple Data Channels Scenario

In this subsection, we show the results of the simulations for the multiple data channels scenario. We study the impact of traffic load, data packet sizes and channel numbers.

In Fig. 4.13, we show the impact of different traffic loads. We randomly deploy 100 nodes and fix the number of data channel as 4. Beamwidth is set as 30° and packet payload size is 1500 bytes. In Fig. 4.13(a), the basic trends of throughput performance are very similar as those with a single data channel. However, we see

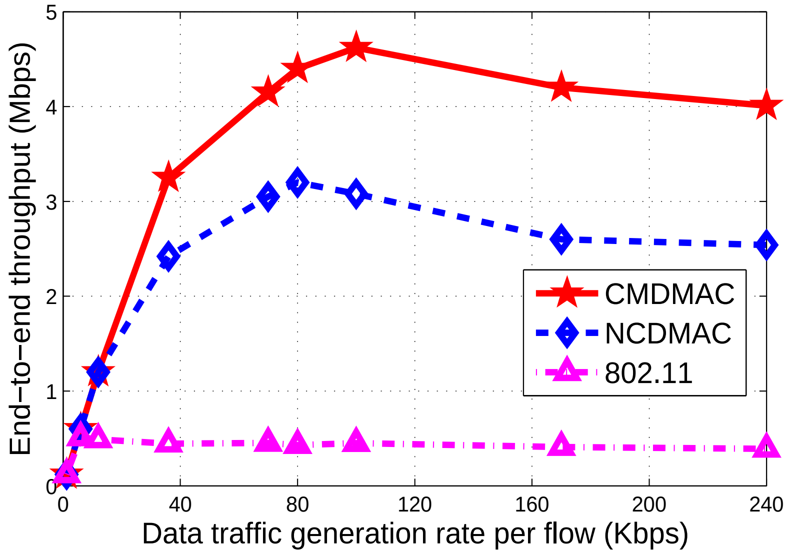

(a) Throughput with different traffic loads.

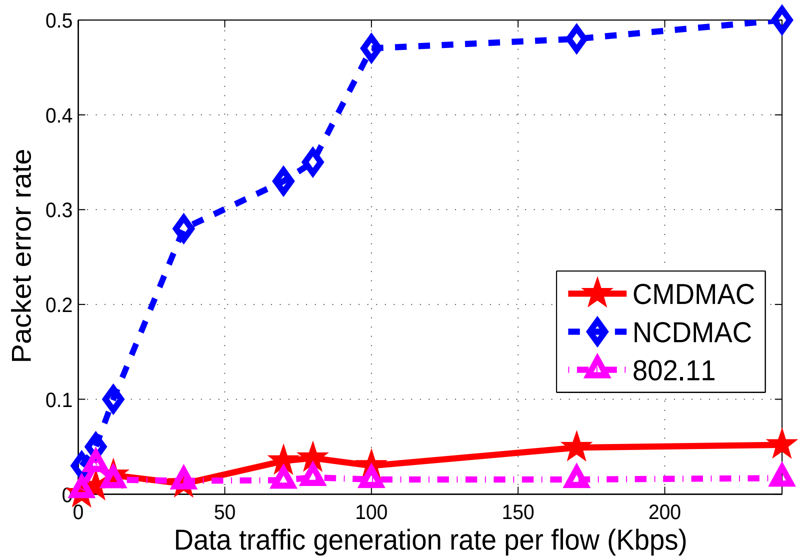

(b) Packet error rate with different traffic loads.

Figure 4.13: Impact of traffic load for multiple data channel scenario.

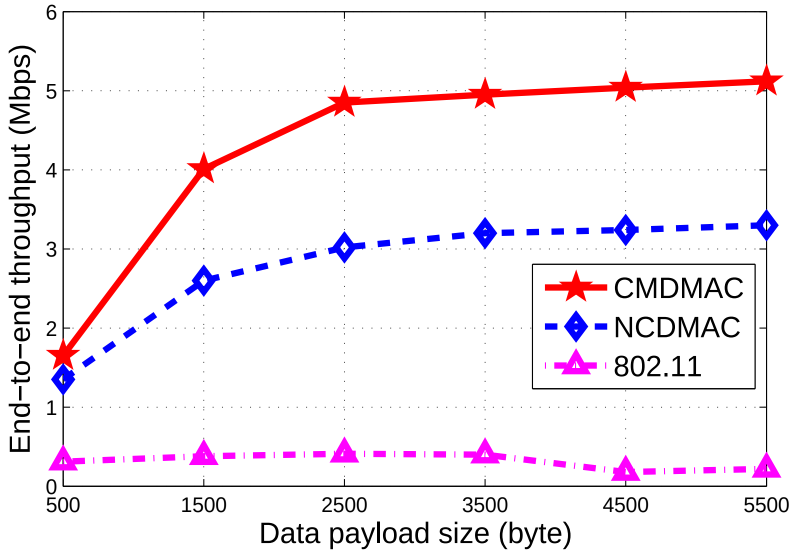

(a) Throughput with different data payload sizes.

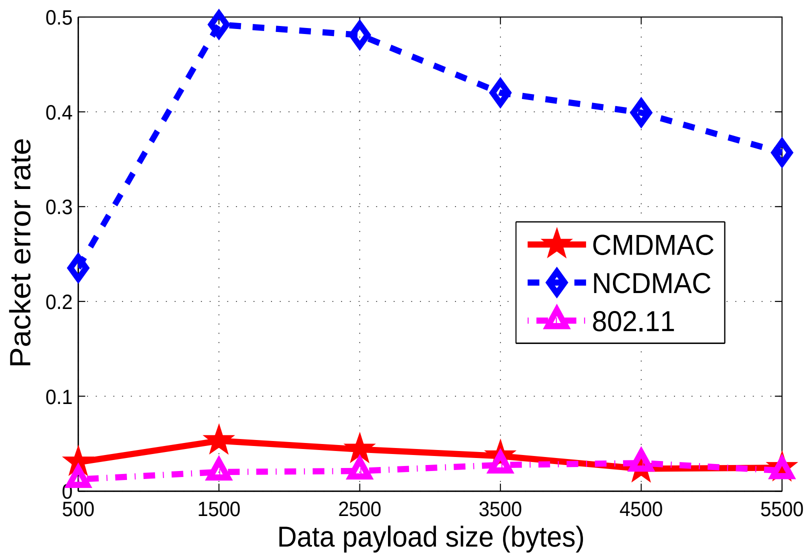

(b) Packet error rate with different data payload sizes.

Figure 4.14: Impact of data payload size for multiple data channel scenario.

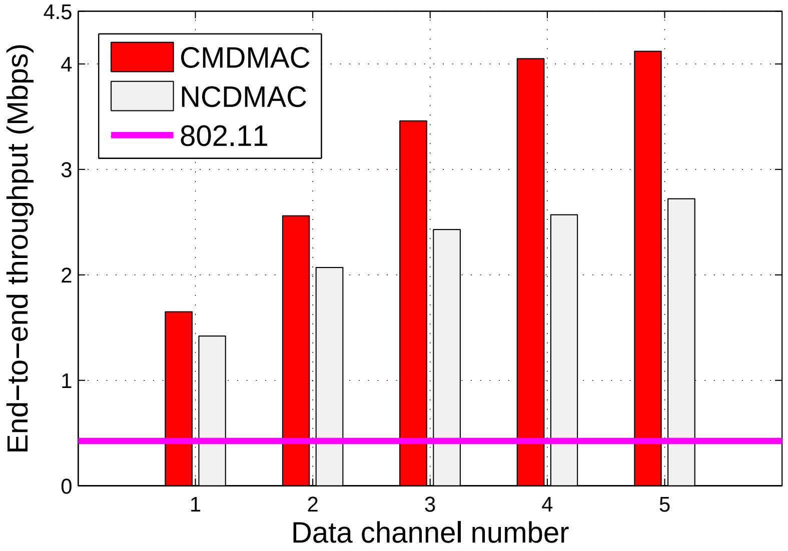

(a) Throughput with different data channel numbers.

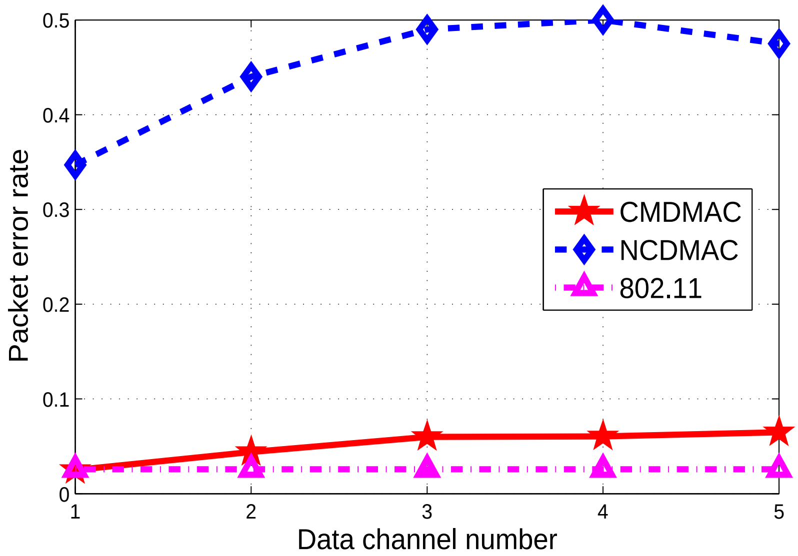

(b) Packet error rate with different data channel numbers.

Figure 4.15: Impact of number of data channels for multiple data channel scenario.

that the difference between CMDMAC and NCDMAC is much larger than that in the single-data-channel scenario. The reason is as follows. In the single-data-channel case, a Tx with CMDMAC reaps benefit only from DYSA/DYSB by canceling its wrong negotiation. Then, the Tx does nothing but waits for the on-going links to end. However, in the multi-data-channel case, this Tx reaps benefit in two fold: i) cancel current negotiation; and ii) back off and then initialize a new negotiation for another potentially free channel immediately. We observe that CMDMAC outperforms NCDMAC by 42% at saturation break point and 56% at heavy traffic load of 240 Kbps per flow. In Fig. 4.13(b), we see that CMDMAC outperforms NCDMAC for all cases and NCDMAC's PER keeps increasing as traffic load becomes higher. It is also noticed that 802.11 is better than both CMDMAC and NCDMAC in terms of PER. This is because 802.11 is so conservative that a node keeps silent as long as there is another active node inside its carrier sensing range, which also leads to worse spatial sharing and throughput performance.

In Fig. 4.14, we show the impact of different data payloads. 100 nodes are randomly deployed and traffic load is set as 240 Kbps. Data channel number is 4, beamwidth is 30°, and packet payload size is 1500 bytes. In Fig. 4.14(a), we see that the end-to-end throughput keeps increasing with using larger packet sizes. Both CMDMAC and NCDMAC benefit from larger data packet sizes because the larger packet size offsets handshake overheads more effectively. We also notice that the throughput difference between CMDMAC and NCDMAC becomes larger as packet size grows. With larger size packets, the number of packets reduces. Meanwhile, the collision of one packet becomes more harmful to throughput. In Fig. 4.14(b), PERs are stable around 5% for both CMDMAC and 802.11. For NCDMAC, it first increases and then slowly decreases. This phenomenon is due to two contradicting factors: longer data packets are more susceptible to channel conflicts; longer data packets keep nodes on data channels longer hence fewer nodes will be able to start new communication which reduces the possibility of channel conflicts.

In Fig. 4.15, we show the impact of different data channel numbers. One hundred nodes are randomly deployed and traffic load per flow is set to 240 Kbps. Beamwidth is set as 30° and packet payload size is 1500 bytes. In Fig. 4.15(a), we see that aggregate throughput increases with the number of data channels. This is as predicted in to *Proposition 4.3*. Since aggregate throughput is an end-to-end issue and can be affected by topology, routing protocol and many other factors in addition to MAC, we are not surprised that the increase is not linear with the number of data channels. In Fig. 4.15(b), we show PER for CMDMAC, NCDMAC and 802.11. While 802.11 provides nearly 2% PER, that of CMDMAC is around 5%. For NCDMAC, PER increases with more data channels at first. As the number of data channel keeps increasing to 5, the PER starts to reduce slightly. To understand this, we assume there are an infinite number of data channels. Then, the collision possibility should be zero as each link can get a free channel. This special case gives the hint for the slight decrease with 5 data channels.

4.7.4 Mobile Scenario

In Fig. 4.16, the impact of mobility is studied for both single and multiple channel scenarios. The traffic load per flow is set to 240 Kbps. The number of nodes are 50 and 100 for 1 and 4 data channels, respectively. The beamwidth is set as 30° and the traffic load is 240 Kbps. The topology dimension is 500 meters by 500 meters. The packet payload size is 1500 bytes. The NIT updating mechanism in Subsection 4.5.1 is used. As compared to static scenario (in Fig. 4.15(a)), the performance degradation is about 11% for the single-data-channel case and 15% for the multi-data-channel case, at a speed of 4 m/s. This is due to the reason that the cooperators do not have the correct location information. Thus, they may fail to recognize the potential hidden terminals

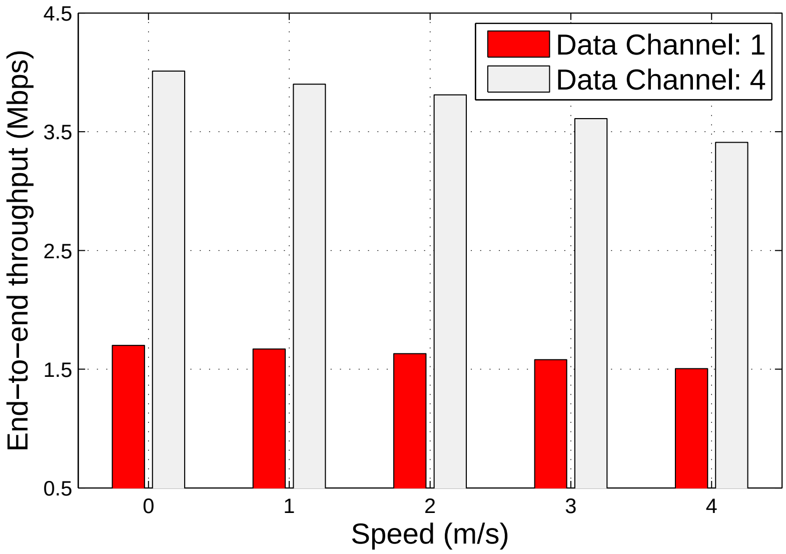

Figure 4.16: Impact of mobility.

or they may deny the negotiation which should be permitted. Both these two actions may harm the performance.

4.7.5 Comparisons with DMAC, CDMAC, MMAC and CAMMAC

We compare CMDMAC with other benchmark directional MACs and multi-channel MACs. As we cannot compare to all the existing protocols, we perform a comparison with the more popular benchmark protocols, which provide clear algorithm description and simulation settings. Therefore, it is convenient for future researchers to compare our work with other non-mentioned protocols who also compare to those benchmark works. All of the comparisons use a single half-duplex transceiver while CDMAC [133] and MMAC [71] require clock synchronization. For the purpose of comparison, all results are with the same parameters settings as reported in the relevant papers.

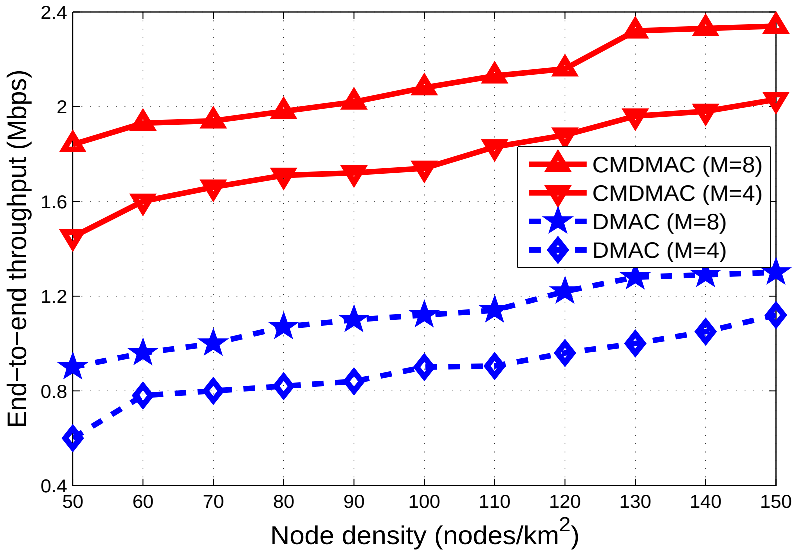

Figure 4.17: Comparison with DMAC. (channel capacity: 2 Mbps; packet size: 1000 bytes; traffic load per flow: 25 packets/second; G_m/G_s: 30 dB; number of nodes: 25; number of flows: 25; number of data channels: 1.)

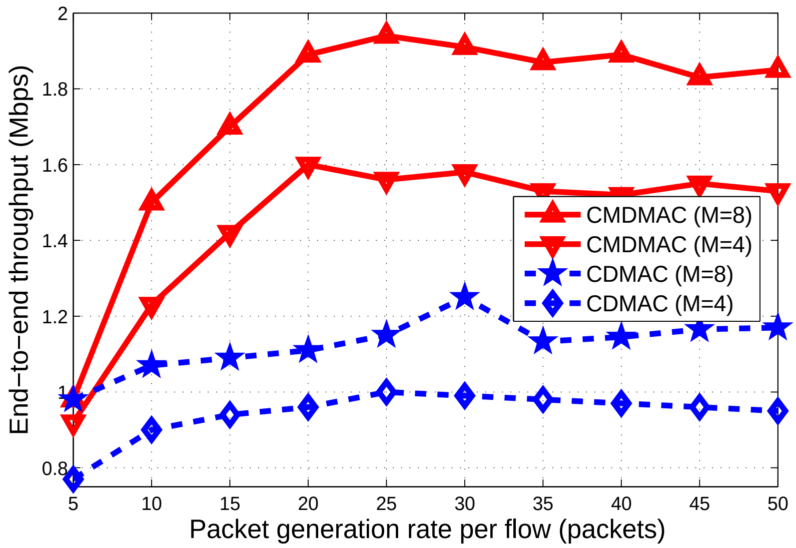

Figure 4.18: Comparison with CDMAC. (channel capacity: 2 Mbps; packet size: 1000 bytes; topology dimensions: 645 m * 645 m; G_m/G_s: 30 dB; number of nodes: 25; number of flows: 25; number of data channels: 1.)

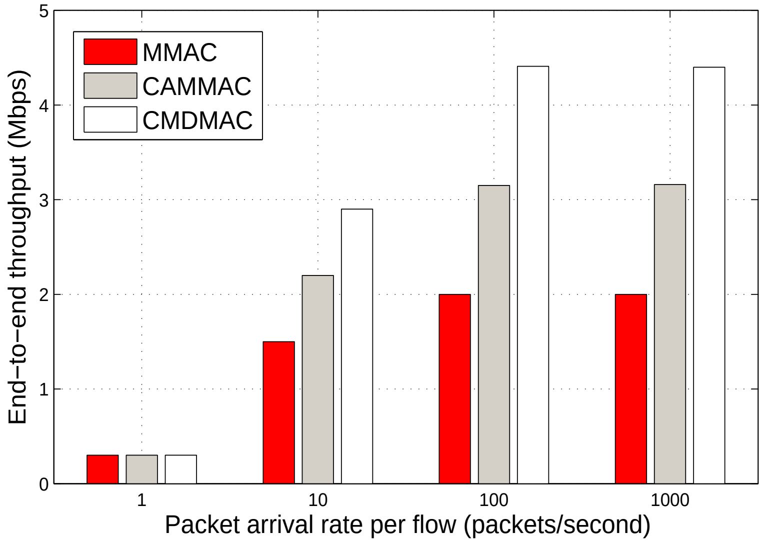

Figure 4.19: Comparison with MMAC and CAMMAC. (channel capacity: 2 Mbps; packet size: 1024 bytes; number of channels: 4; topology dimensions: 500 m * 500 m; number of nodes: 100; number of flows: 40; G_m/G_s: 10 dB; sector width: 30°.)

4.7.5.1 Comparison with DMAC [124]

DMAC is proposed for asynchronous directional networks and often used as benchmark for studying other directional MAC protocols. The number of nodes is fixed while the network size is adjusted according to the nodes densities in this comparison. In Fig. 4.17, M represents the sector number. 25 nodes are deployed randomly and 25 flows are initiated. It is assume that there is only 1 data channel and channel capacity is 2 Mbps. Packet size is 1000 bytes and Traffic load per flow is set as 25 packet/second. It is clear that CMDMAC outperforms DMAC in terms of throughput with both 45° and 90° beamwidths for all the nodes densities. As a benchmark in directional MAC design, the shortfall of DMAC is mainly in the carrier sensing scheme. Although directional virtual carrier sensing is proposed in DMAC design, this function is not comprehensive and DMAC mainly depends on pure carrier sensing to determine whether the channel is available. With this kind of carrier sensing approach, DMAC cannot solve the deafness and hidden terminal problems properly, which leads to lower performance as compared to CMDMAC. We also notice that only one channel is needed to implement DMAC, while at least two channels are needed to implement CMDMAC. We observe that there are multiple channels available in the unlicensed band, for example 802.11a has twelve channels. Therefore, it is no problem if one of them is dedicated as the control channel. Moreover, our CMDMAC can work in a multi-channel scenario and benefit from the multiple data channels, while DMAC does not do that.

4.7.5.2 Comparison with CDMAC [133]

CDMAC is proposed for synchronous directional networks by using contention window to solve hidden terminal problem. The packet generation rate is varied from 5 to 50 in this comparison. In Fig. 4.18, M represents the sector number. 25 nodes are deployed randomly in a 645 meters by 645 meters area. There is 1 data channel with capacity as 2 Mbps. Packet size is set as 1000 bytes. Ratio of G_m towards G_s is set as 30 dB. And the flow number is 25. For both CMDMAC and CDMAC, it is not surprising that narrower beamwidths provide better performance by providing higher spatial sharing possibilities. Also, it is shown that CDMAC quickly saturates with higher packet generation rate, while CMDMAC can provide about 56% and 60% larger throughput performance than CDMAC (M=8) and CDMAC (M=4) respectively. Again, we want to point out that CDMAC works on a single channel while CMDMAC works with separate control channel and data channel. However, we also notice that the advantage of CMDMAC also comes with solving the hidden terminal problem. In CDMAC, the network is divided into a master-slave structure. While the deafness and hidden terminal problems are solved within a local group hosted by a master, there will be packet collisions at the borders of different groups.

Moreover, to deliver a packet from one group to another, a node has to wait for a long time to join another group. Further, since CDMAC uses clock synchronization and divides the time into master node selection window, slaves iterative contention window and data transmission window, it is hard to decide the optimum values of the window sizes. For example, a long contention window will be wasted under light load, while the time may not be enough for the slaves to reserve data links if the contention is severe.

4.7.5.3 Comparison with MMAC [71] and CAMMAC [3]

We compare our CMDMAC to two multi-channel MACs, MMAC and CAMMAC. In this comparison, CMDMAC and CAMMAC use 3 data channels to maintain the fairness towards MMAC. CMDMAC uses a 30° antenna beam. MMAC needs clock synchronization. In Fig. 4.19, 100 nodes are randomly deployed in a 500 meters by 500 meters area. 40 data flows are initiated in the network. G_m/G_s for each antenna is 10 dB and sector width is 30°. There are 4 channels with capacity being 2 Mbps. Packet size is 1024 bytes.We see that these three MACs have the same throughput for light-load networking scenarios. For the saturated case, CMDMAC achieves about 2.23 times the throughput of MMAC. While CAMMAC can be understood as an omni-directional version of CMDMAC, CMDMAC with 30° achieves about 1.40 times the throughput of CAMMAC. This is due to the spatial sharing gain provided by directional transmission.

4.8 Chapter Summary

Observing that multiple radios or network-wide synchronization may not be available in directional ad hoc networks, we propose CMDMAC which employs single radio to solve deafness and hidden terminal problems asynchronously. In CMDMAC, idle terminals in the control channel actively participate in the negotiation procedures of their neighbors and help them identify available data channels. Theoretical analysis is provided and NS-2 simulations are used to validate the protocol's performance. Comparison with popular benchmarks shows that CMDMAC reduces PER effectively and provides better throughput performance.

Chapter 5

Conclusions and Future Work

In this chapter, we summarize the main contributions of this thesis, and present some suggestions for future work.

5.1 Conclusions

In this thesis, we have focused on studying link scheduling and MAC techniques with an aim to improve throughput performance by cooperation in wireless networks. Since cooperation is a very broad concept, we confined it within MAC sublayer in this thesis. Several topics have been investigated and the results of performance analysis have shown that cooperation helps improve throughput.

In Chapter 2, we considered using cooperative relay service in cellular networks. In such cellular networks, we proposed that UEs might be served by multiple MTs from same or different cellular providers. With cooperative relay service among neighboring MTs, UEs might have better networking experience by employing bandwidth aggregation. We extended the opportunistic link scheduling algorithm to maximize overall throughput of cooperative cellular networks, and formulated it as an optimization problem. The optimal solution was provided and the various proofs were established. Besides theoretical analysis, comprehensive simulations were performed. The results have demonstrated that the proposed cooperative opportunistic scheduling algorithms can achieve better throughput performance as compared to the non-cooperative schemes. We also observed that the fairness requirement was met for all UEs no matter whether they were served by single or multiple MTs. In summary, this work has provided a promising scheduling algorithm which introduces cooperation in cellular networks.

In Chapter 3, we investigated using cooperative relay service in 60 GHZ WPANs. In the studied 60 GHz WPAN, we proposed to use cooperative data relay service to improve networking throughput performance. The reasons for studying 60 GHz WPAN are as follows. First, transmission in 60 GHz frequency band experiences severe path loss due to the channel property. Second, transmission in this band possessed weak signal strength once the line-of-sight path get blocked by obstacles. We delved into the throughput maximization problem with considering different traffic demands, namely achievable and bursty demand. With joint treatment of relay assignment and link scheduling, throughput maximization issues in cooperative 60 GHz WPAN were formulated as linear programming problems. The problems were then solved by the column generation method, and comprehensive simulations were performed for both cooperative and non-cooperative WPANs. Further, the effects of using different spatial reuse strategies and antenna models were demonstrated. The results have shown that cooperative WPANs outperform non-cooperative ones in terms of throughput in all cases. The proposed cooperative scheme was also compared to an existing benchmark and demonstrated better throughput performance. This work has provided a pioneering investigation on throughput maximization with jointly considering relay assignment and link scheduling in cooperative 60 GHz WPANs.

In Chapter 4, we studied the use of cooperative information sharing to design an efficient MAC protocol which eliminates packet conflicts in multi-channel directional ad hoc networks. The main challenges in designing MAC protocols for ad hoc networks are the hidden terminal and deafness problems. The mainstream solution towards these problems is either using a radio dedicated for control messages or time synchronization for regulating terminals' behavior. Observing that multiple radios or network-wide synchronization might not be available in multi-channel directional ad hoc networks, we proposed CMDMAC which employed single radio to solve deafness and hidden terminal problems via the use of asynchronous cooperation. In CMDMAC, idle terminals in control channel actively participate in negotiation procedures of their neighbors and assisted them in identifying available data channels based on local channel usage records. Theoretical analysis was provided and NS2 simulations were used to validate CMDMAC's performance. The results have shown that CMDMAC can significantly reduce packet conflicts and effectively improve throughput performance as compared to non-cooperative NCDMAC. Further, comparison with popular benchmarks has demonstrated that CMDMAC may provide better throughput performance. This part of work has deepened the understanding of using cooperation and information sharing in multi-channel directional ad hoc networks.

5.2 Future Work

In the future, we propose to research following aspects to investigate cooperation in wireless communication. Below four topics are highlighted which the researchers may work on in the near future.

5.2.1 Cooperative Uplink Scheduling in Cellular Networks

In this thesis, we investigated cooperative downlink scheduling in cellular networks. However, in practice, there are also cases when uplink transmission is needed. For example, people may update their Twitter or Facebook by writing or uploading photos in their mobile terminals. To further improve uplink transmission rate, we would like to study the scenario when idle mobile terminals can be used to participate in the uplink transmission of other terminals in cellular networks.

5.2.2 Link Scheduling with Physical Interference Model

In this thesis, we assumed that protocol interference model is used when we study the throughput maximization problems in 60 GHz WPAN. However, in practice, interference from different devices may get accumulated in such cases, protocol interference model may not be accurate in calculating SNRs for transceivers. To overcome this inaccuracy, we would like to investigate throughput maximization problem in 60 GHz WPAN with a physical interference model.

5.2.3 Energy-Efficient Cooperative Directional MAC

In this thesis, the main focus of using cooperation in CMDMAC was to reduce packet conflicts and improve networking throughput. However, in practice, another important concern in designing MAC protocol for directional ad hoc networks is energy efficiency. With all devices trying to participate in solving hidden terminal problem for neighbors, the energy consumption can be large because they cannot enter the idle mode. We would like to design and develop a scheme which can make CMDMAC more energy-efficient.

5.2.4 Cooperative Transmission in Multi-Homing Environment

In this thesis, we have focused on using cooperation in homogeneous networks. In practice, one mobile device may have multiple access interfaces, and this device is often termed as a multi-homing device. For example, there are usually at least one WiFi radio and one cellular radio in most smart phones. We also observe that different wireless technologies are usually used separately. This makes having multiple access interfaces less meaningful. We would like to investigate schemes which can make multiple interfaces cooperate in data transmission.

Appendix A

Appendices to Chapter 2

A.1 Proof of Proposition 2.1

$Q^\sharp$ is used to represent the schemes except Q^* to gain the supported rate of UE_j. As mentioned in Section 2.3, for any timeslot of any UE with SMMTSU, we have

$$R_j = \max \left(D_i \cdot \mathbf{1}_{\{\mathrm{MT}_i \in \mathrm{UE}_j\}} \right)_{i=1}^{N}. \tag{A.1}$$

With $Q^\sharp$, we have

$$R_j^{'} = D_{\{i=Q^\sharp (D_i \cdot \mathbf{1}_{\{\mathrm{MT}_i \in \mathrm{UE}_j\}})_{i=1}^{N}\}}. \tag{A.2}$$

Here, we have changed the problem of scheduling MTs with some of them serving the same UEs into the problem of scheduling UEs. We could treat UEs as MTs, because data rate of each UE at any timeslot has been specified. For $j = 1, 2, ..., M$, we set $H_j = R_j$, $H_j^{'} = R_j^{'}$, $\varphi_j = \varphi_j^{'} = \tau_j$, where $\boldsymbol{H}$ and $\boldsymbol{H}'$ are the supported data rate vectors for two set of MTs and $\boldsymbol{\varphi}$ and $\boldsymbol{\varphi}'$ are the fairness requirements. Based on [1], it is known that their scheduling policy $Q^{''}$ is optimal for the scenario where there is no UE_B, we have

$$E\left[\sum_{j=1}^{M} R_j \cdot \mathbf{1}_{\{Q=j\}}\right] = E\left[\sum_{i=1}^{N} D_i \cdot \mathbf{1}_{\{Q=j\ \&\ Q^*=i\}}\right] = E\left[\sum_{j=1}^{M} H_j \cdot \mathbf{1}_{\{Q''=j\}}\right], \tag{A.3}$$

$$E\left[\sum_{j=1}^{M} R_j^{'} \cdot \mathbf{1}_{\{Q=j\}}\right] = E\left[\sum_{i=1}^{N} D_i \cdot \mathbf{1}_{\{Q=j\ \&\ Q^{\sharp}=i\}}\right] = E\left[\sum_{j=1}^{M} H_j^{'} \cdot \mathbf{1}_{\{Q''=j\}}\right]. \quad \text{(A.4)}$$

Based on $H_j \geq H_j^{'}$,

$$E\left[\sum_{j=1}^{M} H_j \cdot \mathbf{1}_{\{Q''=j\}}\right] \geq E\left[\sum_{j=1}^{M} H_j^{'} \cdot \mathbf{1}_{\{Q''=j\}}\right]. \quad \text{(A.5)}$$

Thus,

$$E\left[\sum_{i=1}^{N} D_i \cdot \mathbf{1}_{\{Q=j\ \&\ Q^{*}=i\}}\right] \geq E\left[\sum_{i=1}^{N} D_i \cdot \mathbf{1}_{\{Q=j\ \&\ Q^{\sharp}=i\}}\right]. \quad \text{(A.6)}$$

For we do not specify $Q^{\sharp}$, our policy is optimal.

A.2 Proof of Proposition 2.3

We assume that there are N MTs and M UEs in this system and $M < N$ which means there exist UE_Bs. The D_i, R_j, $\overline{R}_j$ and C_j are defined the same as in Section 2.3. For the overall system, we have

$$E\left[\sum_{j=1}^{M} R_j \cdot \mathbf{1}_{\{Q=j\}}\right] = \sum_{i=1}^{N} E\left[D_i \cdot \mathbf{1}_{\{Q=j\ \&\ Q^{*}=i\}}\right]. \quad \text{(A.7)}$$

Setting $m_j = \sum_{i=1}^{N} \mathbf{1}_{\{\mathrm{MT}_i \in \mathrm{UE}_j\}}$ and $C_j = \sum_{i=1}^{N} D_i \cdot \mathbf{1}_{\{\mathrm{MT}_i \in \mathrm{UE}_j\}}$, we have

$$\begin{aligned}\sum_{i=1}^{N} E\left[D_i \cdot 1_{\{Q=j\ \&\ Q^{*}=i\}}\right] =& \sum_{j=1}^{M} \frac{1}{m_j} \cdot E\left[C_j \cdot \mathbf{1}_{\{Q=j\}}\right] \\ &+ \sum_{j=1}^{M} \frac{1}{m_j} \cdot E\left[(m_j - 1) \cdot R_j \cdot \mathbf{1}_{\{Q=j\}}\right] \\ &- \sum_{j=1}^{M} \frac{1}{m_j} \cdot E\left[\mathrm{sum}(\overline{\boldsymbol{R}}_j \cdot \mathbf{1}_{\{Q=j\}})\right]. \end{aligned} \quad \text{(A.8)}$$

Equation (A.8) achieves its minimum value when all the elements in $\overline{\boldsymbol{R}}_j$ are with the same value of R_j. Therefore, we have

$$E\left[\sum_{j=1}^{M} R_j \cdot \mathbf{1}_{\{Q=j\}}\right] \geqslant \sum_{j=1}^{N} \frac{1}{m_j} \cdot E\left[C_j \cdot \mathbf{1}_{\{Q=j\}}\right]. \quad \text{(A.9)}$$

A.3 Proof of Proposition 2.5

In Fig. 2.4, UE$_j$ is randomly located (with uniform distribution) in the grey cell. We use s to represent UE$_j$'s location. We define

$$C_j(s) = \sum_{i=1}^{N} D_i(s) \cdot \mathbf{1}_{\{\mathrm{MT}_i \in \mathrm{UE}_j\}} \,. \tag{A.10}$$

Further, we divide the MT_Bs serving UE$_j$ into serving two virtual UEs, namely UE$_{j_1}$ and UE$_{j_2}$. For the case of using the same provider A, the expectation of the throughput of UE$_j$ (located at s) in terms of time is

$$\begin{aligned} E\left[R_{\mathrm{A},j}(s)\right] =& E\left[\sum_{i=1}^{N} D_{\mathrm{A},i}(s) \cdot \mathbf{1}_{\{Q=j \& Q^*=i \& \mathrm{MT}_i \in \mathrm{UE}_j\}}\right] \\ =& E\left[C_{\mathrm{A},j}(s).\mathbf{1}_{\{Q=j\}} - \sum_{i=1}^{N} D_{\mathrm{A},i}(s) \cdot \mathbf{1}_{\{Q=j \& Q^* \neq i \& \mathrm{MT}_i \in \mathrm{UE}_j\}}\right] \,. \end{aligned} \tag{A.11}$$

For the purpose of later proof procedure, we now assume UE$_{j_1}$ and UE$_{j_2}$ are independently scheduled by provider A. Moreover, we use $D^{'}_{\cdot,i}$ to represent the supported data rate in this "2-UE" case for the convenience of explanation. The sum of their throughput expectation in terms of time is

$$\begin{aligned} E\left[R^{'}_{\mathrm{A},j_1}(s) + R^{'}_{\mathrm{A},j_2}(s)\right] \quad = \quad & E\left[\sum_{i=1}^{N} D^{'}_{\mathrm{A},i}(s) \cdot \mathbf{1}_{\{Q=j_1 \& Q^*=i \& \mathrm{MT}_i \in \mathrm{UE}_{j_1}\}}\right] \\ & + E\left[\sum_{i=1}^{N} D^{'}_{\mathrm{A},i}(s) \cdot \mathbf{1}_{\{Q=j_2 \& Q^*=i \& \mathrm{MT}_i \in \mathrm{UE}_{j_2}\}}\right] \,. \end{aligned} \tag{A.12}$$

Rewrite this equation,

$$\begin{aligned} E\left[R^{'}_{\mathrm{A},j_1}(s) + R^{'}_{\mathrm{A},j_2}(s)\right] \quad = \quad & E\left[C^{'}_{\mathrm{A},j_1}(s) \cdot \mathbf{1}_{\{Q=j_1\}} + C^{'}_{\mathrm{A},j_2}(s) \cdot \mathbf{1}_{\{Q=j_2\}}\right] \\ & - E\left[\sum_{i=1}^{N} D^{'}_{\mathrm{A},i}(s) \cdot \mathbf{1}_{\{Q=j_1 \& Q^* \neq i \& \mathrm{MT}_i \in \mathrm{UE}_{j_1}\}}\right] \\ & - E\left[\sum_{i=1}^{N} D^{'}_{\mathrm{A},i}(s) \cdot \mathbf{1}_{\{Q=j_2 \& Q^* \neq i \& \mathrm{MT}_i \in \mathrm{UE}_{j_2}\}}\right] \,. \end{aligned} \tag{A.13}$$

We notice that

$$C^{'}_{\mathrm{A},j_1}(s) \cdot \mathbf{1}_{\{Q=j_1\}} + C^{'}_{\mathrm{A},j_2}(s) \cdot \mathbf{1}_{\{Q=j_2\}} \leq C_{\mathrm{A},j}(s) \cdot \mathbf{1}_{\{Q=j\}}. \tag{A.14}$$

Moreover, for the indicator functions in (A.11) and (A.13), we have

$$\mathbf{1}_{\{Q=j\&Q^*\neq i\&\mathrm{MT}_i\in\mathrm{UE}_j\}} = \mathbf{1}_{\{Q=j_1\&Q^*\neq i\&\mathrm{MT}_i\in\mathrm{UE}_{j_1}\}} + \mathbf{1}_{\{Q=j_2\&Q^*\neq i\&\mathrm{MT}_i\in\mathrm{UE}_{j_2}\}}. \tag{A.15}$$

When UE_j is scheduled as one unity and $\mathbf{1}_{\{Q=j\&Q^*\neq i\}} = 1$, MT_i cannot be the MT with best supported data rate. In other words, if UE_j is scheduled, the unselected MT_i with $D_{\mathrm{A},i}$ cannot be the one with maximum D_{A} among those MTs serving UE_j. However, when 2 virtual UEs are scheduled independently, fairness constraint is kept between the UEs. This means, the unselected MT_i with $D'_{\mathrm{A},i}$ may be the maximum data rate among the D'_{A}s. Therefore,

$$\begin{aligned}&E\left[\sum_{i=1}^{N} D_{\mathrm{A},i}(s)\cdot\mathbf{1}_{\{Q=j\&Q^*\neq i\&\mathrm{MT}_i\in\mathrm{UE}_j\}}\right]\\ \leq &E\left[\sum_{i=1}^{N} D'_{\mathrm{A},i}(s)\cdot\mathbf{1}_{\{Q=j\&Q^*\neq i\&\mathrm{MT}_i\in\mathrm{UE}_j\}}\right].\end{aligned} \tag{A.16}$$

Combining (A.14)(A.15)(A.16), we have

$$E\left[R_{\mathrm{A},j}(s)\right] \geq E\left[R'_{\mathrm{A},j_1}(s) + R'_{\mathrm{A},j_2}(s)\right]. \tag{A.17}$$

For the case that the services are provided by different (two) cellular providers, we assume that UE_{j_1} is served by provider A while UE_{j_2} is served by provider B.

$$\begin{aligned}E\left[R'_{\mathrm{A},j_1}(s) + R'_{\mathrm{B},j_2}(s)\right] &= E\left[\sum_{i=1}^{N} D'_{\mathrm{A},i}(s)\cdot\mathbf{1}_{\{Q=j_1\&Q^*=i\&\mathrm{MT}_i\in\mathrm{UE}_{j_1}\}}\right]\\ &+E\left[\sum_{i=1}^{N} D'_{\mathrm{B},i}(s)\cdot\mathbf{1}_{\{Q=j_2\&Q^*=i\&\mathrm{MT}_i\in\mathrm{UE}_{j_2}\}}\right].\end{aligned} \tag{A.18}$$

Comparing the right hand side in (A.18) with that in (A.12), we notice that the only difference is between $D'_{\mathrm{A},i}(s)$ and $D'_{\mathrm{B},i}(s)$. Recall that the cell of A and B are absolutely the same, and UE_{j_2} is randomly located in the cell (of A or B). Thus, if we take the expectation in terms of location ($E_S[\cdot]$), we have

$$E_S[E(R'_{\mathrm{A},j_2}(s))] = E_S\left[E\left(R'_{\mathrm{B},j_2}(s)\right)\right]. \tag{A.19}$$

Combining (A.17) and (A.19), we have

$$\begin{aligned} E_S\left[E\left(R_{\mathrm{A},j}(s)\right)\right] \geq & E_S[E(R'_{\mathrm{A},j_1}(s)+R'_{\mathrm{A},j_2}(s))] \\ = & E_S\left[E\left(R'_{\mathrm{A},j_1}(s)+R'_{\mathrm{B},j_2}(s)\right)\right] \ . \end{aligned} \tag{A.20}$$

This supports our proposition. The main focus of this chapter is on two-cellular-providers case. However, this proof can be extended to multiple (more than two) providers case.

Appendix B

Appendices to Chapter 4

B.1 Proof of Proposition 4.2

$O_{A,R}$ and $O_{A,r}$ are used to represent the concentric circles with their centers at A. $O_{B,R}$ and $O_{B,r}$ are used to represent the concentric circles with their centers at B. For simplicity, we set R equals 1. With α being $arccot(\frac{D}{2})$, the area $S_{A,B}$ covered by $O_{A,R}$ and $O_{B,R}$ is

$$S_{A,B}(D) = 2\pi - 2\alpha + D \cdot sin(\alpha) \ . \tag{B.1}$$

The grey area, which is the exclusion region of this link, is symmetrical about both X and Y axis. For the grey part in the range of $x \in (-\infty, \frac{D}{2}]$ and $y \in [0, +\infty)$, it is $\frac{1}{4}$ of the whole grey area and is named as S_{CS}. S_{CS} is determined by r, D and θ. In the Fig. 4.7, it is clear that the function of line AC is

$$y = f_1(x, D, \theta) : y = (D - x) \cdot tan(\theta) \ . \tag{B.2}$$

The function of $O_{A,R}$ is

$$y = f_2(x, D) : y^2 + (x + D)^2 = R^2 \ . \tag{B.3}$$

The function of $O_{B,r}$ is

$$y = f_3(x) : y^2 + x^2 = r^2 \; . \tag{B.4}$$

We set

$$y = f_4(x, D, \theta) : y = max(f_1(x, D, \theta), f_2(x, D), f_3(x)). \tag{B.5}$$

For D (or x) outside certain function's definition domain, the value of this function is deemed as 0 in (B.5). For the reason that S_{CS} is related to D, we have

$$S_{CS}(D, \theta) = \int_{min(-r, D-R)}^{\frac{D}{2}} f_4(x, D, \theta) dx \; . \tag{B.6}$$

For certain $x \in (\infty, \frac{D}{2}]$, $D \in [0, R]$ and $\theta_1 \geq \theta_2$, we have

$$f_1(x, D, \theta_1) \geq f_1(x, D, \theta_2) \; . \tag{B.7}$$

Therefore, we have

$$f_4(x, D, \theta_1) \geq f_4(x, D, \theta_2) \; , \tag{B.8}$$

and

$$S_{CS}(D, \theta_1) \geq S_{CS}(D, \theta_2) \; . \tag{B.9}$$

For the PSSG, we have

$$\frac{S_{A,B}(D)}{S_{CS}(D, \theta_1)} \leq \frac{S_{A,B}(D)}{S_{CS}(D, \theta_2)} \; . \tag{B.10}$$

For the averaged PSSG, we have

$$f_{PSSG}(\theta) = \frac{1}{R} \cdot \int_0^R \frac{S_{A,B}(D)}{4 \cdot S_{CS}(D, \theta)} dD \; . \tag{B.11}$$

Based on (B.10) and (B.11), we have

$$f_{PSSG}(\theta_1) \leq f_{PSSG}(\theta_2). \tag{B.12}$$

(B.12) means the PSSG becomes smaller with larger θ, which illustrate why wider antenna beams bring smaller spatial sharing gains.

B.2 Possible Spatial Sharing Gain

D is the distance between $O_{B,R}$ and $O_{A,R}$. For the simplicity, we assume R to be 1. With our system model and based on (4.2), we get r is 0.5619. The beamwidth is now 30°. The function of the $O_{B,r}$, l_{AC} and $O_{A,R}$ above x axis is as below.

$$\begin{cases} g_1(x) = \sqrt{r^2 - x^2}\ , \\ g_2(x) = tan(\frac{\pi}{12}) \cdot (D - x)\ , \\ g_3(x) = \sqrt{1 - (x - D)^2}\ . \end{cases} \tag{B.13}$$

The exclusion region of directional transmission with $D \in [0, 0.4381)$ is similar to Fig. 4.7 and its area is as follows.

$$\begin{aligned} f_1(D) = &4 \cdot \left[\int_{x_1}^{x_0} g_1(x)dx + \int_{x_2}^{x_1} g_2(x)dx \right. \\ &\left. + \int_{x_3}^{x_2} g_3(x)dx \right], \end{aligned} \tag{B.14}$$

where

$$\begin{cases} x_0 = \frac{D}{2}, \\ x_1 = \frac{2D \cdot tan^2(\frac{\pi}{12}) - \sqrt{4D^2 \cdot tan^4(\frac{\pi}{12}+1) \cdot (D^2 \cdot tan^2(\frac{\pi}{12}) - r^2)}}{2 \cdot (tan^2(\frac{\pi}{12})+1)}, \\ x_2 = D - cos(\frac{\pi}{12}), \\ x_3 = D - 1. \end{cases} \tag{B.15}$$

For $D \in [0.4381, 0.4671)$, the exclusion region is

$$\begin{aligned} f_2(D) = &4 \cdot \left[\int_{x_1'}^{x_0'} g_1(x)dx + \int_{x_2'}^{x_1'} g_2(x)dx \right. \\ &\left. + \int_{x_3'}^{x_2'} g_3(x)dx + \int_{x_4'}^{x_3'} g_1(x)dx \right], \end{aligned} \tag{B.16}$$

where

$$\begin{cases} x_0^{'} = \frac{D}{2}, \\ x_1^{'} = \frac{2D \cdot tan^2(\frac{\pi}{12}) - \sqrt{4D^2 \cdot tan^4(\frac{\pi}{12}+1) \cdot (D^2 \cdot tan^2(\frac{\pi}{12}) - r^2)}}{2 \cdot (tan^2(\frac{\pi}{12})+1)}, \\ x_2^{'} = D - cos(\frac{\pi}{12}), \\ x_3^{'} = \frac{D^2+r^2-1}{2D}, \\ x_4^{'} = -r. \end{cases} \tag{B.17}$$

For $D \in [0.4671, 1]$, the exclusion region is

$$f_3(D) = 2\pi r^2 - 2r^2 \cdot acos(\frac{D}{2r}) + r \cdot D \cdot sin(acos(\frac{D}{2r})) \tag{B.18}$$

The exclusion region of the omni-directional transmission link is

$$f_4(D) = 2\pi - 2 \cdot acos(\frac{D}{2}) + D \cdot sin(acos(\frac{D}{2})) \ . \tag{B.19}$$

Based on (B.11), the PSSG with 30° beam is

$$\begin{aligned} \text{PSSG} = & \int_0^{0.4381} \frac{f_4(D)}{f_1(D)} dD + \int_{0.4381}^{0.4671} \frac{f_4(D)}{f_2(D)} dD \\ & + \int_{0.4671}^{1} \frac{f_4(D)}{f_3(D)} dD \ . \end{aligned} \tag{B.20}$$

With MATLAB, we get the numerical value is 2.57.

Bibliography

[1] X. Liu, E. K. P. Chong, and N. B. Shroff, "Opportunistic transmission scheduling with resource-sharing constraints in wireless networks," *Selected Areas in Communications, IEEE Journal on*, vol. 19, no. 10, pp. 2053–2064, Oct 2001.

[2] J. Qiao, B. Cao, X. Zhang, X. Shen, and J. W. Mark, "Efficient concurrent transmission scheduling for cooperative millimeter wave systems," in *Proceeding of IEEE Global Communications Conference (GLOBECOM)*, Anaheim, USA, Dec 2012, pp. 4187–4192.

[3] T. Luo, M. Motani, and V. Srinivasan, "Cooperative asynchronous multichannel mac: Design, analysis, and implementation," *Mobile Computing, IEEE Transactions on*, vol. 8, no. 3, pp. 338–352, Jan 2009.

[4] K. J. R. Liu, A. Sadek, W. Su, and A. Kwasinski, *Cooperative communications and networking*. Cambridge: Cambridge University Press, 2008.

[5] E. L. Hahne and R. G. Gallager, "Round robin scheduling for fair flow control in data communication networks," DTIC Document, Tech. Rep., 1986.

[6] E. L. Hahne, "Round-robin scheduling for max-min fairness in data networks," *Selected Areas in Communications, IEEE Journal on*, vol. 9, no. 7, pp. 1024–1039, Sept 1991.

[7] B. Hajek and G. Sasaki, “Link scheduling in polynomial time,” *Information Theory, IEEE Transactions on*, vol. 34, no. 5, pp. 910–917, Sept 1988.

[8] Q. Liu, X. Wang, and G. B. Giannakis, “A cross-layer scheduling algorithm with qos support in wireless networks,” *Vehicular Technology, IEEE Transactions on*, vol. 55, no. 3, pp. 839–847, May 2006.

[9] Y. Cao and V. O. Li, “Scheduling algorithms in broadband wireless networks,” *Proceedings of the IEEE*, vol. 89, no. 1, pp. 76–87, Jan 2001.

[10] H. Kim, K. Kim, Y. Han, and S. Yun, “A proportional fair scheduling for multicarrier transmission systems,” in *Proceeding of IEEE Vehicular Technology Conference (VTC)*, Los Angeles, USA, Sep 2004, pp. 409–413.

[11] Y. D. Chung and M.-H. Kim, “Qem: A scheduling method for wireless broadcast data,” in *Proceeding of IEEE International Conference on Database Systems for Advanced Applications*, Hsinchu, China, Apr 1999, pp. 135–142.

[12] S.-M. Cheng, P. Lin, D.-W. Huang, and S.-R. Yang, “A study on distributed/centralized scheduling for wireless mesh network,” in *Proceedings of ACM International Conference on Wireless Communications and Mobile Computing*, Vancouver, Canada, Jul 2006, pp. 599–604.

[13] M. Andrews and L. Zhang, “Scheduling algorithms for multi-carrier wireless data systems,” in *Proceedings of ACM International Conference on Mobile Computing and Networking (MOBICOM)*, Honolulu, USA, Aug 2007, pp. 3–14.

[14] P. Ansel, Q. Ni, and T. Turletti, “An efficient scheduling scheme for ieee 802.11e,” in *Proceeding of Modeling and Optimization in Mobile, Ad Hoc and Wireless Networks*, London, UK, Mar 2004, pp. 24–26.

[15] M. M. Rashid, E. Hossain, and V. K. Bhargava, “Controlled channel access scheduling for guaranteed qos in 802.11 e-based wlans,” *Wireless Communications, IEEE Transactions on*, vol. 7, no. 4, pp. 1287–1297, Apr 2008.

[16] B. Ji, C. Joo, and N. B. Shroff, “Delay-based back-pressure scheduling in multihop wireless networks,” *Networking, IEEE/ACM Transactions on*, vol. 21, no. 5, pp. 1539–1552, Apr 2013.

[17] ——, “Throughput-optimal scheduling in multi-hop wireless networks without per-flow information,” *Networking, IEEE/ACM Transactions on*, vol. 21, no. 2, pp. 634–647, Jul 2013.

[18] A. Bedekar, S. Borst, K. Ramanan, P. Whiting, and E. Yeh, “Downlink scheduling in cdma data networks,” in *Proceeding of IEEE Global Telecommunications Conference (GLOBECOM)*, Rio de Janeiro, Brazil, Dec 1999, pp. 2653–2657.

[19] H. Boche and M. Wiczanowski, “Optimal scheduling for high speed uplink packet access-a cross-layer approach,” in *Proceeding of IEEE Vehicular Technology Conference (VTC)*, Los Angeles, USA, Sep 2004, pp. 2575–2579.

[20] D. Wu and R. Negi, “Downlink scheduling in a cellular network for quality-of-service assurance,” *Vehicular Technology, IEEE Transactions on*, vol. 53, no. 5, pp. 1547–1557, Sept 2004.

[21] L. Xu, X. Shen, and J. W. Mark, “Dynamic fair scheduling with qos constraints in multimedia wideband cdma cellular networks,” *Wireless Communications, IEEE Transactions on*, vol. 3, no. 1, pp. 60–73, Jan 2004.

[22] X. Liu, E. K. Chong, and N. B. Shroff, "A framework for opportunistic scheduling in wireless networks," *Computer Networks*, vol. 41, no. 4, pp. 451–474, Jan 2003.

[23] S. S. Kulkarni and C. Rosenberg, "Opportunistic scheduling policies for wireless systems with short term fairness constraints," in *Proceeding of IEEE Global Telecommunications Conference (GLOBECOM)*, San Francisco, USA, Dec 2003, pp. 533–537.

[24] A. K. Khattab and K. M. Elsayed, "Opportunistic scheduling of delay sensitive traffic in ofdma-based wireless," in *proceedings of IEEE International Symposium on on World of Wireless, Mobile and Multimedia Networks*, Buffalo, USA, Jun 2006, pp. 279–288.

[25] H. Yomo and P. Popovski, "Opportunistic scheduling for wireless network coding," in *Proceeding of IEEE International Conference on Communications (ICC)*, Glasgow, UK, Jun 2007, pp. 5610–5615.

[26] S. Deb, V. Mhatre, and V. Ramaiyan, "Wimax relay networks: opportunistic scheduling to exploit multiuser diversity and frequency selectivity," in *Proceedings of ACM International Conference on Mobile Computing and Networking (MOBICOM)*, Hong Kong, China, May 2008, pp. 163–174.

[27] D. Zheng, W. Ge, and J. Zhang, "Distributed opportunistic scheduling for ad hoc networks with random access: an optimal stopping approach," *Information Theory, IEEE Transactions on*, vol. 55, no. 1, pp. 205–222, Jan 2009.

[28] R. Urgaonkar and M. J. Neely, "Opportunistic scheduling with reliability guarantees in cognitive radio networks," *Mobile Computing, IEEE Transactions on*, vol. 8, no. 6, pp. 766–777, Feb 2009.

[29] S. Jin, M. Choi, K. Kim, and S. Choi, “Opportunistic spatial reuse in ieee 802.15. 3c wireless personal area networks,” *Vehicular Technology, IEEE Transactions on*, vol. 62, no. 2, pp. 824–834, Feb 2013.

[30] Y. Zhe, L. Cai, and W.-s. Lu, “Practical scheduling algorithms for concurrent transmissions in rate-adaptive wireless networks,” *Engine*, 2010.

[31] I. K. Son, S. Mao, M. X. Gong, and Y. Li, “On frame-based scheduling for directional mmwave wpans,” in *Proceeding of IEEE International Conference on Computer Communication (INFOCOM)*, Orlando, USA, Mar 2012, pp. 2149–2157.

[32] W. Lee, K. Noh, S. Kim, and J. Heo, “Efficient cooperative transmission for wireless 3d hd video transmission in 60ghz channel,” *Consumer Electronics, IEEE Transactions on*, vol. 56, no. 4, pp. 2481–2488, Dec 2010.

[33] Q. Chen, X. Peng, J. Yang, and F. Chin, “Spatial reuse strategy in mmwave wpans with directional antennas,” in *Proceeding of IEEE Global Communications Conference (GLOBECOM)*, Anaheim, USA, Dec 2012, pp. 5392–5397.

[34] S. Singh, F. Ziliotto, U. Madhow, E. Belding, and M. Rodwell, “Blockage and directivity in 60 ghz wireless personal area networks: from cross-layer model to multihop mac design,” *Selected Areas in Communications, IEEE Journal on*, vol. 27, no. 8, pp. 1400–1413, Oct 2009.

[35] E.-J. Kim and S. Youm, “Selective cooperative transmission in ad hoc networks with directional antennas,” *International Journal of Distributed Sensor Networks*, vol. 2013, Nov 2013.

[36] X. Zhang, S. Zhou, X. Wang, Z. Niu, X. Lin, D. Zhu, and M. Lei, “Improving network throughput in 60ghz wlans via multi-ap diversity,” in *Proceeding of IEEE International Conference on Communications (ICC)*, Ottawa, Canada, Jun 2012, pp. 4803–4807.

[37] J. Qiao, L. X. Cai, X. Shen, and J. W. Mark, “Enabling multi-hop concurrent transmissions in 60 ghz wireless personal area networks,” *Wireless Communications, IEEE Transactions on*, vol. 10, no. 11, pp. 3824–3833, Oct 2011.

[38] ——, “Stdma-based scheduling algorithm for concurrent transmissions in directional millimeter wave networks,” in *Proceeding of IEEE International Conference Communications (ICC)*, Ottawa, Canada, Jun 2012, pp. 5221–5225.

[39] L. X. Cai, L. Cai, X. Shen, and J. W. Mark, “Spatial multiplexing capacity analysis of mmwave wpans with directional antennae,” in *Proceeding of IEEE Global Telecommunications Conference (GLOBECOM)*, Washington D.C., USA, Dec 2007, pp. 4744–4748.

[40] ——, “Rex: a randomized exclusive region based scheduling scheme for mmwave wpans with directional antenna,” *Wireless Communications, IEEE Transactions on*, vol. 9, no. 1, pp. 113–121, Jan 2010.

[41] J.-H. Liu and H.-L. Chao, “Joint relay selection and scheduling algorithm for inter-piconet communications in millimeter wave wireless personal area networks,” in *Proceeding of IEEE International Symposium on Personal Indoor and Mobile Radio Communications (PIMRC)*, Toronto, Canada, Sep 2011, pp. 1119–1123.

[42] P. Dutta, V. Mhatre, D. Panigrahi, and R. Rastogi, “Joint routing and scheduling in multi-hop wireless networks with directional antennas,” in *Proceeding of*

IEEE International Conference on Computer Communication (INFOCOM), San Diego, USA, Mar 2010, pp. 1–5.

[43] Z. Lan, J. Wang, J. Gao, C.-S. Sum, F. Kojima, T. Baykas, H. Harada, and S. Kato, “Directional relay with spatial time slot scheduling for mmwave wpan systems,” in *Proceeding of IEEE Vehicular Technology Conference (VTC)*, Taipei, China, May 2010, pp. 1–5.

[44] Z. Lan, L. A. Lu, X. Zhang, C. Pyo, and H. Harada, “A space-time scheduling assisted cooperative relay for mmwave wlan/wpan systems with directional antenna,” in *Proceeding of IEEE Global Telecommunications Conference (GLOBECOM)*, Houston, USA, Dec 2011, pp. 1–6.

[45] H. Su and X. Zhang, “Joint link scheduling and routing for directional-antenna based 60 ghz wireless mesh networks,” in *Proceeding of IEEE Global Telecommunications Conference (GLOBECOM)*, Honolulu, USA, Dec 2009, pp. 1–6.

[46] Z. Yang, L. Cai, and W.-S. Lu, “Practical scheduling algorithms for concurrent transmissions in rate-adaptive wireless networks,” in *Proceeding of IEEE International Conference on Computer Communications (INFOCOM)*, San Diego, USA, Mar 2010, pp. 1–9.

[47] N. Challa and H. Cam, “Cost-aware downlink scheduling of shared channels for cellular networks with relays,” in *Proceeding of IEEE International Conference on Performance, Computing, and Communications*, Phoenix, USA, Apr 2004, pp. 793–798.

[48] H. Viswanathan and S. Mukherjee, “Performance of cellular networks with relays and centralized scheduling,” *Wireless Communications, IEEE Transactions on*, vol. 4, no. 5, pp. 2318–2328, Sept 2005.

[49] L. Huang, M. Rong, L. Wang, Y. Xue, and E. Schulz, “Resource scheduling for ofdma/tdd based relay enhanced cellular networks,” in *Proceeding of IEEE Wireless Communications and Networking Conference (WCNC)*, Hong Kong, China, Mar 2007, pp. 1544–1548.

[50] O. Oyman, “Opportunistic scheduling and spectrum reuse in relay-based cellular ofdma networks,” in *Proceeding of IEEE Global Telecommunications Conference (GLOBECOM)*, Washington D.C., USA, Dec 2007, pp. 3699–3703.

[51] W.-G. Ahn and H.-M. Kim, “Proportional fair scheduling in relay enhanced cellular ofdma systems,” in *Proceeding of IEEE International Symposium on Personal Indoor and Mobile Radio Communications (PIMRC)*, Cannes, France, Sep 2008, pp. 1–4.

[52] L. Xiao and L. Cuthbert, “A two-hop proportional fairness scheduling algorithm for relay based ofdma systems,” in *Proceeding of IEEE International Conference on Wireless Communications, Networking and Mobile Computing (WICOM)*, Dalian, China, Sep 2008, pp. 1–4.

[53] H. Chen, X. Xie, and H. Wu, “A queue-aware scheduling algorithm for multihop relay wireless cellular networks,” in *Proceeding of IEEE Mobile WiMAX Symposium*, Napa Valley, CA, Jul 2009, pp. 63–68.

[54] C.-Y. Hong and A.-C. Pang, “3-approximation algorithm for joint routing and link scheduling in wireless relay networks,” *Wireless Communications, IEEE Transactions on*, vol. 8, no. 2, pp. 856–861, Feb 2009.

[55] ——, “Link scheduling with qos guarantee for wireless relay networks,” in *Proceeding of IEEE International Conference on Computer Communication (INFOCOM)*, Rio De Janeiro, Brazil, Apr 2009, pp. 2806–2810.

[56] O. Oyman, “Opportunistic scheduling and spectrum reuse in relay-based cellular networks,” *Wireless Communications, IEEE Transactions on*, vol. 9, no. 3, pp. 1074–1085, Mar 2010.

[57] Y. Wang, H. K. Garg, and M. Motani, “Downlink scheduling for user equipment served by multiple mobile terminals,” in *Proceeding of IEEE Global Telecommunications Conference (GLOBECOM)*, Houston, USA, Dec 2011, pp. 1–5.

[58] ——, “Downlink scheduling for user equipment served by multiple mobile terminals in cellular systems,” *Computer Networks*, vol. 57, no. 3, pp. 668–681, Oct 2013.

[59] Z. Genc, G. M. Olçer, E. Onur, and I. Niemegeers, “Improving 60 ghz indoor connectivity with relaying,” in *Proceeding of IEEE International Conference on Communications (ICC)*, Cape Town, South Africa, May 2010, pp. 1–6.

[60] Z. Lan, C.-S. Sum, J. Wang, T. Baykas, F. Kojima, H. Nakase, and H. Harada, “Relay with deflection routing for effective throughput improvement in gbps millimeter-wave wpan systems,” *Selected Areas in Communications, IEEE Journal on*, vol. 27, no. 8, pp. 1453–1465, Oct 2009.

[61] N. Abramson, “The aloha system: another alternative for computer communications,” in *Proceedings of ACM Joint Computer Conference*, Atlantic City, USA, May 1970, pp. 281–285.

[62] P. Karn, “Maca-a new channel access method for packet radio,” in *ARRL/CRRL Amateur Radio Computer Networking Conference*, London, Canada, Sep 1990, pp. 134–140.

[63] K. Biba, "An update to the hybrid wireless mac protocol supporting asynchronous and synchronous msdu delivery services," *IEEE 802.11*, vol. 11, no. 92, p. 14, 1992.

[64] L. Kleinrock and F. A. Tobagi, "Packet switching in radio channels: Part i–carrier sense multiple-access modes and their throughput-delay characteristics," *Communications, IEEE Transactions on*, vol. 23, no. 12, pp. 1400–1416.

[65] V. Bharghavan, A. Demers, S. Shenker, and L. Zhang, "Macaw: a media access protocol for wireless lan's," in *ACM SIGCOMM Computer Communication Review*, vol. 24, no. 4, 1994, pp. 212–225.

[66] J. Garcia-Luna-Aceves and C. L. Fullmer, "Performance of floor acquisition multiple access in ad-hoc networks," in *Proceeding of IEEE Symposium on Computers and Communications*, Athens, Greece, Jun 1998, pp. 63–68.

[67] ——, "Floor acquisition multiple access (fama) in single-channel wireless networks," *Mobile Networks and Applications*, vol. 4, no. 3, pp. 157–174, Oct 1999.

[68] S.-L. Wu, C.-Y. Lin, Y.-C. Tseng, and J.-P. Sheu, "A new multi-channel mac protocol with on-demand channel assignment for multi-hop mobile ad hoc networks," in *Proceeding of IEEE International Symposium on Parallel Architectures, Algorithms and Networks*, Dallas, USA, Dec 2000, pp. 232–237.

[69] A. Adya, P. Bahl, J. Padhye, A. Wolman, and L. Zhou, "A multi-radio unification protocol for ieee 802.11 wireless networks," in *Proceeding of IEEE International Conference on Broadband Networks (BROADNETS)*, San Jose, USA, Oct 2004, pp. 344–354.

[70] R. Maheshwari, H. Gupta, and S. R. Das, "Multichannel mac protocols for wireless networks," in *Proceeding of IEEE International Conference on Sensor, Mesh and Ad Hoc Communications and Networks (SECON)*, Reston, USA, Sep 2006, pp. 393–401.

[71] J. So and N. H. Vaidya, "Multi-channel mac for ad hoc networks: handling multi-channel hidden terminals using a single transceiver," in *Proceedings of ACM International Symposium on Mobile Ad Hoc Networking and Computing (MOBIHOC)*, Tokyo, Japan, May 2004, pp. 222–233.

[72] J. Chen, S.-T. Sheu, and C.-A. Yang, "A new multichannel access protocol for ieee 802.11 ad hoc wireless lans," in *Proceeding of IEEE International Symposium on Personal, Indoor and Mobile Radio Communications (PIMRC)*, Beijing, China, Sep 2003, pp. 2291–2296.

[73] J. Zhang, G. Zhou, C. Huang, S. H. Son, and J. A. Stankovic, "Tmmac: An energy efficient multi-channel mac protocol for ad hoc networks," in *Proceeding of IEEE International Conference on Communications (ICC)*, Glasgow, UK, Jun 2007, pp. 3554–3561.

[74] P. Bahl, R. Chandra, and J. Dunagan, "Ssch: slotted seeded channel hopping for capacity improvement in ieee 802.11 ad-hoc wireless networks," in *Proceedings of ACM International Conference on Mobile Computing and Networking (MOBICOM)*, Tokyo, Japan, May 2004, pp. 216–230.

[75] K. Bian, J.-M. Park, and R. Chen, "Control channel establishment in cognitive radio networks using channel hopping," *Selected Areas in Communications, IEEE Journal on*, vol. 29, no. 4, pp. 689–703, Mar 2011.

[76] Y. Zhang, Q. Li, G. Yu, and B. Wang, "Etch: Efficient channel hopping for communication rendezvous in dynamic spectrum access networks," in

Proceeding of IEEE International Conference on Computer Communications (INFOCOM), Shanghai, China, Apr 2011, pp. 2471–2479.

[77] Z. Huang, C.-C. Shen, C. Srisathapornphat, and C. Jaikaeo, “A busy-tone based directional mac protocol for ad hoc networks,” in *Proceeding of IEEE Military Communication Conference (MILCOM)*, Anaheim, USA, Oct 2002, pp. 1233–1238.

[78] H. Gossain, C. Cordeiro, and D. P. Agrawal, “Mda: An efficient directional mac scheme for wireless ad hoc networks,” in *Proceeding of IEEE International Conference on Global Telecommunications Conference (GLOBECOM)*, St. Louis, USA, Dec 2005, pp. 3633–3637.

[79] J. Wang, Y. Fang, and D. Wu, “Syn-dmac: A directional mac protocol for ad hoc networks with synchronization,” in *Proceeding of IEEE Military Communications Conference (MILCOM)*, Atlantic City, USA, Oct 2005, pp. 2258–2263.

[80] M. Takata, M. Bandai, and T. Watanabe, “A mac protocol with directional antennas for deafness avoidance in ad hoc networks,” in *Proceeding of IEEE International Conference on Global Telecommunications Conference (GLOBECOM)*, Washington D.C., USA, Dec 2007, pp. 620–625.

[81] T. Ueda, S. Tanaka, D. Saha, S. Roy, and S. Bandyopadhyay, “An efficient mac protocol with direction finding scheme in wireless ad hoc network using directional antenna,” in *Proceeding of IEEE Radio and Wireless Conference (RAWCON)*, Boston, USA, Aug 2003, pp. 233–236.

[82] R. R. Choudhury and N. Vaidya, “Deafness: A mac problem in ad hoc networks when using directional antennas,” in *Proceeding of IEEE International*

Conference on Network Protocols (ICNP), Berlin, Germany, Oct 2004, pp. 283–292.

[83] M. Takata, M. Bandai, and T. Watanabe, “Ri-dmac: a receiver-initiated directional mac protocol for deafness problem,” *International Journal of Sensor Networks*, vol. 5, no. 2, pp. 79–89, Apr 2009.

[84] A. Acharya, A. Misra, and S. Bansal, “Design and analysis of a cooperative medium access scheme for wireless mesh networks,” in *Proceeding of IEEE International Conference on Broadband Networks (BROADNETS)*, San Jose, USA, Oct 2004, pp. 621–631.

[85] J. Zheng and M. Ma, “Qos-aware cooperative medium access control for mimo ad-hoc networks,” *IEEE Communications Letters*, vol. 14, no. 1, pp. 48–50, Jan 2010.

[86] K. Tan, Z. Wan, H. Zhu, and J. Andrian, “Code: cooperative medium access for multirate wireless ad hoc network,” in *Proceeding of IEEE International Conference on Sensor, Mesh and Ad Hoc Communications and Networks (SECON)*, San Diego, USA, Jun 2007, pp. 1–10.

[87] H. Zhu and G. Cao, “rdcf: A relay-enabled medium access control protocol for wireless ad hoc networks,” *Mobile Computing, IEEE Transactions on*, vol. 5, no. 9, pp. 1201–1214, Jul 2006.

[88] H. Shin, Y. Kim, S. Pack, and C.-h. Kang, “A distributed relay mac protocol in wimedia wireless personal area,” in *Proceeding of IEEE International Symposium on Parallel and Distributed Processing with Applications (ISPA)*, Sydney, Australia, Dec 2008, pp. 784–789.

[89] C.-T. Chou, J. Yang, and D. Wang, “Cooperative mac protocol with automatic relay selection in distributed wireless networks,” in *Proceeding of IEEE International Conference on Pervasive Computing and Communications Workshops (PerCom)*, New York, USA, Mar 2007, pp. 526–531.

[90] W. Wang, C.-K. Seo, and S.-J. Yoo, “Power aware multi-hop packet relay mac protocol in uwb based wpans,” in *Mobile Ad-hoc and Sensor Networks*. Springer, Jan 2005, pp. 580–592.

[91] T. Guo and R. Carrasco, “Crbar: Cooperative relay-based auto rate mac for multirate wireless networks,” *Wireless Communications, IEEE Transactions on*, vol. 8, no. 12, pp. 5938–5947, Dec 2009.

[92] M. Khalid, Y. Wang, I.-h. Ra, and R. Sankar, “Two-relay-based cooperative mac protocol for wireless ad hoc networks,” *Vehicular Technology, IEEE Transactions on*, vol. 60, no. 7, pp. 3361–3373, Sept 2011.

[93] P. Liu, Z. Tao, and S. Panwar, “A cooperative mac protocol for wireless local area networks,” in *Proceeding of IEEE International Conference on Communications (ICC)*, Seoul, Korea, May 2005, pp. 2962–2968.

[94] P. Ju, W. Song, and D. Zhou, “Survey on cooperative medium access control protocols,” *IET Communications*, vol. 7, no. 9, pp. 893–902, Aug 2013.

[95] T. Luo, M. Motani, and V. Srinivasan, “Cam-mac: A cooperative asynchronous multi-channel mac protocol for ad hoc networks,” in *Proceeding of IEEE International Conference on Broadband Communications, Networks and Systems (BROADNETS)*, San Jose, USA, Oct 2006, pp. 1–10.

[96] Y. Wang, M. Motani, H. K. Garg, Q. Chen, and T. Luo, “Directional medium access control for ad hoc networks: A cooperation-based approach,” in

Proceeding of IEEE International Conference on Networks (ICON), Singapore, Dec 2013, pp. 1–6.

[97] Y. Wang, H. K. Garg, and M. Motani, "Multi-channel directional medium access control for ad hoc networks: A cooperative approach," in *Proceeding of IEEE International Conference on Communications (ICC)*, Sydney, Australia, Jun 2014, pp. 53–58.

[98] Y. Wang, X. Kang, H. K. Garg, M. Motani, and Q. Chen, "Throughput maximization for 60 ghz wpans via device cooperation," *IEEE Communications Letters*, vol. 18, no. 92, pp. 1–4, Mar 2014.

[99] Y. Wang, H. K. Garg, M. Motani, X. Kang, and Q. Chen, "Link scheduling and relay assignment for cooperative 60 ghz wpans," to submit.

[100] Y. Wang, M. Motani, H. K. Garg, Q. Chen, and T. Luo, "Cooperative multi-channel directional medium access control for ad hoc networks," *Systems, IEEE Journal*, submitted.

[101] F. Blomer, "Scheduling for streaming users in hsdpa," Ph.D. dissertation, M. Sc thesis, Munich Univ. of Technol., Munich, Germany, 2003.

[102] T. E. Kolding, F. Frederiksen, and M. Preben, "Performance aspects of wcdma systems with high speed downlink packet access (hsdpa)," in *Proceeding of IEEE Vehicular Technology Conference (VTC)*, Birmingham, USA, May 2002, pp. 477–481.

[103] X. Liu, E. K. P. Chong, and N. Shroff, "Transmission scheduling for efficient wireless resource utilization with minimum-performance guarantees," in *Proceeding of IEEE Vehicular Technology Conference (VTC)*, Atlantic City, USA, Oct 2001, pp. 824–828.

[104] M. Andrews, L. Qian, and A. Stolyar, “Optimal utility based multi-user throughput allocation subject to throughput constraints,” in *Proceeding of IEEE International Conference on Computer Communications (INFOCOM)*, Miami, USA, Mar 2005, pp. 2415–2424.

[105] S. H. Ali, K.-D. Lee, and V. C. Leung, “Throughput constrained opportunistic scheduling in cellular data networks,” *Vehicular Technology, IEEE Transactions on*, vol. 58, no. 3, pp. 1396–1406, May 2009.

[106] A. Farrokh and V. Krishnamurthy, “Opportunistic scheduling for streaming multimedia users in high-speed downlink packet access (hsdpa),” *Multimedia, IEEE Transactions on*, vol. 8, no. 4, pp. 844–855, Nov 2006.

[107] G. T. . v7.3.0, “Physical layer procedures (fdd) (release 7),” pp. 35–40, 2006.

[108] S.-Y. Jeon and D.-H. Cho, “Channel adaptive cqi reporting schemes for hsdpa systems,” *Communications Letters, IEEE*, vol. 10, no. 6, pp. 459–461, Jun 2006.

[109] K. Freudenthaler, A. Springer, and J. Wehinger, “Novel sinr-to-cqi mapping maximizing the throughput in hsdpa,” in *Proceeding of IEEE Wireless Communications and Networking Conference (WCNC)*, Hong Kong, China, Sep 2007, pp. 2231–2235.

[110] G. T. . v7.3.0, “User equipment (ue) radio transmission and reception (fdd) (release 7),” pp. 98–104, 2005.

[111] Ericsson, Motorola, and Nokia, “Common hsdpa system simulation assumptions,” *Communications Letters, IEEE*, vol. 10, no. 6, pp. 459–461, 2006.

[112] M. Gudmundson, “Correlation model for shadow fading in mobile radio systems,” *Electronics letters*, vol. 27, no. 23, pp. 2145–2146, 1991.

[113] [Online]. Available: http://cp.literature.agilent.com/litweb/pdf/5990-9697EN.pdf

[114] L. L. Yang, “60ghz: opportunity for gigabit wpan and wlan convergence,” *ACM SIGCOMM Computer Communication Review*, vol. 39, no. 1, pp. 56–61, Jan 2009.

[115] J. Zhang, H. Wu, Q. Zhang, and B. Li, “Joint routing and scheduling in multi-radio multi-channel multi-hop wireless networks,” in *Proceeding of IEEE International Conference on Broadband Networks (BROADNETS)*, Boston, USA, Oct 2005, pp. 631–640.

[116] A. Capone, I. Filippini, and F. Martignon, “Joint routing and scheduling optimization in wireless mesh networks with directional antennas,” in *Proceeding of IEEE International Conference on Communications (ICC)*, Beijing, China, May 2008, pp. 2951–2957.

[117] A. Capone, G. Carello, I. Filippini, S. Gualandi, and F. Malucelli, “Routing, scheduling and channel assignment in wireless mesh networks: optimization models and algorithms,” *Ad Hoc Networks*, vol. 8, no. 6, pp. 545–563, Aug 2010.

[118] Z. Yang, Q. Zhang, and Z. Niu, “Throughput improvement by joint relay selection and link scheduling in relay-assisted cellular networks,” *Vehicular Technology, IEEE Transactions on*, vol. 61, no. 6, pp. 2824–2835, Jul 2012.

[119] Y. Cheng, X. Cao, X. S. Shen, D. M. Shila, and H. Li, “A systematic study of the delayed column generation method for optimizing wireless networks,” in *Proceedings of the 15th ACM international symposium on Mobile ad hoc networking and computing (MOBIHOC)*. Philadelphia, USA: ACM, 2014, pp. 23–32.

[120] Q. Chen, J. Tang, D. T. C. Wong, X. Peng, and Y. Zhang, "Directional cooperative mac protocol design and performance analysis for ieee 802.11 ad wlans," *Vehicular Technology, IEEE Transactions on*, vol. 62, no. 6, pp. 2667–2677, Jul 2013.

[121] I. C. Society, *IEEE Std 802.11ad-2012*, 2012.

[122] G. Desaulniers, J. Desrosiers, and M. M. Solomon, *Column generation*. New York: Springer, 2005.

[123] "www-01.ibm.com/software/commerce/optimization/cplex-optimizer."

[124] M. Takai, J. Martin, R. Bagrodia, and A. Ren, "Directional virtual carrier sensing for directional antennas in mobile ad hoc networks," in *Proceedings of ACM international Symposium on Mobile Ad Hoc Networking and Computing (MOBIHOC)*, Lausanne, Switzerland, Jun 2002, pp. 183–193.

[125] R. R. Choudhury, X. Yang, R. Ramanathan, and N. Vaidya, "On designing mac protocols for wireless networks using directional antennas," *Mobile Computing, IEEE Transactions on*, vol. 5, no. 5, pp. 477–491, Mar 2006.

[126] Y. Takatsuka, M. Takata, M. Bandai, and T. Watanabe, "A mac protocol for directional hidden terminal and minor lobe problems," in *Proceeding of IEEE Wireless Telecommunications Symposium (WTS)*, Pomona, Canada, Apr 2008, pp. 210–219.

[127] J.-J. Chang, W. Liao, and J.-R. Lai, "On reservation-based mac protocol for ieee 802.11 wireless ad hoc networks with directional antenna," *Vehicular Technology, IEEE Transactions on*, vol. 60, no. 6, pp. 2669–2679, Jul 2011.

[128] A. Arora, M. Krunz, and A. Muqattash, "Directional medium access protocol (dmap) with power control for wireless ad hoc networks," in *Proceeding of*

IEEE Global Telecommunications Conference (GLOBECOM), Dallas, USA, Dec 2004, pp. 2797–2801.

[129] T. Korakis, G. Jakllari, and L. Tassiulas, “Cdr-mac: A protocol for full exploitation of directional antennas in ad hoc wireless networks,” *Mobile Computing, IEEE Transactions on*, vol. 7, no. 2, pp. 145–155, Feb 2008.

[130] W. Na, L. Park, and S. Cho, “Deafness-aware mac protocol for directional antennas,” in *Proceeding of IEEE International Conference on Consumer Electronics (ICCE)*, Las Vagas, USA, Jan 2013, pp. 625–626.

[131] S. Motegi, H. Sekiya, J. Ma, K. Sanada, and S. Sakata, “A directional mac protocol with the data-frame fragmentation and short busy advertisement signal for mitigating the directional hidden node problem,” in *Proceeding of IEEE International Symposium on Personal Indoor and Mobile Radio Communications (PIMRC)*, Sydney, Australia, Sept 2012, pp. 393–398.

[132] A. A. Abdullah, L. Cai, and F. Gebali, “Dsdmac: Dual sensing directional mac protocol for ad hoc networks with directional antennas,” *Vehicular Technology, IEEE Transactions on*, vol. 61, no. 3, pp. 1266–1275, Mar.

[133] J. Wang, H. Zhai, P. Li, Y. Fang, and D. Wu, “Directional medium access control for ad hoc networks,” *Wireless Networks*, vol. 15, no. 8, pp. 1059–1073, 2009.

[134] A. Nasipuri, J. Zhuang, and S. R. Das, “A multichannel csma mac protocol for multihop wireless networks,” in *Proceeding of IEEE Wireless Communications and Networking Conference (WCNC)*, New Orleans, USA, Sep 1999, pp. 1402–1406.

[135] A. Tzamaloukas and J. Garcia-Luna-Aceves, “Channel-hopping multiple access,” in *Proceeding of IEEE International Conference on Communications (ICC)*, New Orleans, USA, Jun 2000, pp. 415–419.

[136] H.-S. W. So, G. Nguyen, and J. Walrand, “Practical synchronization techniques for multi-channel mac,” in *Proceedings of ACM International Conference on Mobile Computing and Networking (MOBICOM)*, Los Angeles, USA, Sept 2006, pp. 134–145.

[137] X. Zhang and H. Su, “Cream-mac: cognitive radio-enabled multi-channel mac protocol over dynamic spectrum access networks,” *Selected Topics in Signal Processing, IEEE Journal of*, vol. 5, no. 1, pp. 110–123, Jan 2011.

[138] W. S. Jeon, J. A. Han, and D. G. Jeong, “A novel mac scheme for multichannel cognitive radio ad hoc networks,” *Mobile Computing, IEEE Transactions on*, vol. 11, no. 6, pp. 922–934, Apr 2012.

[139] M. Timmers, S. Pollin, A. Dejonghe, L. Van der Perre, and F. Catthoor, “A distributed multichannel mac protocol for multihop cognitive radio networks,” *Vehicular Technology, IEEE Transactions on*, vol. 59, no. 1, pp. 446–459, Jan 2010.

[140] L. T. Tan and L. B. Le, “Distributed mac protocol for cognitive radio networks: Design, analysis, and optimization,” *Vehicular Technology, IEEE Transactions on*, vol. 60, no. 8, pp. 3990–4003, Aug 2011.

[141] R. Ramanathan, “On the performance of ad hoc networks with beamforming antennas,” in *Proceedings of ACM International Symposium on Mobile Ad Hoc Networking and Computing (MOBIHOC)*, Long Beach, USA, Oct 2001, pp. 95–105.

[142] I. W. Group, *Wireless LAN medium access control (MAC) and physical layer (PHY) specifications*, 1999.

List of Publications

Journal Papers

1. Y. Wang, H. K. Garg, and M. Motani, “Downlink Scheduling for User Equipment Served by Multiple Mobile Terminals in Cellular Systems,” *Elsevier Journal of Computer Networks* , vol. 57, issue 3, pp. 668 - 681, Feb 2013.

2. Y. Wang, X. Kang, H. K. Garg, M. Motani, and Q. Chen, “Throughput Maximization for 60 GHz WPANs Via Device Cooperation,” *IEEE Communication Letters*, vol. 18, issue 5, pp. 785 - 788, May 2014.

3. Y. Wang, M. Motani, H. K. Garg, Q. Chen, and T. Luo, “Cooperative Multi-Channel Directional Medium Access Control for Ad Hoc Networks,” *IEEE Systems Journal*, submitted.

4. Y. Wang, H. K. Garg, M. Motani, X. Kang, and Q. Chen, “Link Scheduling And Relay Assignment For Cooperative 60 GHz WPANs,” prepare to submit.

Conference Papers

1. Y. Wang, M. Motani, H. K. Garg, Q. Chen, and T. Luo, “Multi-channel Directional Medium Access Control for Ad Hoc Networks: A Cooperative Approach,” in *Proc. IEEE International Conference on Communications 2014*

(ICC '14), Sydney, Australia, June 2014.

2. Y. Wang, H. K. Garg, and M. Motani, "Directional Medium Access Control for Ad Hoc Networks: A Cooperation-Based Approach," in *Proc. IEEE International Conference on Networks 2013 (ICON '13)*, Singapore, December 2013.

3. Y. Wang, H. K. Garg, and M. Motani, "Downlink Scheduling for User Equipment Served by Multiple Mobile Terminals," in *Proc. IEEE Global Communications Conference 2011 (GLOBECOM '11)*, Houston, USA, December 2011.